ANALYTICAL AND EXPERIMENTAL STABILITY OF EARTH ANCHORS

By

HAMED SALEM SAEEDY

Diploma of Technology
Kingston College of Technology
Kingston on Thames
Surrey, England
1962

Diploma of Technology
Twickenham College of Technology
Twickenham
Middlesex, England
1963

Master of Science
Colorado State University
Fort Collins, Colorado
1968

Submitted to the Faculty of the Graduate College
of the Oklahoma State University
in partial fulfillment of the requirements
for the Degree of
DOCTOR OF PHILOSOPHY
May, 1971

ANALYTICAL AND EXPERIMENTAL STABILITY OF EARTH ANCHORS

Thesis Approved:

J. V. Parcher
Thesis Adviser

T. Allan Haliburton

Wm. Ward Hasty

R. L. Lowery

O. D. Dunham
Dean of the Graduate College

To my Grandmother, parents, and son,

Adi, for all their suffering, and

patience during my absence.

ACKNOWLEDGEMENTS

The author wishes to express his sincere appreciation and gratitude to the following individuals and organizations:

To Dr. James V. Parcher, Thesis Adviser and Chairman of the Advisory Committee, for his valuable counsel and continuous advice throughout this study; and to Dr. T. A. Haliburton, member of the Advisory Committee, for his sincere help and valuable suggestions throughout this investigation.

To Drs. M. A. Hady and R. L. Lowry, members of the Advisory Committee, for their significant suggestions and expressed interest during this work.

To Dr. J. W. N. Fead, Professor and Head of Civil Engineering Department, and Dr. J. M. Bell, at Colorado State University for their early encouragement.

To the University of Basrah and the School of Civil Engineering, Oklahoma State University, for the financial support.

To Mr. C. Sharp, P. G. Wilson, and A. L. Harris for their assistance in constructing the experimental set up.

To all colleagues in the School of Civil Engineering for their continuous help in the experimental work.

And finally, to the author's wife, Layla, and son, Ali, for the undying love, understanding, and encouragement during the period of the graduate study.

H. S. Saeedy

TABLE OF CONTENTS

LIST OF TABLES

LIST OF FIGURES

CHAPTER I

INTRODUCTION

1.1 General

Earth anchors are generally used to provide necessary resistance for uplift pressures to which certain types of structures are subjected. For example, submerged structures such as pipelines, tunnels and storage containers are subjected to uplift hydrostatic pressures and should, therefore, be provided with earth anchors to achieve the required stability. Earth anchors may also be used to counteract the overturning couples acting on tall towers, such as those used for different types of communications and power transmission as indicated by Giffels (10) and Markowsky (19). It is also becoming general practice to use earth anchors in retaining structures, spillways and dams to reduce the use of external bracing.

Unlike the supporting mechanism provided by conventional footings and foundations, which are designed to resist compression forces, earth anchors are designed to provide adequate tie-back resistance to the applied tensile forces.

1.2 Purpose and Scope of Investigation

Earth anchors play an important role in the field of Civil Engineering. With the increasing variety of uses to which earth anchors are put, it is becoming more and more important that their

behavior and capability to provide the required support be more fully understood. While conventional footings and foundations have been thoroughly investigated, both theoretically and practically, no comprehensive method for designing anchor foundations is available.

This study is directed toward providing a rational approach for determining the ultimate vertical pull-out capacity of circular disc anchor plates buried in sand. This is believed to be an important step along the way to a more general solution of the problem.

The theoretical study developed herein is based on the assumption that the soil mass at failure is at a state of limiting equilibrium. In this case, the resistance of the anchor to the uplift forces is provided by three components: (1) the dead weight of the foundation, (2) the vertical component of the shear force produced by mobilizing the shear strength of the soil, and (3) the weight of the mass of the soil bounded by the rupture surface, which is lifted by the anchor plate.

In this investigation experimental work was carried out on anchors embedded in sand under different moisture conditions: (1) dry sand, (2) submerged sand, and (3) submerged sand drained prior to testing. Data collected from the experimental work were compared with predictions based on the theoretically formulated approach, to evaluate the validity of the theoretical relationship. Furthermore, experimental data were utilized to determine the significant effects of varying the depth of embedment and diameter of the anchor plate.

Although the testing program was performed on a single type of s soil, which was Ottawa Sand, the analytical solution was generalized to cover a variety of cohesionless soils having different values of Φ and γ.

CHAPTER II

LITERATURE REVIEW

2.1 General

Anchor foundations have been categorized as shallow or deep, depending on their mode of failure. They are characterized as shallow when a definite slip surface appears on the surface of the soil at failure, and as deep anchors when there is no observable slip surface, Turner (30).

The critical depth at which the transition from shallow to deep anchor takes place depends on the geometry of the anchor. According to Baker and Kondner (2), shallow anchors are those having depth to diameter ratio smaller than six, while deep anchors have a ratio of depth to diameter greater than six. Both Meyerhof (23) and Mariupol-skii (18) commented on the behavior of shallow and deep anchors. However, they did not precisely delineate the point at which the transition from one to the other occurs.

Previous investigations directed toward a solution of earth anchor problems may be classified under the following forms:

a) Theoretical and semi-theoretical methods.

b) Laboratory or model tests.

c) Full scale or prototype tests carried out in the field.

2.2 Theoretical and Semi-Theoretical Methods

2.2.1 Friction Cylinder Method

As noted by Balla (3), the friction cylinder method was the early approach to analyze the pullout capacity of anchors. The method was developed by Majer (1955). Majer assumed that the breaking-out mass of earth takes the form of a vertical cylinder, with the same cross section as the plan projection of the anchor plate. To calculate the anchor capacity, the shear resistance along the surface of this cylinder is added to the dead weight of earth, Figure 1a.

2.2.2 Soil Cone Method

The soil cone method was devised by Mors (1957). According to Balla (3), the failure surface is assumed to enclose a truncated cone of soil extending above the anchor plate with an apex angle of $(90^{o} + \Phi)$, Figure 1b. The pullout capacity of the anchor is determined by calculating the weight of the soil mass within the truncated cone.

Pullout capacities of anchors calculated using either one of the above methods do not generally agree with the results of tests conducted in field and laboratory. The disagreement arises partly because the assumed failure surfaces differ from the real one, and partly because the shearing strength of the soil is ignored in the soil cone method.

2.2.3 Balla's Method

The method presented by Balla (3), was based on observations of small scale models of anchors tested in sand. He assumed that the meridian section of the rupture surface may be represented by circular

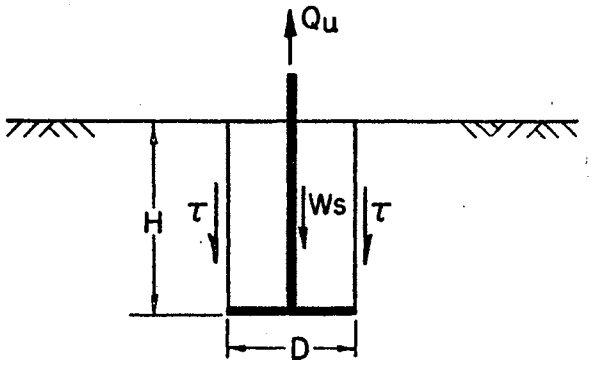

(a) FRICTION CYLINDER METHOD

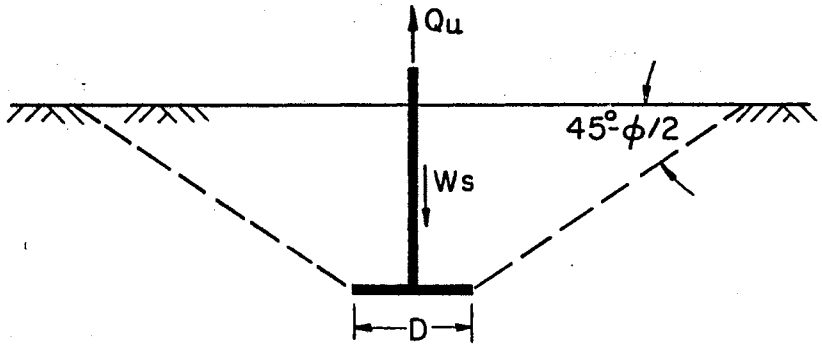

(b) SOIL CONE METHOD

Figure 1. Early Methods for Calculating Uplift Capacity

arcs, as shown in Figure 2. In this figure, it is evident that the failure surface originates at the top surface of the plate as a vertical tangent, curves outwards and intersects the ground level at an angle equal to $45 - \Phi/2$.

The ultimate resistance was considered to be composed of the dead weight of the anchor, the weight of the breaking-out soil mass, and the shearing resistance on the sliding surface. To determine the shearing resistance along the sliding surfaces, Balla used Kotter's equation. In his analysis he assumed that the state of stress was plane, in order to simplify the solution. The actual state of stress is a spatial axial-symmetric state of stress.

The theoretical value of the uplift capacity of a concrete anchor is given by Balla's expression:

$$Q_u = H^3 \cdot \gamma\{F_1(\Phi, H/D) + (c/\gamma H) \cdot F_2(\Phi, H/D) + F_3(\Phi, H/D)\} + G, \quad (2.1)$$

where

H = the depth of soil above the plate,

γ = unit weight of soil,

D = diameter of anchor plate,

c = unit cohesion of soil,

G = the product of volume of anchor and difference in unit weight of concrete and soil, and

F_1, F_2, F_3 are complex functions of Φ and H/D;

their numerical values are plotted in reference (3).

Balla's method is limited to earth anchors having relative depths, $H/D \leq 4$. The experimental results obtained from model anchors were in reasonable agreement with values computed by Equation (2.1).

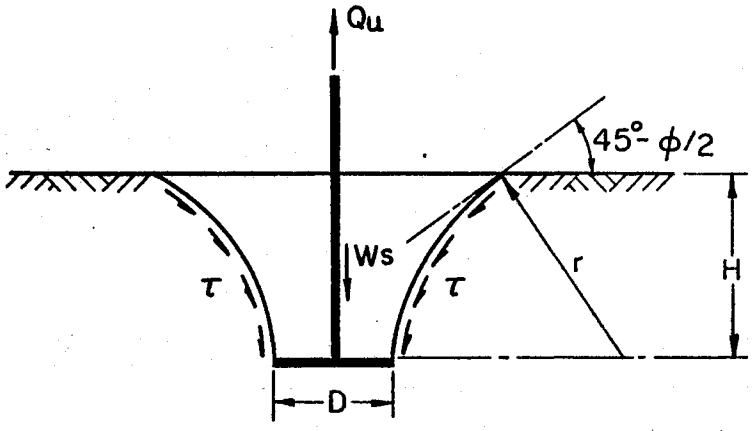

Figure 2. Balla's Method for Uplift Capacity

2.2.4 Vesic's Method

Vesic's theory (31) pertaining to cratering by explosives was adapted for a solution of the earth anchor problem by Esquivel (9). Vesic's theory was developed through studies of cratering mechanics, for the problem of expansion of a spherical cavity near the surface of a semi-infinite, homogeneous, isotropic solid.

According to Vesic, if the cavity is close enough to the soil surface, a point explosive charge will shear away the soil above a cavity of radius R_1 (Figure 3), whose value depends on the characteristics of the explosive charge. A similar approach can be applied to the case of a shallow anchor plate, by assuming the horizontal anchor plate of a radius R_1 and the pullout pressure equal to the ultimate cavity pressure q_u, Ali (1).

This axially symmetric problem has been solved by assuming that the normal and shear stress distribution and the statically correct angles along the rupture surface are equivalent to those found in the corresponding two-dimensional problem. The rupture surface was assumed to be formed by the revolution of a circular slip line about the axis of symmetry. The equilibrium of the ruptured mass would give the ultimate cavity pressure q_u in the following form:

$$q_u = c\bar{F}_c + \gamma Z\bar{F}_q \qquad (2.2)$$

where $\bar{F}_c$ and $\bar{F}_q$ are cavity breakthrough factors that were evaluated and presented in tabular form by Bhatnagar (4).

The above method was applied to analyze experimental data obtained from shallow and deep anchors tested in both cohesive and cohesionless

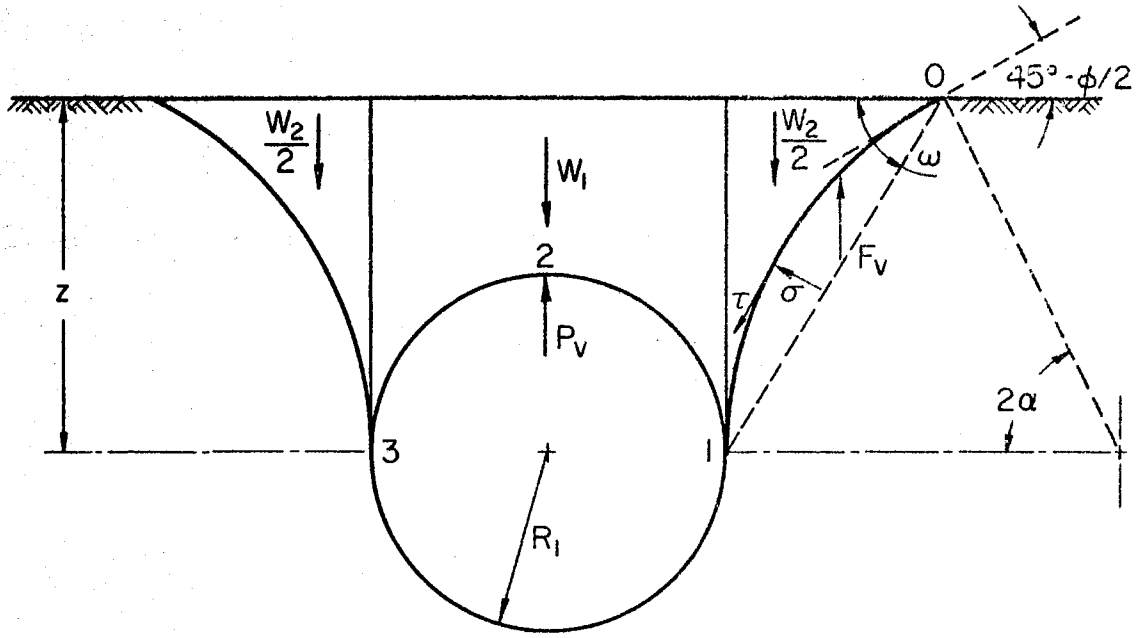

Figure 3. Expansion of a Spherical Cavity Close to the Surface (After Vesic)

soils. However, the correlation of experimental and theoretical results was not consistent (Esquivel (9) and Bhatnagar (4)).

2.2.5 Mariupol'skii's Method

Mariupol'skii (18) has outlined a method for estimating the ultimate pullout resistance of earth anchors. According to Mariupol'skii, the ultimate uplift capacity of a shallow earth anchor is determined by the dead weight of the anchor, the weight of the column of soil (abcd in Figure 4a) above the anchor plate, and the friction and cohesive forces along the external surface of the soil cylinder abcd. The friction forces increase as the soil above the anchor plate is compressed by the upward movement of the anchor. Owing to the development of tensile stresses, a separation of a certain volume of earth in the form of a cone with a curvilinear generatrix would eventually occur.

The ultimate load capacity of a shallow anchor is given by:

$$Q_u = G + \pi/4(D^2 - D_0^2)\left[\frac{\gamma H\left\{1 - \left(\frac{D_0}{D}\right)^2 + (2k \cdot H/D)\tan\Phi\right\} + 4cH/D}{1 - (D_0/D)^2 - 2nH/D}\right] \qquad (2.3)$$

where

G = weight of anchor,

k = coefficient of lateral earth pressure, and

n = parameter depending on Φ.

In the case of a deep anchor, Mariupol'skii assumed that when the anchor stresses have reached the limiting condition, the work done in displacing the anchor plate vertically through a distance, S, is equivalent to the work needed to expand a cylindrical cavity of a height, S, and diameter, D_0, to a cavity of a diameter, D, with the same height,

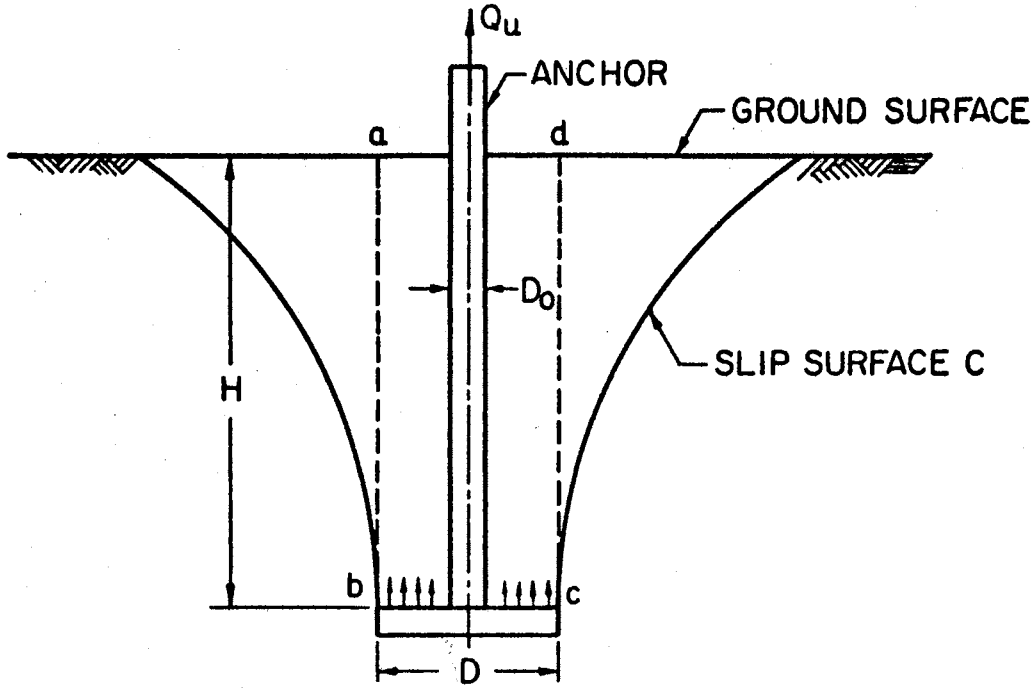

(a) SLIP SURFACE FORMED BY SHALLOW ANCHOR

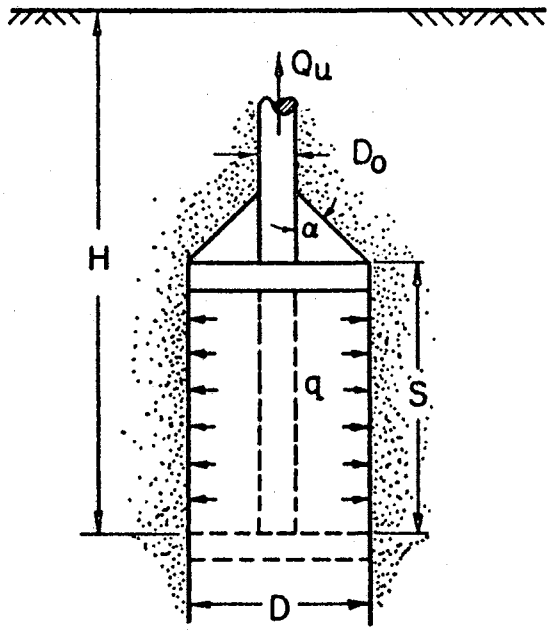

(b) ACTION OF A DEEP ANCHOR

Figure 4. Mariupol' skii's Method for Uplift Capacity

S (Figure 4b). In Mariupol'skii's analysis the capacity of a deep anchor was given by:

$$Q_u = G + \frac{\pi q(D^2 - D_o^2)}{4 - 2 \tan \Phi} + f\pi D_o l \qquad (2.4)$$

where

q = radial pressure under which the cavity expanded,

l = effective length of anchor stem = $H - (D - D_o)$, and

f = friction between anchor stem and soil.

Mariupol'skii suggested that, to determine the uplift capacity of anchors by means of Equations (2.3) and (2.4), the lower value of the two should be used. Thus, no definite criterion was set for distinguishing shallow from deep anchors.

The evaluation of parameters included in Equations (2.3) and (2.4), particularly k and q, involve tedious mathematical work.

2.2.6 Matsuo's Method

According to Matsuo (20) the failure surface is best described by a combined logarithmic spiral curve and its tangential straight line, the lower part of the sliding curve being the logarithmic spiral, and the upper part the straight line.

The combined curve should be that which yields the minimum value of the uplift capacity Q_u. This particular curve is to be selected from many curves drawn by a process of trial and error, similar to those methods used for solving retaining wall and slope stability problems.

The ultimate load capacity is given by:

$$Q_u = G + V + T \qquad (2.5)$$

where

G = weight of anchor,

V = volume of soil mass included in the sliding surface, and

T = vertical component of the resultant shearing resistance acting along the sliding surface.

Matsuo developed rather cumbersome equations and graphs to evaluate the terms included in the parameters V and T.

According to Sams (26), Matsuo concluded from model tests that his procedure was more appropriate for small H/D ratios than for the larger values associated with deep anchors.

2.2.7 Meyerhof's Method

Meyerhof (23) has formulated a semi-theoretical approach to analyze the uplift capacity of earth anchors, based on simplifying assumptions for the complex form of the actual rupture surface. The simplified failure surface that he used is a vertical cylindrical surface above the anchor plate.

The uplift capacity for shallow anchors was expressed as follows:

$$Q_u = cHD + \tfrac{1}{2}(s\pi\gamma DH^2 k_u \tan \Phi) + W \qquad (2.6)$$

where

W = weight of the lifted soil and anchor,

s = shape factor governing the passive earth pressure on a convex cylindrical wall, and

k_u = nominal uplift coefficient of earth pressure on vertical plane through footing edge.

Furthermore, Equation (2.6) was modified to yield a solution for deep anchors, by assuming the failure surface to extend vertically above the anchor plate to a height, H_t, less than the total depth of embedment, H. The values for the limiting height H_t were presented in a tabular form by Meyerhof.

The load capacity of deep anchors was given by:

$$Q_u = \pi cDH_t + \tfrac{1}{2}\{\pi s\gamma D(2H - H_t)k_u \tan \Phi + W \quad . \qquad (2.7)$$

All terms of Equation (2.7) were previously defined.

2.3 Experimental Investigations

As an adjunct to the theoretical solutions, experimental investigations are essential to determine the values of certain parameters and to help in explaining behavior that is difficult to account for theoretically. Experimental data are also used to verify analytical findings.

Experimental investigations reported in this section are only those conducted to describe and elaborate on the behavior of the earth anchor.

2.3.1 Baker and Kondner's Experimental and Field Tests

Numerous tests were conducted by Baker and Kondner (2) on model anchors, made of flat, circular steel plates ¼ inch thick, with diameters of 1, 1.5, 2, and 3 inches. The anchors were embedded at depths ranging from 3 to 21 inches in air-dried uniform silica sand with a friction angle of $\Phi = 42^{o}$, and an average unit weight $\gamma = 112$ pcf. The results of this investigation are summarized in Chapter VII.

The experimental data of this investigation were used to define the limits between shallow and deep anchors. For shallow anchors, where a definite failure circle was observed on the surface of the sand, the relative depth was found to be ($H/D < 6$). For deep anchors where ($H/D > 6$), no rise or at most a very slight rise of the sand surface was observed in the vicinity of the anchor rod, at failure.

Baker and Kondner plotted the dimensionless parameters $Q_u/D^3\gamma$ versus H/D, to show that the plot was insensitive to changes in the parameter D/t, where D is diameter of the anchor plate and t is thickness of the plate, for the value $H/D < 6$.

The ultimate load capacity for shallow anchors was expressed by:

$$Q_u = C_1 HD^2\gamma + C_2 H\gamma \tag{2.8}$$

and for deep anchors by:

$$Q_u = 170D^3\gamma + C_3 D^2 t\gamma + C_4 HDt\gamma \tag{2.9}$$

where C_1, C_2, C_3, and C_4 are empirical constants that depend on the internal angle of friction and the relative density of the cohesionless material, D_r.

According to Baker and Kondner, Equations (2.8) and (2.9) are not applicable to anchors with values of $D/t < 1$, since such anchors act primarily as friction piles.

The application of Equations (2.8) and (2.9) using Baker and Kondner's constants would be limited to a particular type of soil, since the values of C_1, C_2, C_3, and C_4 need to be established empirically for each separate set of values for Φ and D_r.

2.3.2 Duke University Model Testing

As reported by Esquivel (9), Bhatnagar (4), and Ali (1), model tests were conducted at Duke University on vertical anchors embedded in sand, silty clay and soft bentonite clay, respectively. The loading apparatus used to extract the anchor was of the stress controlled type. Some of the experimental data were tabulated and compared with the solution developed in this study in Chapter VII. It may be noted here that most of the experimental results were within a tolerable range of discrepancy, for anchors embedded at shallow depths (Bhatnagar (4)).

Esquivel (9), pointed out that no satisfactory theory is available for determining the pullout resistance of earth anchors in cohesionless soils.

2.3.3 Colorado State University Model Testing

An extensive testing program was conducted by Sams (26) to determine how anchor stability problems related to cohesive soils might be modeled quantitatively in the laboratory. Ottawa sand was used in the tests, with cohesion being simulated artificially through vacuum confinement. The anchor system was made up of a circular bevel-edged plate connected to a shaft through its center. The bevel-edged plate was used to simulate a plate without thickness in order to eliminate the effect of side friction. After the shaft was placed vertically in position at the required depth, sand was poured around the sides of the container in a random manner sloping down at an angle equal to the angle of repose to a point near the anchor plate. This arrangement produced a conical shaped cavity with the anchor plate at the apex.

According to Sams, the above method of placing the soil leaves only the volume of possible influence to be filled with soil in such a manner that the strength properties of the soil are predictable. The remaining conical cavity was filled by adopting a more orderly and uniform procedure.

This method of placing the soil was quite different from those adopted by other investigators, (2) and (9), and probably produces conditions that differ considerably from those that would exist in field situations. Other investigators have placed the soil in uniform layers to avoid imposing an artificial condition that could control the location or shape of the slip surface. A brief discussion is given in Chapter V concerning the effect produced by the shape of the anchor plate.

CHAPTER III

ANALYTICAL APPROACH

3.1 Failure Mechanism

In order to analyze the stability of earth anchors, one should consider the physical behavior of the anchor-soil system during the loading process. Loading of an anchor to its ultimate carrying capacity may be achieved by using a loading system that controls either the rate of stress increase or the rate of strain. The latter system was adopted throughout this investigation which allowed the measurement of the accumulated load imposed on the anchor plate as the anchor was progressively displaced at a constant rate of strain in the vertical direction.

Prior to any displacement, the anchor and the soil surrounding it are at rest. As soon as displacement commences, the resultant force, Q, required to displace the anchor begins to take on a value. The magnitude of Q depends on the anchor weight, the shearing resistance, and weight of the soil that is being displaced. The anchor plate transmits to the overlying soil the displacement force produced by pulling on the vertical anchor rod. Continuing displacement causes internal adjustments in the soil mass under the influence of the overburden pressure until the anchor overcomes the inter-granular and cohesive forces (depending on the type of soil). Those forces resist the displacement and are considered to act along a surface of least

resistance within the mass of soil. Further displacement does not produce an appreciable increase of load; on the contrary, the load may even decrease.

Progressive deformation of the soil as the anchor plate moves upward finally produces a curvilinear rupture surface in the soil mass. In the processes leading to rupture the soil mass has to undergo the following stages of deformation:

1) Prior to displacement of the anchor the soil is in elastic equilibrium. When the anchor begins to be displaced, compression of the overlying soil may take place, approximately according to Hooke's law, with some densification of the soil.

2) As displacement continues, vertical deformation of the soil will be accompanied by some lateral displacement. This stage is regarded as the beginning of rupture of the soil. An indication of the incipient rupture is the bulging which occurs at the soil surface.

3) With continued displacement of the anchor, the shearing resistance of the soil becomes fully mobilized, and the soil fails along some rupture surface. At this stage, plastic equilibrium of the soil and anchor system has been attained.

In earth anchor problems, when no surface surcharge is present, the major principal stress acts horizontally at the ground level. At the line where ground and rupture surfaces intersect, the tangent to the failure surface makes an angle $\alpha_o = 45 - \Phi/2$ with the horizontal surface of soil (Parcher and Means (22, 25)). It is assumed that the sliding surface along which failure occurs takes the form of logarithmic

spiral, that the curve originates with a vertical tangent at the edge of the anchor plate, and that it curves outwardly to intersect the ground level at a statically correct angle α_0.

As pointed out by other investigators; e.g., Baker and Kondner (2), Meyerhof (23), and Balla (3), the above failure mechanism has been observed in anchors embedded at small ratios of relative depths ($H/D < 6$), and it has been observed that the surface of rupture extends to the soil surface.

For values ($H/D > 6$), the compressibility and deformation, and possibly the flow of soil around the anchor plate have usually prevented the rupture surface from propagating to the soil surface. Nevertheless, it has been found that a condition of failure is attained, when deformation continues without an increase in load.

It may be concluded that the dual modes of failure pertaining to anchors are governed by: (1) general shear failure in the case of shallow anchors, and (2) local shear failure, or punching through the overlying soil, in the case of deep anchors (Terzaghi (28)).

3.2 Load-Displacement Characteristics

A typical load-displacement curve obtained from a representative test is shown in Figure 5, which indicates the behavioral characteristics of soil and anchor interaction. This curve is basically a stress-strain relationship. The initial part of the curve (a-b) is almost a straight line, which represents the linear elastic properties of the soil, after which the soil starts to yield. The rate of load increase tends to decrease nonlinearly to point (c). At point (c) the curve is at its flattest slope, being parallel to the horizontal axis,

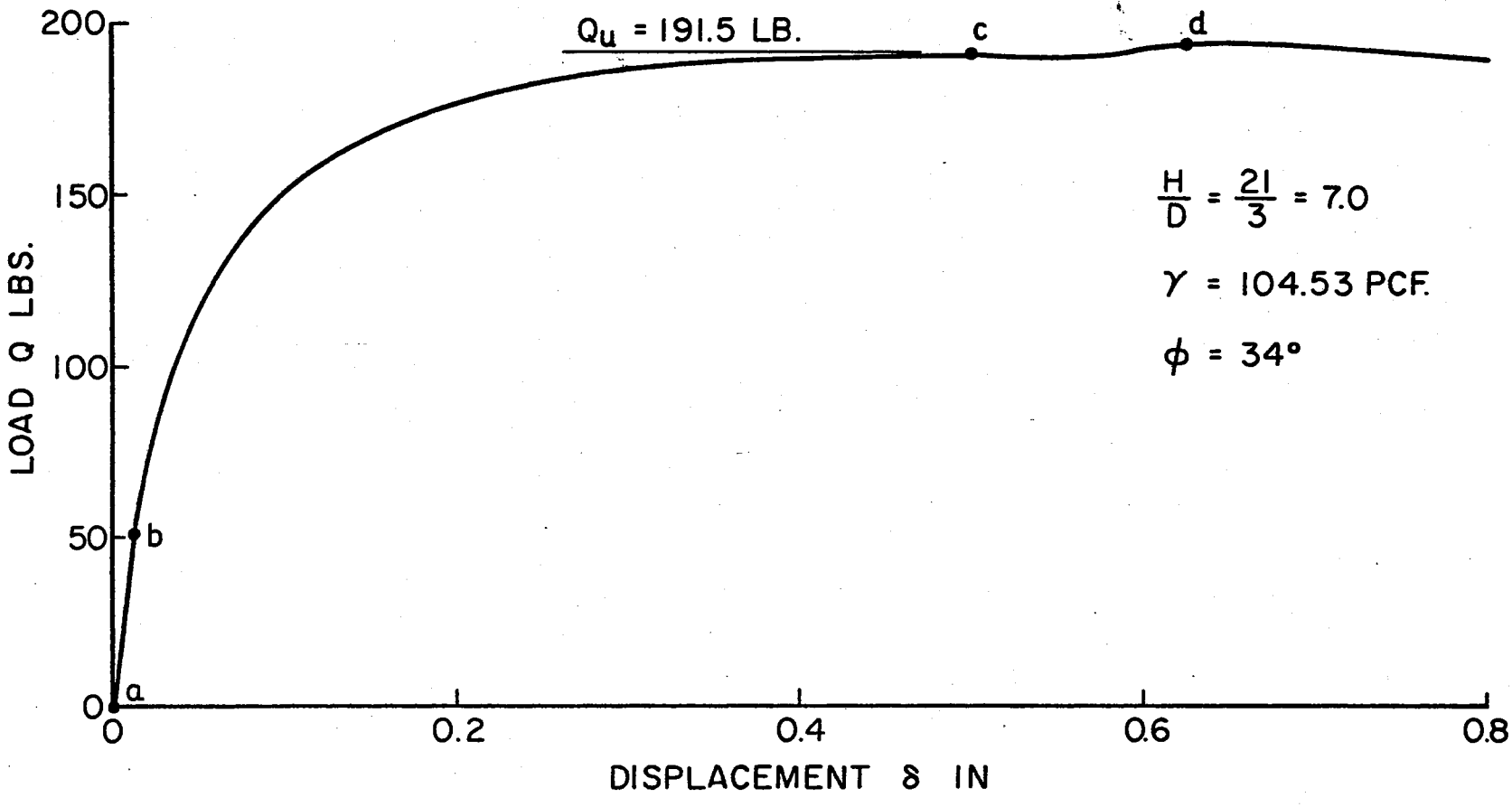

Figure 5. Load-Displacement Characteristic of Earth Anchors

and the ordinate at this point represents the ultimate value of the anchor load. Yong and Warkentin (33) have thoroughly discussed the characteristic soil behavior leading to the state represented at point (c).

The slight hump in the curve at point (d) is characteristic of anchors having $H/D \geq 6.0$, buried in dry sand. The occurrence of such a hump is believed to be due to arching effects of the soil above the region of local failure. At this stage the soil in the vicinity of the anchor plate starts to flow around the plate into the cavity created by displacing the anchor upward. At the same time the shearing stress reaches the limiting value of the shearing strength of the soil.

3.3 Formulation of Solution

Factors governing the stability of earth anchors are the weight and dimensions of the anchor, the shearing resistance of the soil along an assumed sliding surface, and the dead weight of the displaced soil bounded by the sliding surface. Mathematical statements of the latter two components require rather intricate expressions; but these will be kept as simple as possible, consistent with the desire to provide an adequate solution.

For the purpose of analysis, the soil medium is assumed to be homogeneous, isotropic, and of semi-infinite extent. Kotter's differential equation will be utilized to evaluate the distribution and magnitude of the shearing stress, τ. According to Nadai (23) and Brinch Hansen (5), this differential equation lends itself to an evaluation of stresses acting along the failure surface only if the shape of the failure surface is known. It is quite clear that if the

failure surface is incorrectly chosen, the results will be wrong; e.g., see Hansen's (6) reference to the work of Coenen.

Jumikis (14) listed a number of conditions and properties pertaining to Kotter's equation. The following modifications of those conditions are proposed in connection with the analysis of earth anchors:

1) Kotter's equation deals with the critical state of stress, in two dimensions of a semi-infinite mass, bounded by a horizontal surface plane.
2) It yields the distribution of reactive, compressive and shear stresses along the slip surface.
3) It is based purely on theory and the laws of mechanics, and its derivation is scientifically plausible.
4) The original equation was derived for cohesionless soils, and Jaky showed that it is also valid for soils with cohesion (12).
5) It has no restriction as to the form of the slip surface, and may be fitted by either the true form if known, or by a form determined experimentally.
6) The stress components (σ_α, σ_r, and $\tau_{r\alpha}$) are functions of the polar coordinates (r and α).
7) There are two unknowns in Kotter's equation; the shear stress and the form of the rupture surface.

Kotter's differential equation was developed by considering the equilibrium of an infinitesimal element (ABCD) of earth, using the polar coordinates (r, α) as shown in Figure 6.

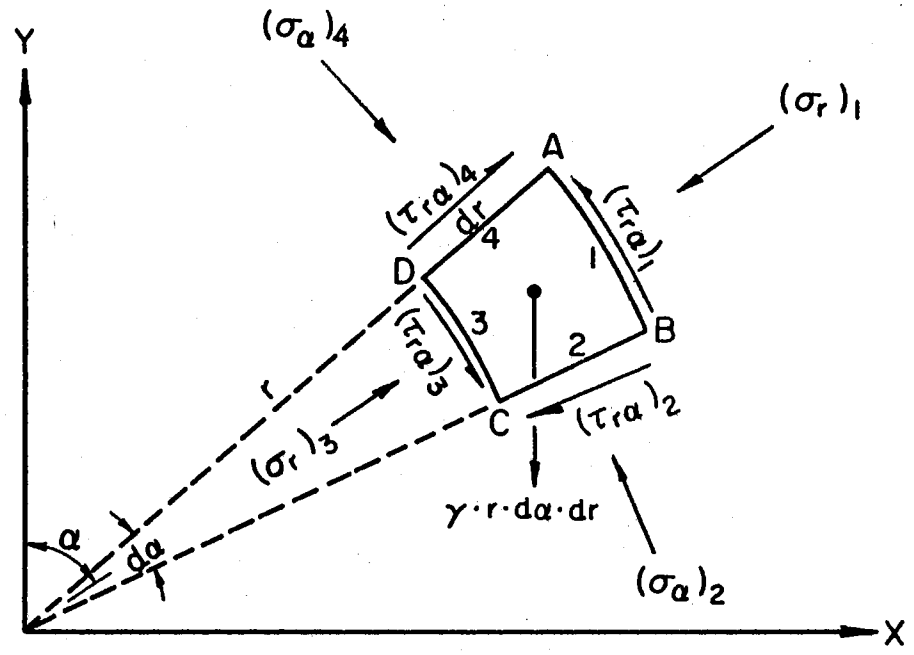

Figure 6. Equilibrium of Earth Infinitesimal Element

Including the rate of change of both σ and τ with respect to r and α, the following will hold true:

Normal Stresses:

$$(\sigma_r)_3 = \sigma_r$$

$$(\sigma_r)_1 = \sigma_r + \frac{\partial \sigma_r}{\partial r} \cdot dr$$

$$(\sigma_\alpha)_4 = \sigma_\alpha$$

$$(\sigma_\alpha)_2 = \sigma_\alpha + \frac{\partial \sigma_\alpha}{\partial \alpha} \cdot d\alpha$$

Shear Stresses:

$$(\tau_{r\alpha})_3 = \tau_{r\alpha}$$

$$(\tau_{r\alpha})_1 = \tau_{r\alpha} + \frac{\partial \tau_{r\alpha}}{\partial r} \cdot dr$$

$$(\tau_{r\alpha})_4 = \tau_{r\alpha}$$

$$(\tau_{r\alpha})_2 = \tau_{r\alpha} + \frac{\partial \tau_{r\alpha}}{\partial \alpha} \cdot d\alpha \ .$$

In accordance with Timoshenko (29), the normal stress component in the radial direction is denoted by σ_r, the normal component in the circumferential direction by σ_α, and the shearing stress component by $\tau_{r\alpha}$.

If forces, including the body force, are summed in the radial and tangential directions, taking inward and downward forces as positive, the following equilibrium equations are obtained:

Σ Radial Forces = 0

$$\{(\sigma_r + \frac{\partial \sigma_r}{\partial r} dr)\cdot(r + dr) \cdot d\alpha - (\sigma_r \cdot r \cdot d\alpha)\} - \{\sigma_\alpha \cdot dr + (\sigma_\alpha + \frac{\partial \sigma_\alpha}{\partial \alpha} d\alpha)\cdot dr\}$$
$$\cdot \sin \frac{d\alpha}{2} + \{(\tau_{r\alpha} + \frac{\partial \tau_{r\alpha}}{\partial \alpha} d\alpha) - (\tau_{r\alpha})\} \cdot dr \cdot \cos \frac{d\alpha}{2} + \gamma \cdot r \cdot dr \cdot d\alpha$$
$$\cdot \cos \alpha = 0 \qquad (3.1)$$

Σ Tangential Forces = 0

$$\{\sigma_\alpha - (\sigma_\alpha + \frac{\partial \sigma_\alpha}{\partial \alpha} d\alpha)\} dr \cdot \cos \frac{d\alpha}{2} - \left[\{(\tau_{r\alpha} + \frac{\partial \tau_{r\alpha}}{\partial r} dr) \cdot (dr d\alpha + r d\alpha)\} - (\tau_{r\alpha} \cdot r d\alpha)\right]$$
$$+ \{(\tau_{r\alpha} + \frac{\partial \tau_{r\alpha}}{\partial \alpha} d\alpha) dr - \tau_{r\alpha} dr\} \sin \frac{d\alpha}{2} + \gamma \cdot r \cdot dr \cdot d\alpha \cdot \sin \alpha = 0 \,. \qquad (3.2)$$

Collecting the common terms and using small angle rotation, then dividing by $(d\alpha \cdot dr)$. Equations (3.1) and (3.2) take the final forms:

$$\sigma_r + \frac{\partial \sigma_r}{\partial r} r - \sigma_\alpha + \frac{\partial \tau_{r\alpha}}{\partial \alpha} + \gamma \cdot r \cdot \cos \alpha = 0 \qquad (3.1a)$$

$$- \frac{\partial \tau_{r\alpha}}{\partial r} r - \frac{\partial \sigma_\alpha}{\partial \alpha} - 2\tau_{r\alpha} + \gamma \cdot r \cdot \sin \alpha = 0 \,. \qquad (3.2a)$$

Applying Coulomb's law to σ_r and $\tau_{r\alpha}$ outside the rupture surface

$$\tau_{r\alpha} - \sigma_r \tan \Phi \leq c \,. \qquad (3.3)$$

Differentiating Equation (3.3) with respect to (α and r)

$$\frac{\partial}{\partial r} (\tau_{r\alpha} - \sigma_r \tan \Phi) = 0 \qquad (3.4)$$

$$\frac{\partial}{\partial \alpha} (\tau_{r\alpha} - \sigma_r \tan \Phi) = 0 \,. \qquad (3.5)$$

For the stresses in the rupture surface, see Mohr's Circle, Figure 7.

$$\sigma_\alpha - \sigma_r = 2\tau_{r\alpha} \tan \Phi \, . \tag{3.6}$$

Differentiation of Equation (3.6) yields:

$$\frac{\partial \sigma_\alpha}{\partial \alpha} - \frac{\partial \sigma_r}{\partial \alpha} = 2 \frac{\partial \tau_{r\alpha}}{\partial \alpha} \tan \Phi \, . \tag{3.7}$$

Now multiplying Equation (3.1a) by tan Φ, then subtracting it from Equation (3.2a) and using the result of Equation (3.4)

$$\frac{\partial \sigma_\alpha}{\partial \alpha} - \frac{\partial \tau_{r\alpha}}{\partial \alpha} \tan \Phi + (\sigma_\alpha - \sigma_r) \tan \Phi - \gamma \cdot r \, (\tan \Phi \cos \alpha + \sin \alpha) = 0 \, . \tag{3.8}$$

Equations (3.4), (3.6), and (3.7) are used to eliminate σ_r and σ_α from Equation (3.8), for simplicity omitting subscripts $r\alpha$ on τ; i.e., $\tau_{r\alpha} = \tau$. Equation (3.8) takes the form:

$$\frac{\partial \tau}{\partial \alpha} + 2\tau \tan \Phi - \gamma r \sin \Phi \sin (\alpha + \Phi) = 0 \, . \tag{3.9}$$

Equation (3.9) is Kotter's differential equation which is valid for the rupture line in cohesive and cohesionless soils. It also has a general application pertaining to the curvature of the slip surface. For circular lines:

$$r = \frac{ds}{d\alpha} = \text{constant} \, . \tag{3.10}$$

Balla (3) and Brinch Hansen (5, 6) outline the analytical solution for circular rupture lines:

$$\tau = K \cdot e^{-2\alpha \cdot \tan \Phi} - [\gamma \cdot r \cdot \sin \Phi \cdot \cos \Psi \cos(\alpha_o + \Phi + \Psi)] \tag{3.11}$$

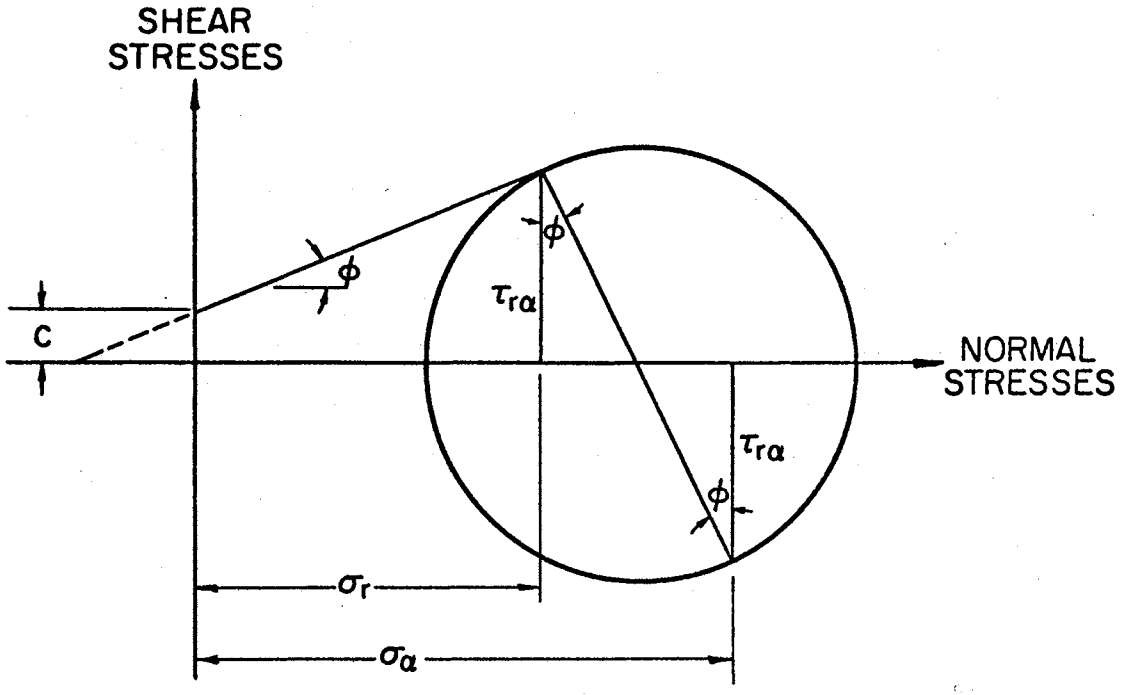

Figure 7. Mohr's Circle for Normal and Shear Stresses

where

Ψ = Arc tan 2 (tan Φ), and

$K = e^{2\alpha_0 \tan \Phi}[\tau_0 + \gamma \cdot r \sin \Phi \cos \Psi \cos(\alpha_0 + \Phi + \Psi)]$.

K is a constant stress found by substituting the following values for the boundary values of α_0 and τ_0 (the shear stress on the rupture surface) at the ground surface:

$$\alpha_0 = \frac{\pi}{4} - \frac{\Phi}{2} \tag{3.12}$$

$$\tau = c(1 + \sin \Phi) \text{ .} \tag{3.13}$$

Throughout this work, the rupture surface curve is assumed to follow a logarithmic spiral curve, the radius of which is given by:

$$r = r_s = \frac{ds}{d\alpha} = 1/\{r_0 \cdot \sqrt{(1 + \tan^2 \Phi \cdot e^{\omega \tan \Phi})}\} \text{ .} \tag{3.14}$$

Jumikis (14) states that use of the logarithmic spiral rupture surface yields a rigorous mathematical solution when applied to stability problems.

3.4 Development of the Logarithmic Spiral Curve

The curved failure surface is approximated by a logarithmic spiral, starting vertically tangential to the edge of the horizontal anchor plate at point (d), Figure 8, and curving outward to point (b) where it intersects the horizontal soil surface at an angle α_0. The particular spiral used in this investigation has the relationship:

$$R_\omega = R_0 e^{\omega \tan \Phi} \tag{3.15}$$

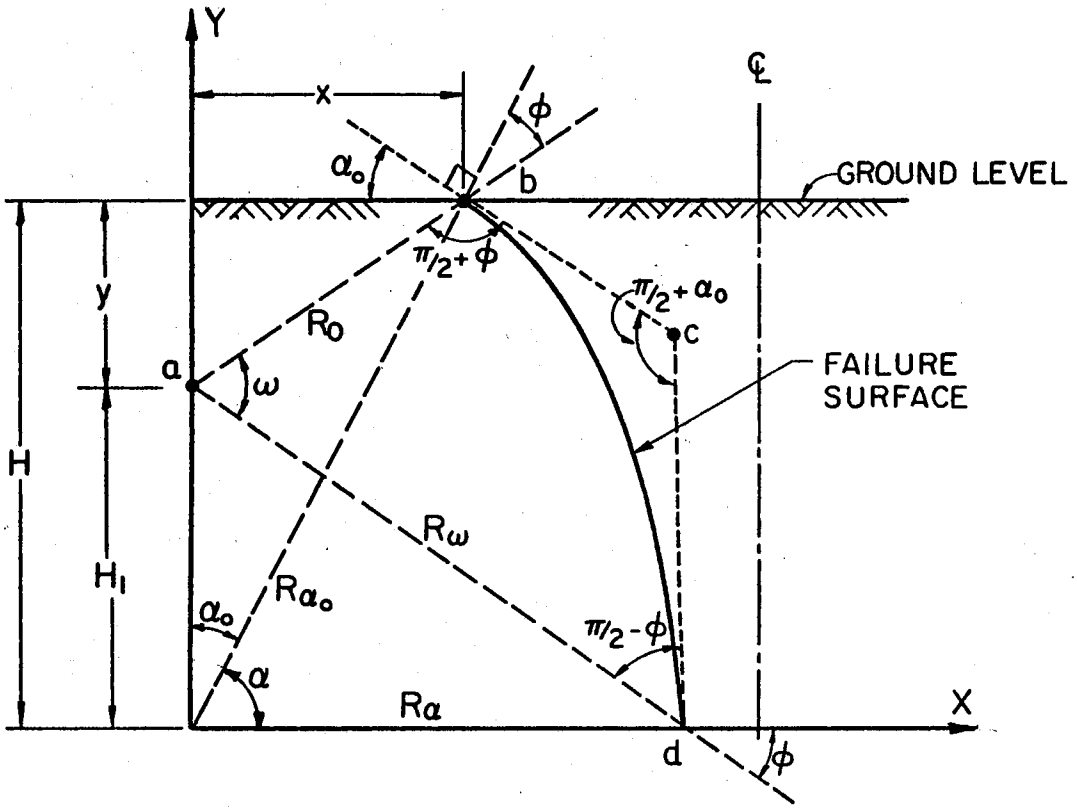

Figure 8. Coordinations of Logarithmic Spiral Curve

in which

R_ω = radius of spiral,

R_o = starting radius (for $\omega = 0$),

e = base of natural logarithms,

ω = polar angle between R_o and R_ω, and

Φ = angle of internal friction of soil.

As noted by Jumikis (15), the logarithmic spiral is particularly advantageous in analytical solutions because every radius, R, forms the angle Φ with a normal to the curve. Since, for impending slip, the full frictional resistance is mobilized, the resultant of the normal frictional stresses at each point acts along a radius of the spiral.

To construct any spiral curve the polar angle, ω, and one of the subtending radii vectors (R_o or R_ω) should be known. The angle, ω, may be found as a function of Φ or α_o by considering the summation of the internal angles in polygon abcd, Figure 8.

$$\Sigma \text{ internal angles} = 2\pi$$

Hence,

$$(\pi/2 + \Phi) + (\pi/2 - \Phi) + (\pi/2 + \alpha_o) + \omega = 2\pi$$

from which

$$\omega = \pi/2 - \alpha_o \quad . \tag{3.16}$$

The pole of the spiral is to be located along the "Y" axis at a horizontal distance, x, from the point where the spiral intersects the surface and at distance, y, from the ground surface as follows:

$$x = H \cdot \tan \alpha_o \tag{3.17}$$

$$y = R_o \cdot \sin(\pi/2 - \alpha_o - \Phi) \quad . \tag{3.18}$$

The initial radius of the spiral is given by:

$$R_0 = (R_{\alpha 0} \cdot \sin \alpha_0)/\cos(\pi/2 - \alpha_0 - \Phi) \qquad (3.19)$$

and the final radius R_w found from Equation (3.15) is:

$$R_w = \{(R_{\alpha 0} \cdot \sin \alpha_0)/\cos(\pi/2 - \alpha_0 - \Phi)\}e^{w \tan \Phi} . \qquad (3.20)$$

The curve which defines the failure surface can now be developed by incrementing angle α_0 to reach the value of angle α, which is equal to $\left(\frac{\pi}{4}\right) + \left(\frac{\Phi}{2}\right)$. For each increment added to α_0, there corresponds a value for R_w. Performance of the computations by means of a high-speed computer permits numerous points on the curve to be defined as a function of the polar coordinates, R and α.

3.5 Numerical Analysis and Computer Solution

To solve Equation (3.9), a computer program was developed to determine the magnitudes of the shear stress, τ, at various points along the failure surface. This was accomplished by using the Runge Kutta technique as outlined by Henrici (11). Vertical components of the shearing stresses were then used to calculate the anchor pull resistance.

The other principal component of anchor pull resistance, the weight of the breaking-out mass of soil, was determined by utilizing a numerical integration using Simpson's Rule (McCracken (21)).

The input parameters in the program are the angle of internal friction Φ, unit weight of soil γ, depth of anchor H, diameter of anchor D, diameter of anchor shaft D_0, plate thickness t, number of

the finite incremented parts of angle α, and the unit weight of the anchor material. Listing of the above program is provided in Appendix A. The calculations were made on the Oklahoma State University IBM Model 360/50 Computer.

CHAPTER IV

EXPERIMENTAL INVESTIGATIONS AND RESULTS

4.1 Properties of the Material Used in Testing

All tests related to this study were conducted on a medium silica sand (Ottawa sand). The sand was sieved to determine the grain size distribution (Figure 9). The gradation curve indicates that the material is uniform, having a uniformity coefficient of 1.74. Microscopic examination revealed that the grains are sub-angular (with a rather smooth surface texture) quartz particles.

The shear strength of the sand in the dry state was determined by standard triaxial tests. Samples were prepared at density of about 104.0 lb./cu.ft., and triaxial cell pressures were varied from 1.5 to 6.0 kg./sq.cm. The angle of internal friction determined from the graphical shear strength envelope was found to be 34^{o} with no intercept on the shear stress axis. Other tests were made using a direct shear machine, shown in Figure 10. The sand was tested in a dry state as well as in a fully saturated state, with the following results:

State of Sand	Density pcf.	Φ^{o}	e	w%
Dry (Hand-packed)	105.3	35.5	0.57	0.0
Saturated (Vibrated)	130.7	40.0	0.464	17.5

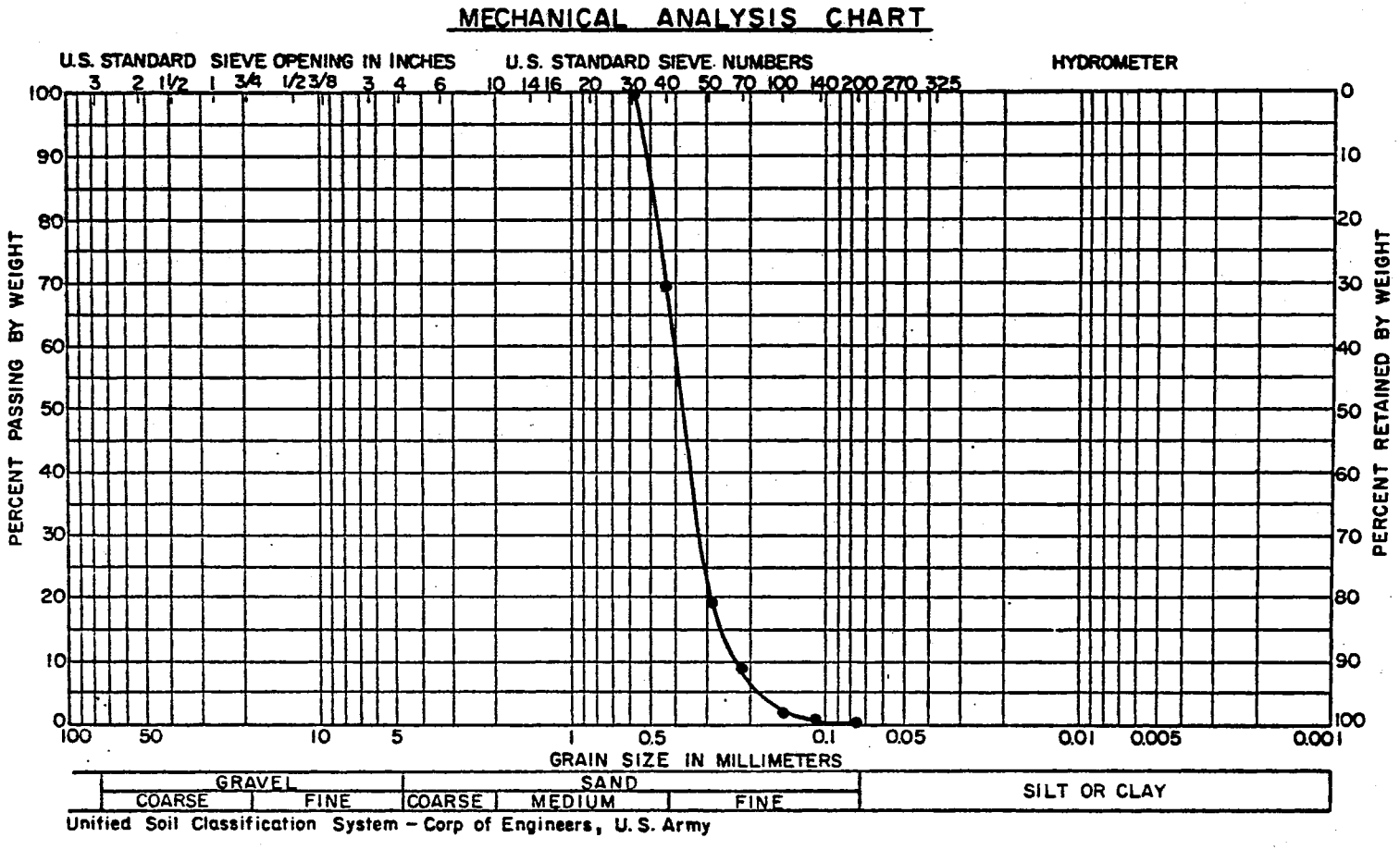

Uniformity Coef.

$$U = \frac{d_{60}}{d_{10}} = \frac{0.4}{0.23} = 1.74 < 5.0 \text{ indicates sand is uniform.}$$

Figure 9. Gradation Curve for the Ottawa Sand

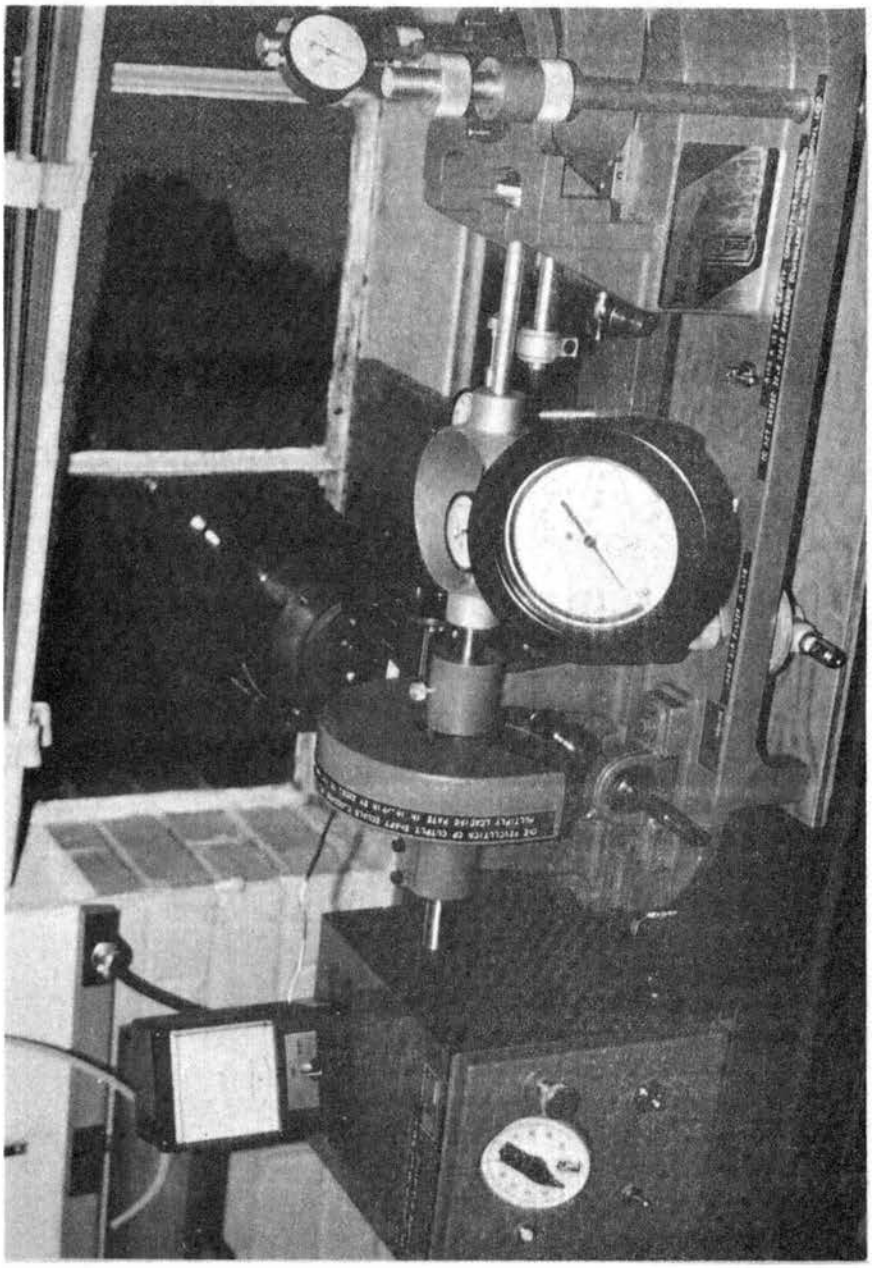

Figure 10. Direct Shear Machine

The angles of internal friction were measured from Figure 11. The values of Φ used throughout this study were 34^{o} for the dry sand as found from the triaxial test for the corresponding density of 104.0 lb./cu.ft.

4.2 Experimental Procedure and Apparatus

The testing program adopted in this investigation consisted of carrying out numerous tests on anchors having plate diameters of 2.0, 3.0, and 3.5 inches, embedded at different depths. The maximum depth used was limited to 29.25 inches by the dimension of the container. Details of the attainable relative depths corresponding to each plate diameter are given in Section 4.3. A consistent procedure was followed to eliminate a variety of possible experimental errors. The procedure can be outlined as follows.

The test box used for all tests was a fabricated lucite container, 2 ft. X 2 ft. in section and 2½ ft. deep, mounted on a movable steel frame, as shown in Figure 12. External stiffeners were added to provide more rigidity. The bottom of the box was filled with sand to the desired depth for the bottom surface of the anchor plate, and the surface was leveled and marked on the lucite walls. The anchor plate, attached to its stem, was then set on the center of this surface. The remainder of the sand was poured from a reasonably constant height of 2.0 feet to form a layer of 2.0 inches in thickness. After each layer was poured, the sand surface was again leveled by means of wooden trowels. This method of placing the sand was continued until the container was filled.

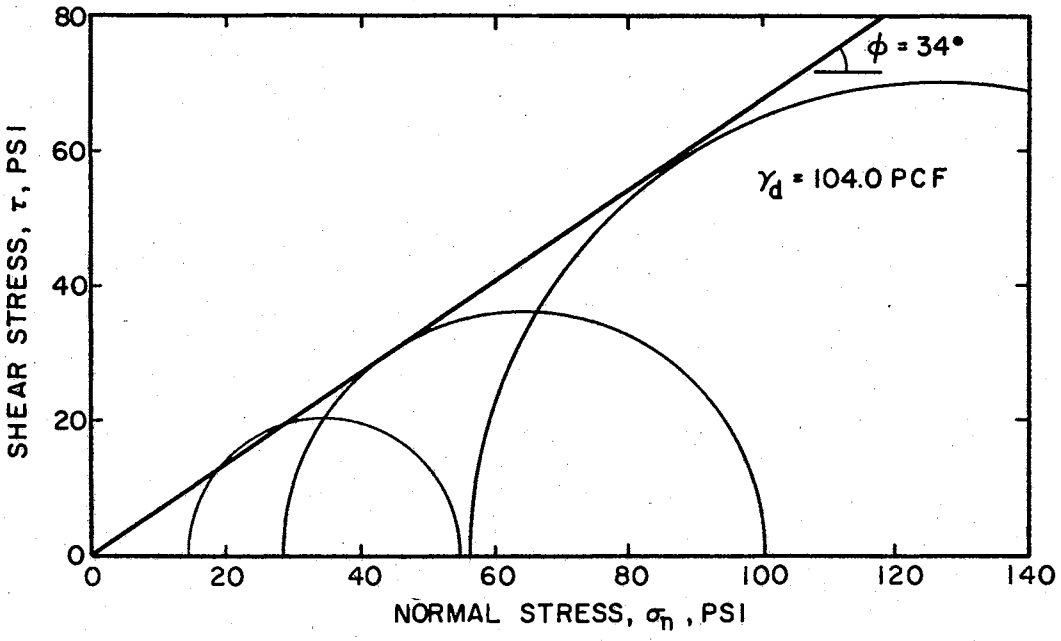

(a) TRIAXIAL TEST RESULTS

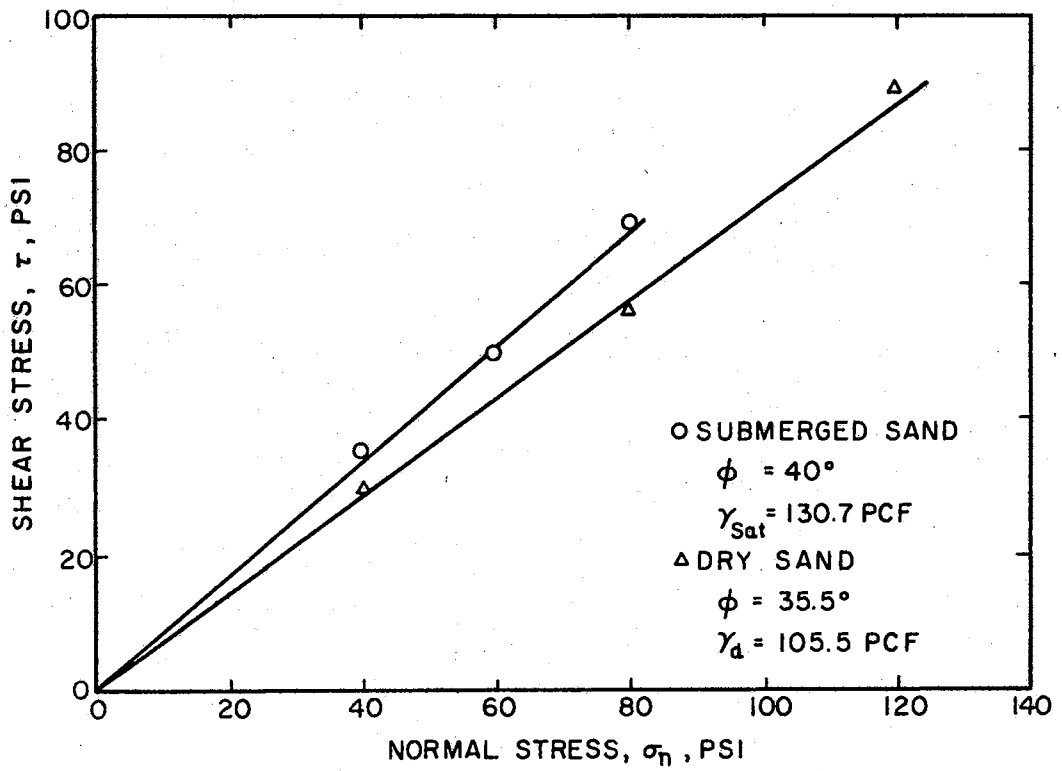

(b) DIRECT SHEAR TEST

Figure 11. Strength Envelopes for Ottawa Sand

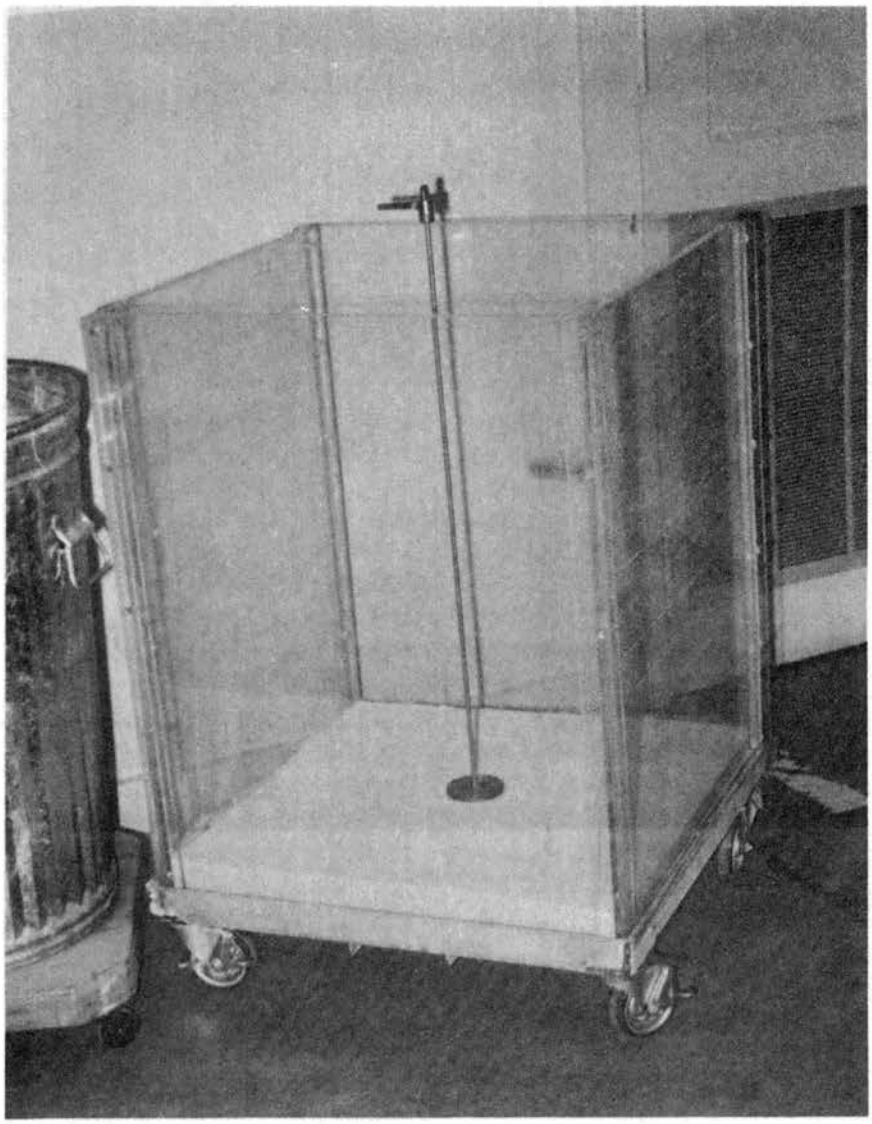

Figure 12. Positioning of Anchor in Dry Sand

The container was then positioned under the loading frame, as shown in Figure 13. After all necessary connections between the anchor shaft and the loading device had been made, as illustrated in Figure 14, the test was started by switching on an electric motor which drives a jack through a variable gear drive as shown in Figure 15. The rate of deformation could be accurately controlled by means of micrometer adjustment located on the drive. This was preset at a rate of 0.005 in./min. throughout the testing program. During the early stages of testing a dial gauge was set to check the rate of deformation. The anchor pull was transmitted through a BLH universal type load cell between the jacking device and the anchor rod. The load cell was connected to a potentiometric strip chart recorder, which was initially set to read zero load after connecting the anchor to the loading system and before commencing any displacement. The load cell and the recorder were calibrated prior to testing. The chart in the recorder was rolled at a constant speed of 6 in./hr. throughout the test. The curve produced by the recorder represents a plot of the load transmitted to the anchor versus time. Since the rate of displacement and the speed of the recorder were known, the time abscissa may be interpreted in terms of the amount of displacement of the anchor corresponding to a specified magnitude of load. In interpreting the results of these tests, failure is assumed to have occurred when the peak load is passed (Figure 5). The ultimate load capacity and the corresponding displacement of the anchor can be determined from those curves. The density of the sand was calculated for each test, using the known volume of the container and the weight of sand used. The average value of the density of the dry sand was about 104.0 lb./cu.ft.

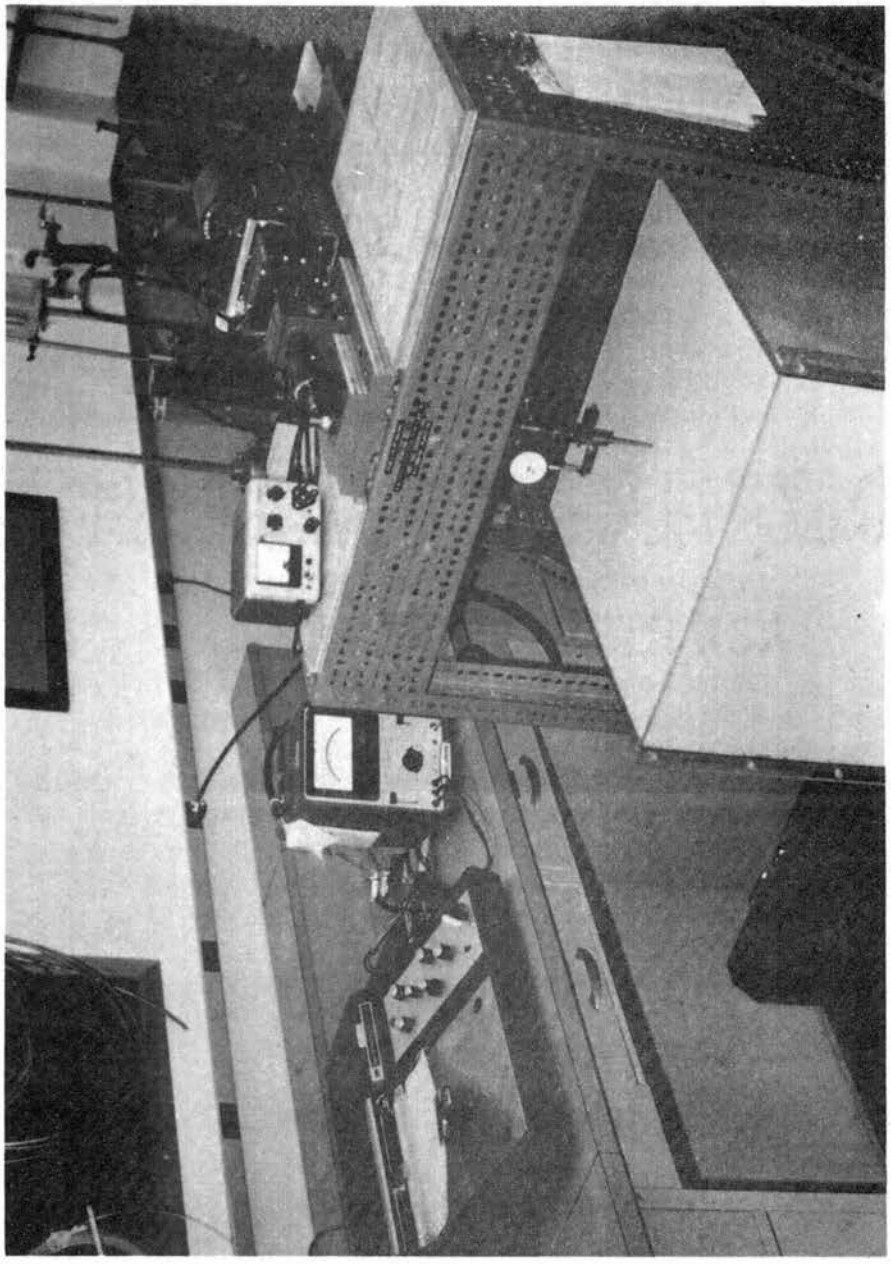

Figure 13. Positioning of Sand Container Under Loading Frame

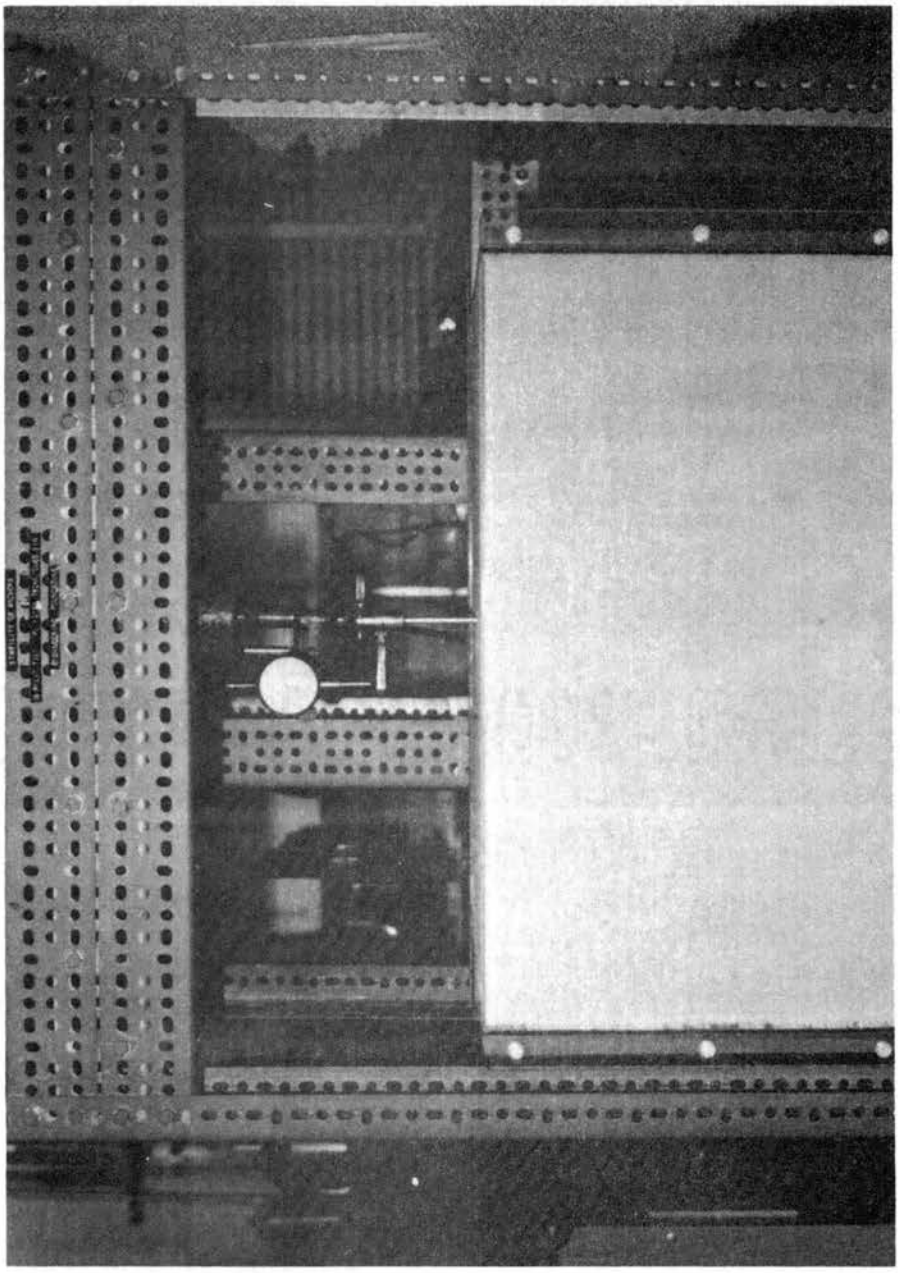

Figure 14. Final Experimental Setup

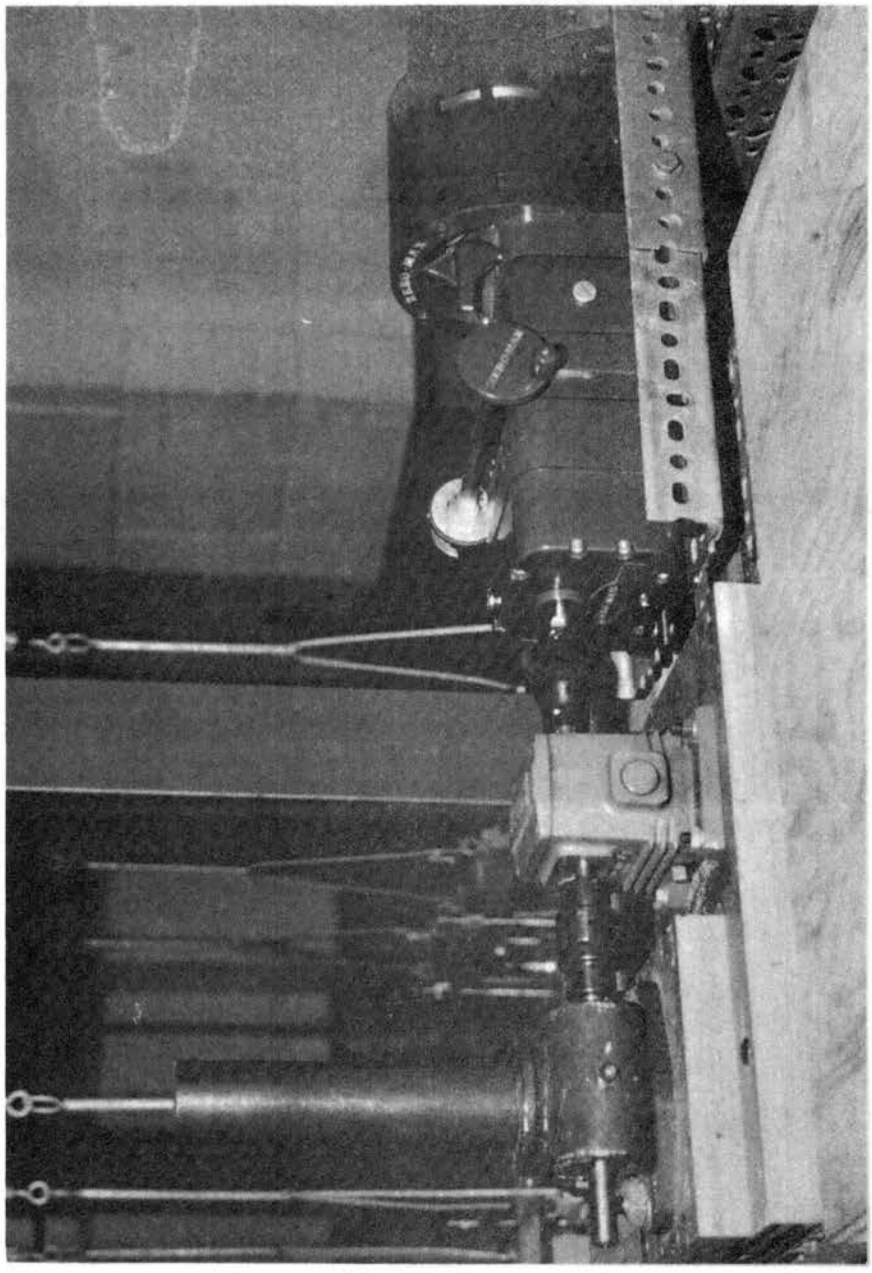

Figure 15. Loading Device

4.3 Testing of Anchors Embedded in Dry Sand

The first set of tests was performed on anchors in dry sand. Those tests employed three sizes of anchor plates (2.0, 3.0, and 3.5 inches in diameter) having a thickness of 3/8 inch and depths of embedments as follows:

Diameter D in.	Depth H in.	Relative Depth H/D
2.0	8.0 to 28.00	4.0 to 14.00
3.0	6.0 to 29.25	2.0 to 9.75
3.5	8.0 to 28.00	2.29 to 8.00

Although the relative displacement between the anchor and the surface of the sand was not measured, it was observed that there was some differential movement. Also, bulging of the surface was noticed. The highest point of the surface was in the vicinity of the shaft, and the bulge vanished at a distance of about four times the plate radius from the centerline of the shaft. This phenomenon was evident only for relative depths of ($H/D \leq 4.0$); for higher values of H/D the surface of the soil did not change during the test. This particular characteristic has been observed by others (2, 9, 20, and 23). The most probable explanation for this behavior is that the ultimate load of shallow anchors corresponds to a general shear failure, whereas that of deep anchors corresponds to a local shear failure. In the latter, a flow of material around the anchor occurs while elastic equilibrium of the upper part of the soil mass is maintained by arching.

The experimental data obtained from those tests are tabulated in Table I. The relationship between depth of embedment and ultimate load

TABLE I

EXPERIMENTAL DATA FOR DRY SAND

Test No.	Depth H (in)	Diameter D (in)	H/D	γ (pcf)	Φ^o	Experimental Q_u (lb)	Ultimate Displacement δ_u (in)
2-1	8.0	2.0	4.0	103.2	34	18.75	0.162
2-2	12.0	2.0	6.0	103.9	34	45.9	0.293
2-3	16.0	2.0	8.0	104.0	34	74.9	0.343
2-4	16.0	2.0	8.0	103.8	34	69.9	0.382
2-5	20.0	2.0	10.0	103.6	34	89.4	0.382
2-6	24.0	2.0	12.0	103.2	34	102.0	0.373
2-7	24.0	2.0	12.0	103.2	34	107.6	0.314
2-8	28.0	2.0	14.0	104.0	34	110.0	0.390
3-1	6.0	3.0	2.0	104.0	34	13.0	0.065
3-2	6.0	3.0	2.0	103.5	34	12.3	0.060
3-3	9.0	3.0	3.0	103.8	34	34.7	0.145
3-4	9.0	3.0	3.0	104.5	34	34.7	0.202
3-5	12.0	3.0	4.0	104.2	34	62.1	0.295
3-6	12.0	3.0	4.0	104.4	34	61.8	0.295
3-7	15.0	3.0	5.0	104.2	34	90.8	0.345
3-8	15.0	3.0	5.0	104.3	34	97.8	0.375
3-9	18.0	3.0	6.0	103.8	34	128.8	0.462
3-10	18.0	3.0	6.0	103.9	34	151.3	0.422
3-11	18.0	3.0	6.0	104.0	34	136.3	0.415
3-12	18.0	3.0	6.0	104.7	34	126.0	0.450
3-13	18.0	3.0	6.0	103.7	34	126.0	0.425
3-14	21.0	3.0	7.0	103.8	34	153.3	0.517
3-15	21.0	3.0	7.0	104.5	34	190.3	0.500
3-16	21.0	3.0	7.0	104.4	34	165.8	0.490
3-17	21.0	3.0	7.0	104.2	34	165.0	0.485
3-18	21.0	3.0	7.0	104.2	34	161.3	0.490
3-19	24.0	3.0	8.0	105.7	34	210.0	0.465
3-20	24.0	3.0	8.0	105.8	34	224.0	0.440
3-21	24.0	3.0	8.0	105.6	34	199.0	0.445
3-22	27.0	3.0	9.0	104.3	34	230.7	0.467
3-23	27.0	3.0	9.0	104.2	34	218.7	0.425
3-24	27.0	3.0	9.0	104.5	34	223.7	0.495
3-25	29.25	3.0	9.75	104.7	34	246.2	0.400
3-26	29.25	3.0	9.75	104.4	34	204.7	0.425
3.5-1	8.0	3.5	2.29	103.5	34	27.0	0.103
3.5-2	12.0	3.5	3.43	104.0	34	73.8	0.225
3.5-3	16.0	3.5	4.57	104.0	34	129.3	0.400
3.5-4	16.0	3.5	4.57	104.0	34	129.3	0.450
3.5-5	20.0	3.5	5.71	103.8	34	182.3	0.485
3.5-6	20.0	3.5	5.71	103.8	34	179.3	0.480
3.5-7	20.0	3.5	5.71	103.5	34	180.3	0.535
3.5-8	24.0	3.5	6.86	104.2	34	253.2	0.450
3.5-9	24.0	3.5	6.86	104.2	34	250.7	0.435
3.5-10	28.0	3.5	8.0	104.3	34	275.7	0.435

capacity are shown graphically in Figure 16, for different sizes of anchor plates.

4.4 Testing of Anchors Embedded in Submerged Sand

Tests similar to those above were carried out on anchor plates 3.0 inches in diameter buried in submerged sand. However, in these tests the anchor was vibrated with a portable concrete vibrator, causing it to sink into the submerged material until the required depth was reached.

The vibration was intended to simplify the procedure for placing the anchor and the soil, though the value of the internal friction angle increased to 40^{o} in the process. The saturated density was kept fairly constant at 130.7 lb./cu.ft. at a moisture content of 17.5 per cent under full submergence.

Submergence of the soil sample was achieved by allowing water to flow through a control valve located at the base of the sand container. The flow of water was adjusted to a very slow rate, so that as much air as possible would be forced out at the free surface (Figure 17). The flow of water was stopped when the water level reached the surface of the soil. Afterward, the testing procedure previously described was followed until failure occurred.

Preparation for each subsequent test was accomplished by vibrating the anchor to the required depth, after which the water was drained from the sand through the flow control inlet. The depth of the anchor was checked, and water was then allowed to flow back into the container. When submergence was completed, the depth of the anchor was checked

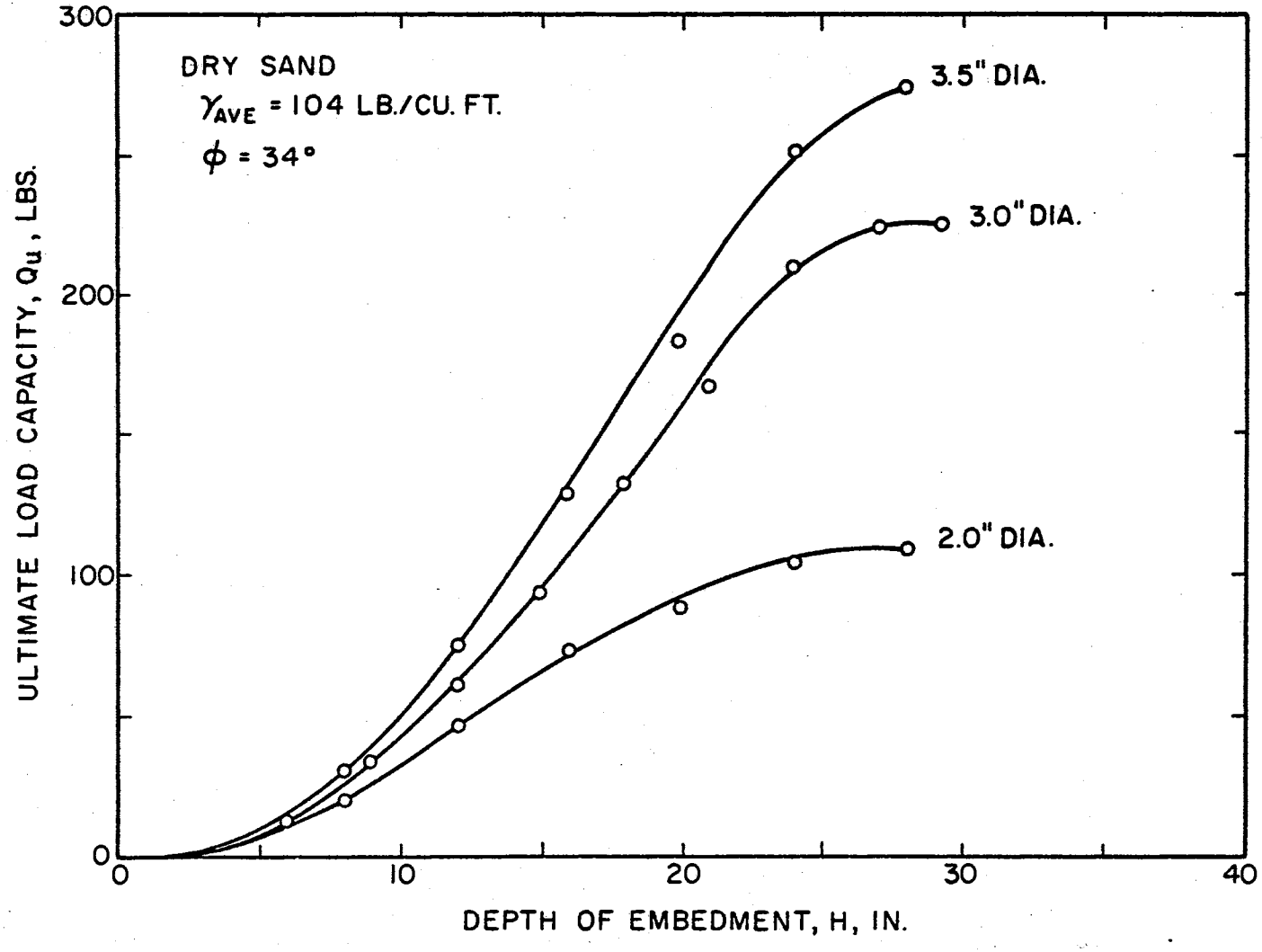

Figure 16. Variation of Q_u with Respect to Depth and Diameter

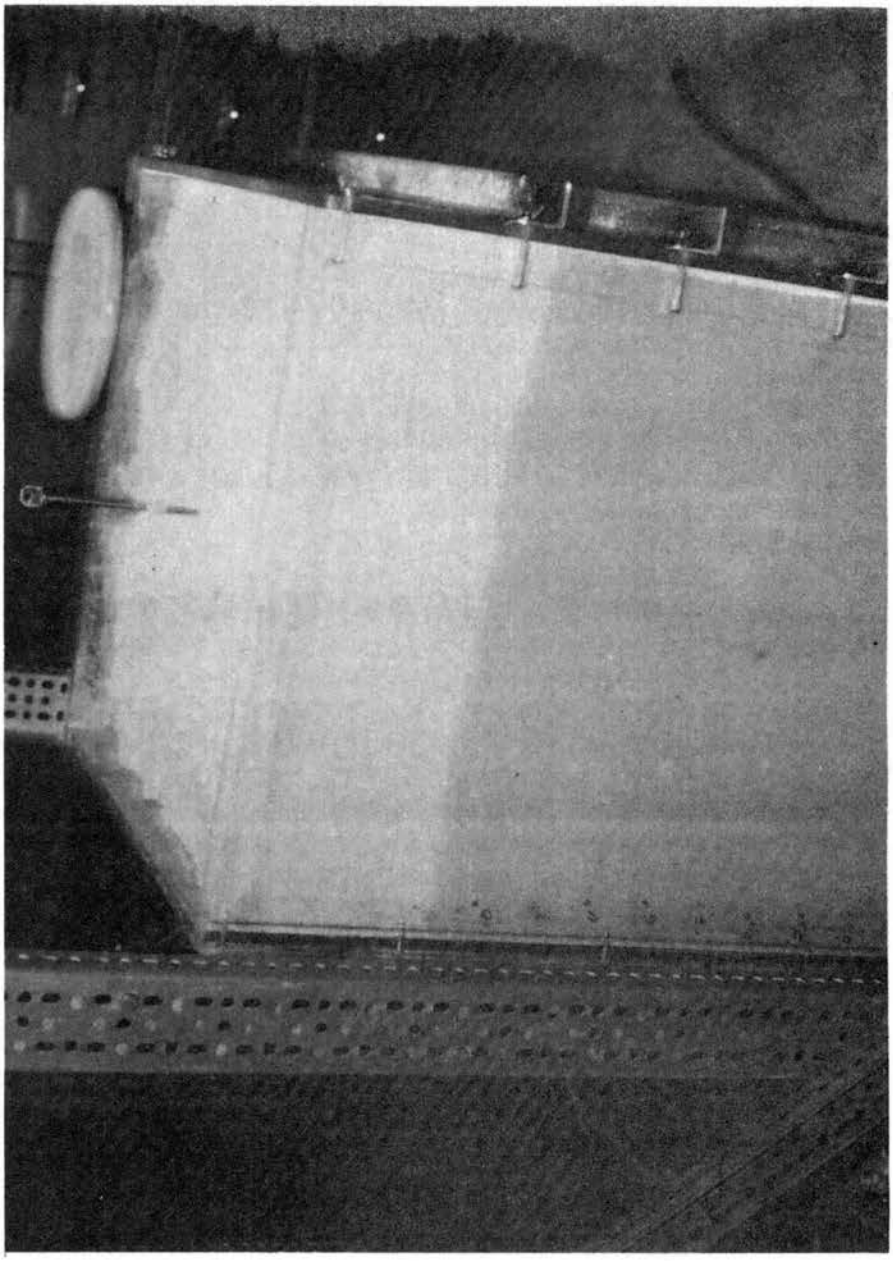

Figure 17. Submerged Testing

again before testing. The experimental results related to this phase of the investigation are tabulated in Table II.

4.5 Testing of Anchors Embedded in Drained Sand

These tests were performed on a submerged, then drained, sand. The experimental procedure was similar to that for submerged sand. The anchor plate diameter was 3.0 inches and the depth was varied from 9.0 to 21.0 inches. In this phase of testing, the soil surface appeared to bulge more, with tension cracks appearing radially as shown in Figures 18 and 19. The disturbed central part of the drained sand was removed by suction using a vacuum cleaner, until a firm surface was exposed, as shown in Figures 19, 20, and 21.

On Figure 21, a dotted line was drawn to delineate the actual shape of the surface along which the failure has developed. It appears that the shape of the failure may be closely represented by a logarithmic spiral curve, as discussed in Section 3.4 of Chapter III.

The data collected from the drained sand tests are presented in Table III. All experimental data obtained from anchors tested in submerged and drained sand are compared graphically in Figure 22. The main purpose of this figure is to show the effects of different soil moisture conditions on the ultimate load capacity of anchors. The comparisons are based on an arbitrarily chosen depth equal to 15.0 inches. The corresponding values of the ultimate capacity, Q_u, varied drastically. The highest resistance was produced by the drained state, probably due to the presence of an apparent cohesion induced by the

TABLE II

SUBMERGED SAND

Test No.	Depth H (in)	Diameter D (in)	H/D	γ (pcf)	Φ^o	Experimental Q_u (lb)	Ultimate Displacement δ_u (in)
1	12.0	3.0	4.0	68.3	40	43.3	0.213
2	12.0	3.0	4.0	68.3	40	45.8	0.215
3	15.0	3.0	5.0	68.3	40	78.0	0.300
4	15.0	3.0	5.0	68.3	40	85.0	0.265
5	18.0	3.0	6.0	68.3	40	139.0	0.390
6	18.0	3.0	6.0	68.3	40	137.0	0.455
7	22.5	3.0	7.5	68.3	40	229.0	0.520
8	24.0	3.0	8.0	68.3	40	294.0	0.428
9	24.0	3.0	8.0	68.3	40	304.0	0.410
10	28.62	3.0	9.5	68.3	40	340.0	0.457
11	28.62	3.0	9.5	68.3	40	346.0	0.462

TABLE III

DRAINED SAND

Test No.	Depth H (in)	Diameter D (in)	H/D	γ (pcf)	Φ^o	Experimental Q_u (lb)	Ultimate Displacement δ_u (in)
1	9.63	3.0	3.21	114.2	40	60.0	0.155
2	14.25	3.0	4.75	114.2	40	212.0	0.275
3	18.25	3.0	6.08	114.2	40	360.0	0.650
4	18.25	3.0	6.08	114.2	40	387.0	0.705
5	21.25	3.0	7.08	114.2	40	457.0	1.250

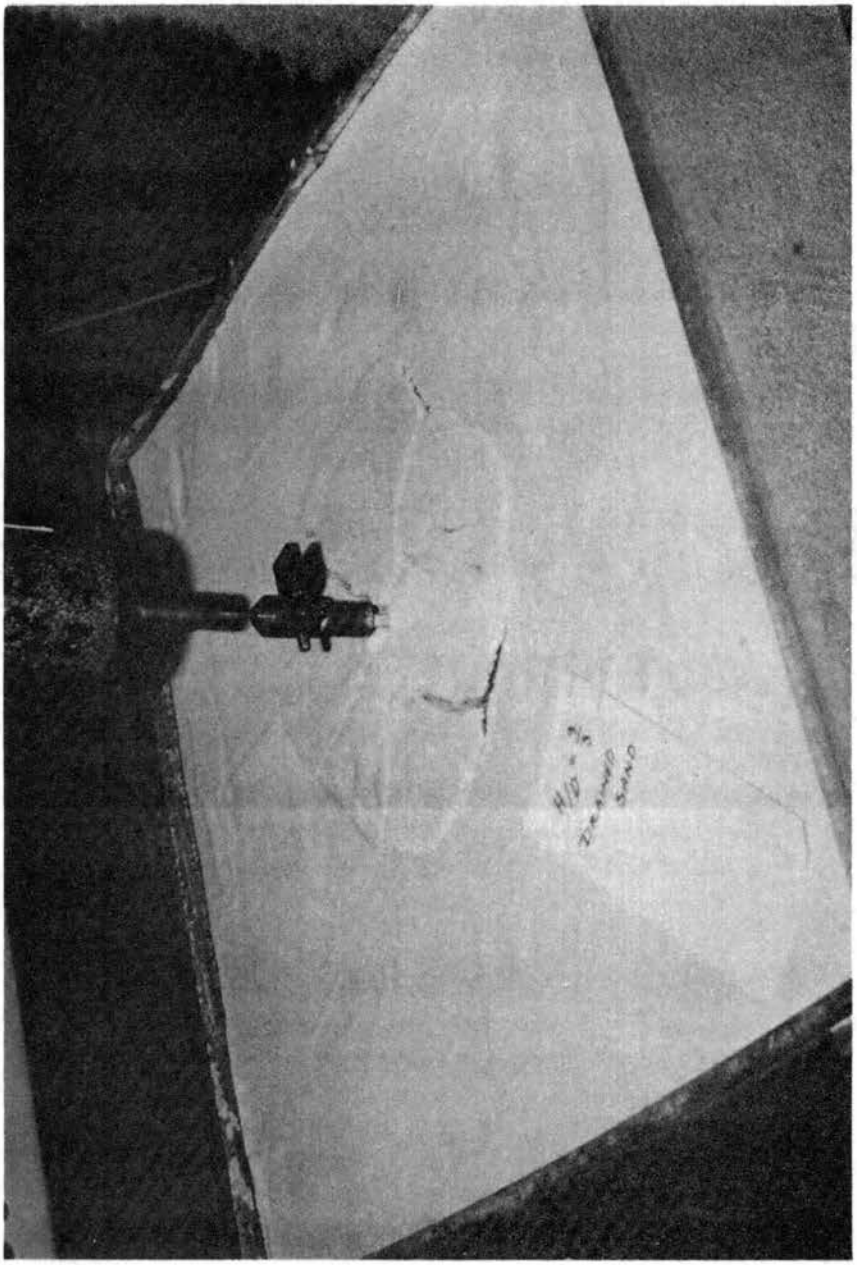

Figure 18. Surface Cracks of Drained Sand

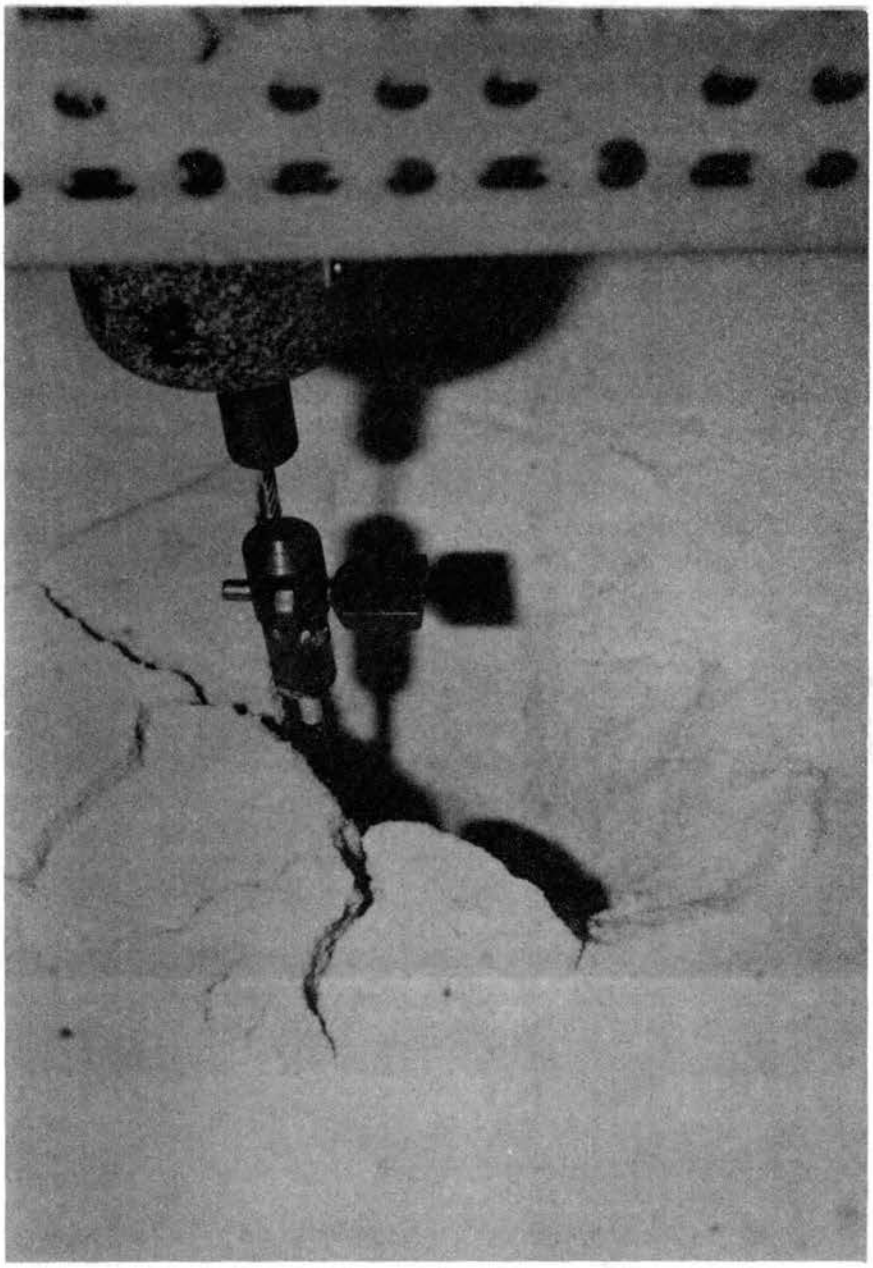

Figure 19. Sectional View Through the Breaking-Out Mass of Soil

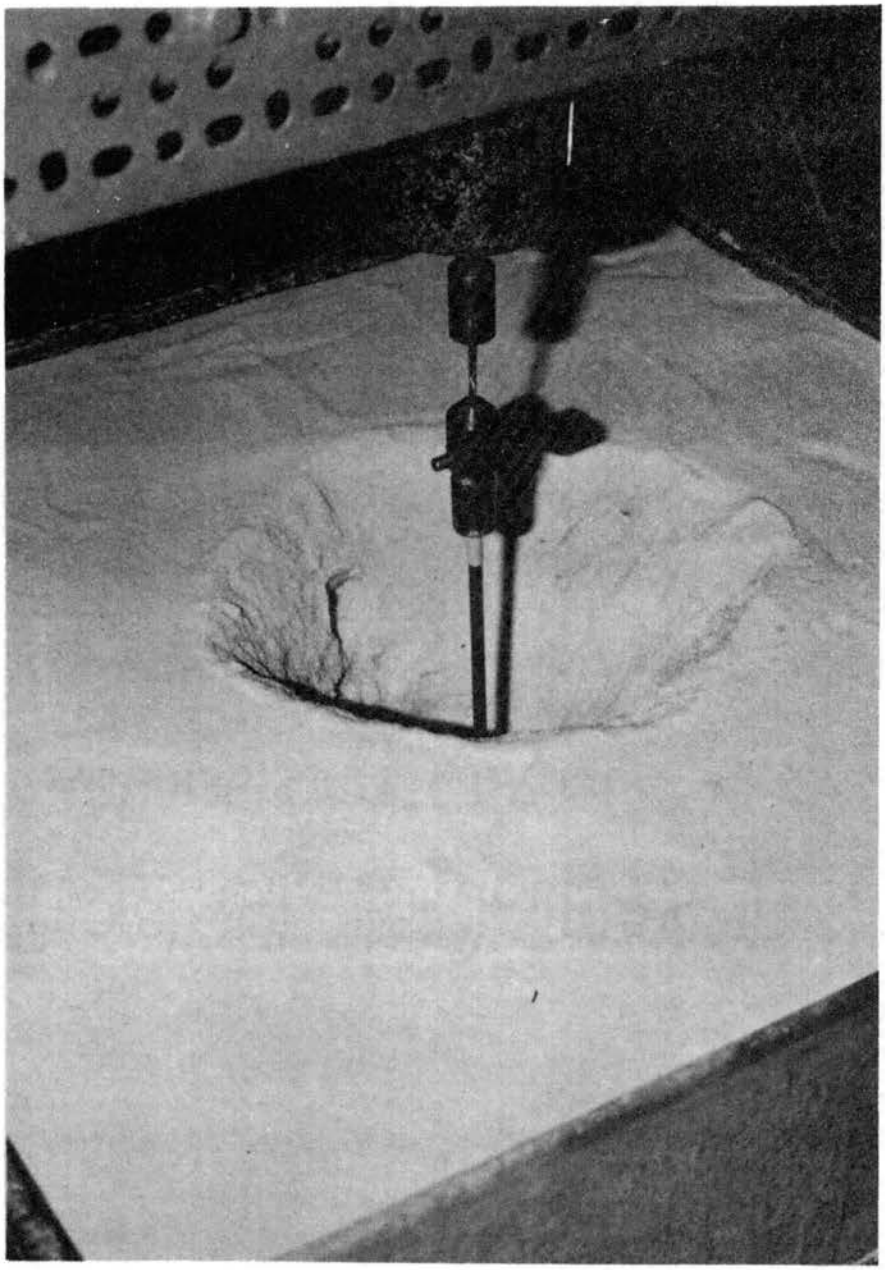

Figure 20. Sectional View Through the Breaking-Out Mass of Soil

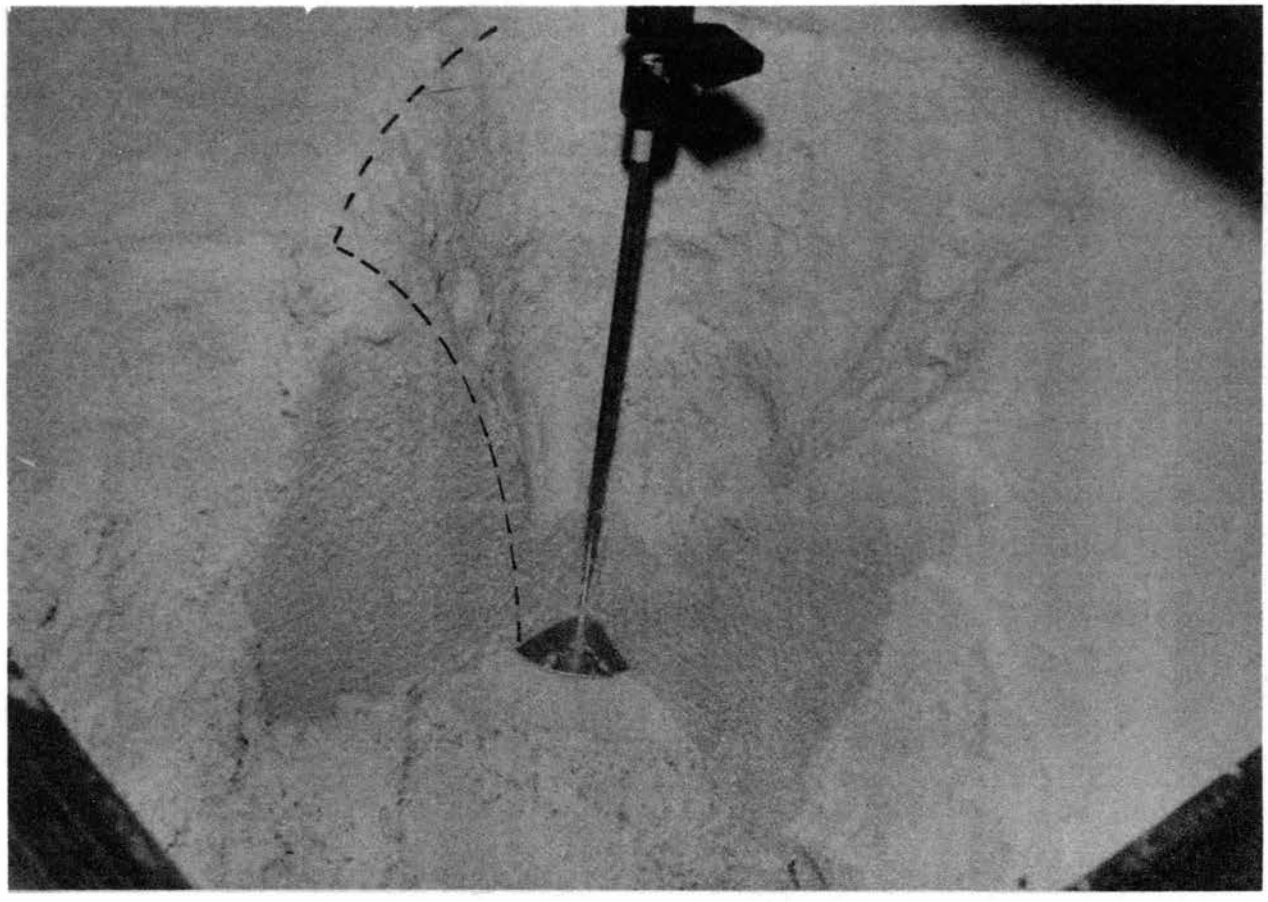

Figure 21. Sectional View Through the Breaking-Out Mass of Soil

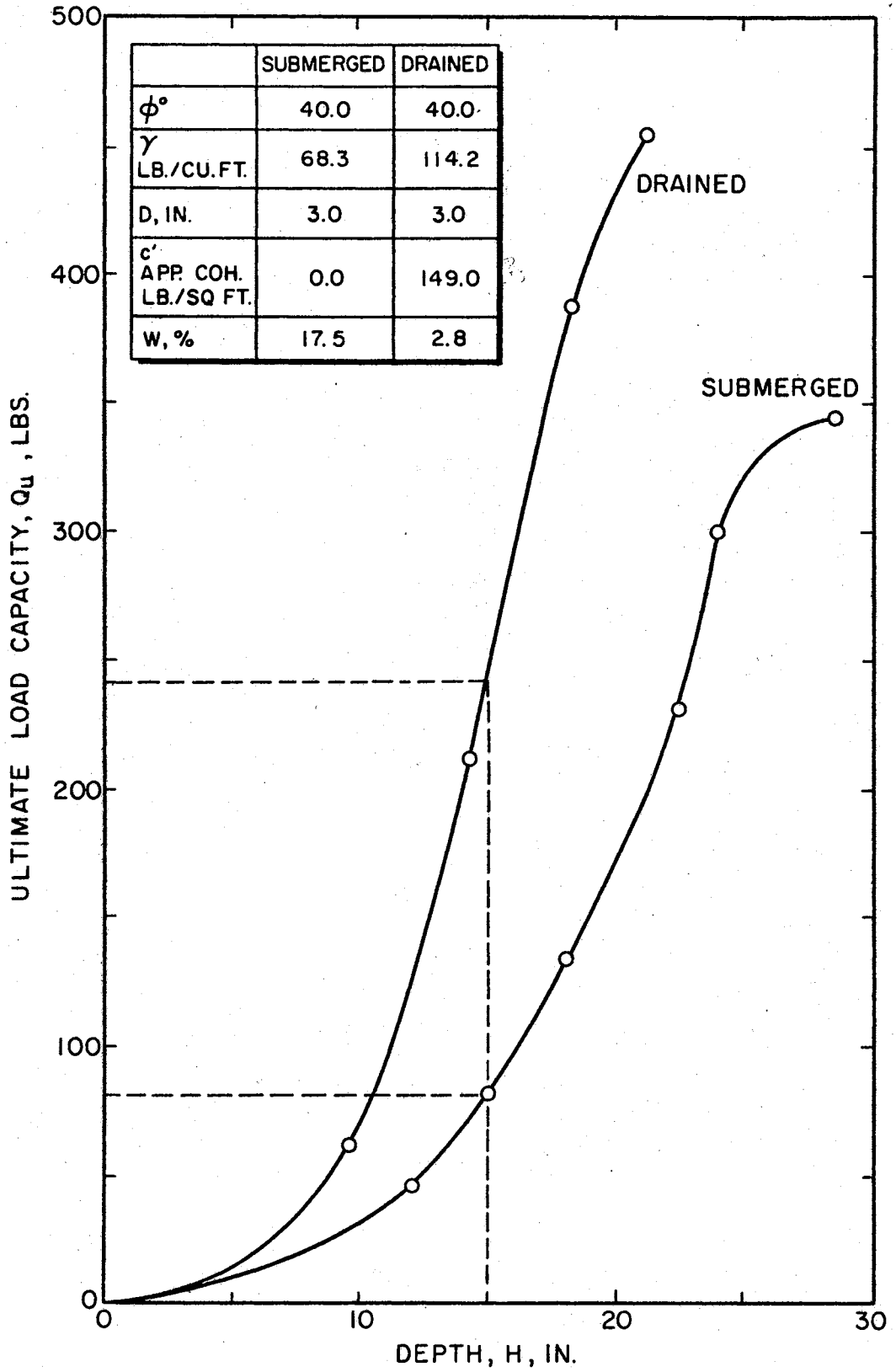

Figure 22. Variation of Load Capacity in Drained and Submerged Sand

internal forces of capillarity. The least value of Q_u was produced by the submerged state, owing to the reduction of the unit weight of soil caused by submergence.

CHAPTER V

DISCUSSION OF RESULTS

5.1 General

The experimental data obtained in this study were used primarily to test the validity of the proposed analytical solution. These data were also compared with data that had been obtained and reported by others, and the latter were used, in addition, to extend the range of experimental data against which the analytical solution could be checked. All of these data served the further purpose of permitting limits to be set for the relative depths at which the anchor behavior is transitional between that of shallow anchors and that of deep ones. The significance of this knowledge in the field of practical application is apparent.

5.2 Effects of Anchor Geometry

There are several factors with respect to anchor geometry that can influence the stability of anchors.

5.2.1 Depth of Embedment

The depth of embedment has an important effect on the magnitude of the resistance to pull. The greater the depth, H, the higher the load capacity, Q_u. However, after a certain depth is reached, the capacity

of the anchor tends to increase at a lesser rate than when the anchor is located at shallower depths. The depth at which a transition occurs appears to be a function of the plate diameter, and the effect is very significant for diameters smaller than 3.0 inches.

Figures 16 and 23 show the variation of Q_u as a function of H and H/D, respectively.

The initial slopes of these curves are rather flat over small ranges of H and H/D. The slopes then increase rather rapidly into a range where the slope is relatively constant. Within this range, a maximim slope is attained, after which there is at first a gradual decrease of slope, followed finally by a portion that is tending toward a horizontal asymptote.

From an engineering point of view, the most efficient anchor performance corresponds to the steepest portion of the curves, extending over a considerable range. There appears to be some limit beyond which greater depth of embedment will not produce a corresponding increase in anchor pull resistance.

Values of H/D corresponding to points of inflection of the curves in Figures 23 and 24, are given below for a considerable range of anchor plate diameters. These are based on data obtained from this investigation and on that reported by Baker and Kondner (2).

Diameter D in.	Relative Depth H/D
1.0	14.0
1.5	9.0
2.0	7.0
3.0	6.0
3.5	6.0

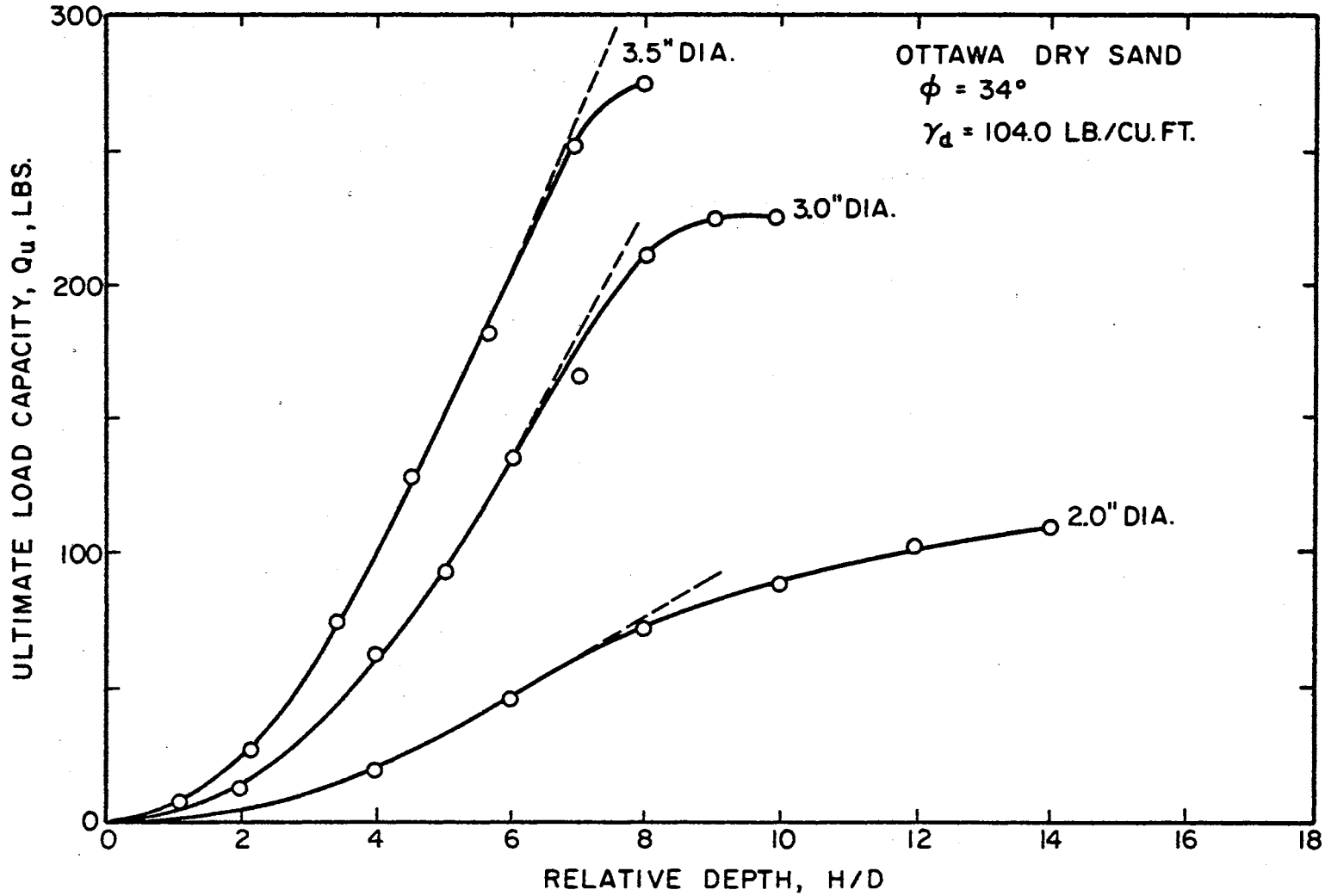

Figure 23. Variation of Q_u Versus H/D (Saeedy's Data)

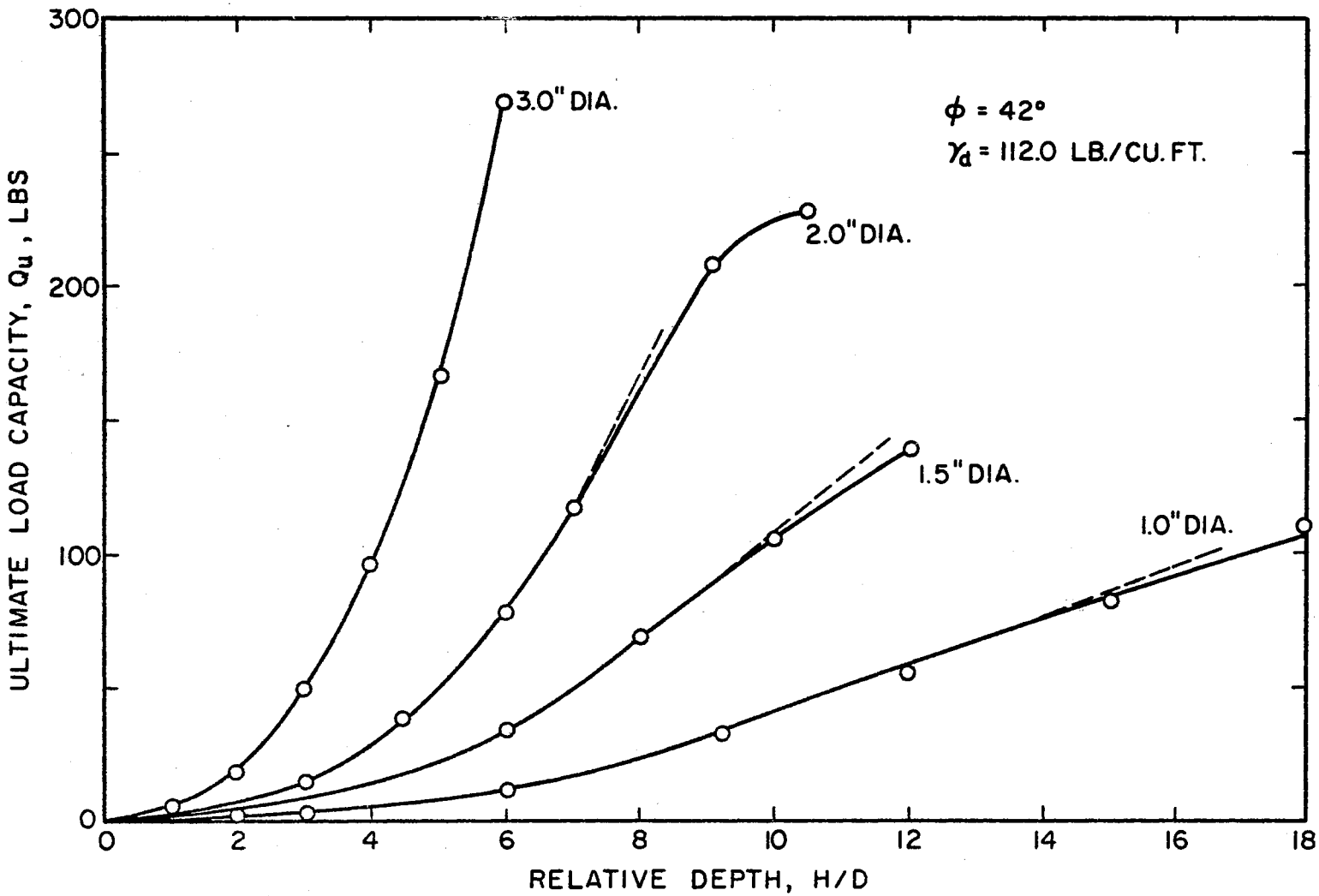

Figure 24. Variation of Q_u Versus H/D (Baker and Kondner's Data)

The mathematical relationship between D and the values of H/D at the point of inflection was found to follow a fourth degree polynomial of determinable coefficients, that is

$$H/D = A_0 + A_1 D + A_2 D^2 + A_3 D^3 + A_4 D^4 \qquad (5.1)$$

where

$A_0 = 27.85971$,

$A_1 = -22.43521$,

$A_2 = 8.441958$,

$A_3 = -1.372482$, and

$A_4 = 0.0806472$.

The utilization, in practice, of depths of embedment greater than that represented by the above value of H/D should be questioned, since greater embedment depths yield diminishing returns in terms of anchor capacity.

5.2.2 Plate Geometry

There is significant increase in the ultimate load capacity with the increase of plate diameter as illustrated in Figure 25. Furthermore, as pointed out by Matsuo (20), anchor plates with equal areas but different shapes yield different pullout capacities. The ultimate load capacity of a square plate is about ten per cent larger than that of a circular plate. Additional effects are produced by bell shaped plates. According to Matsuo, the maximum uplift resistance occurs at $\theta = 15^{\circ}$, where θ is the angle subtended by the sloping side of the bell plate and the horizontal, and is about ten per cent larger than that for a flat plate.

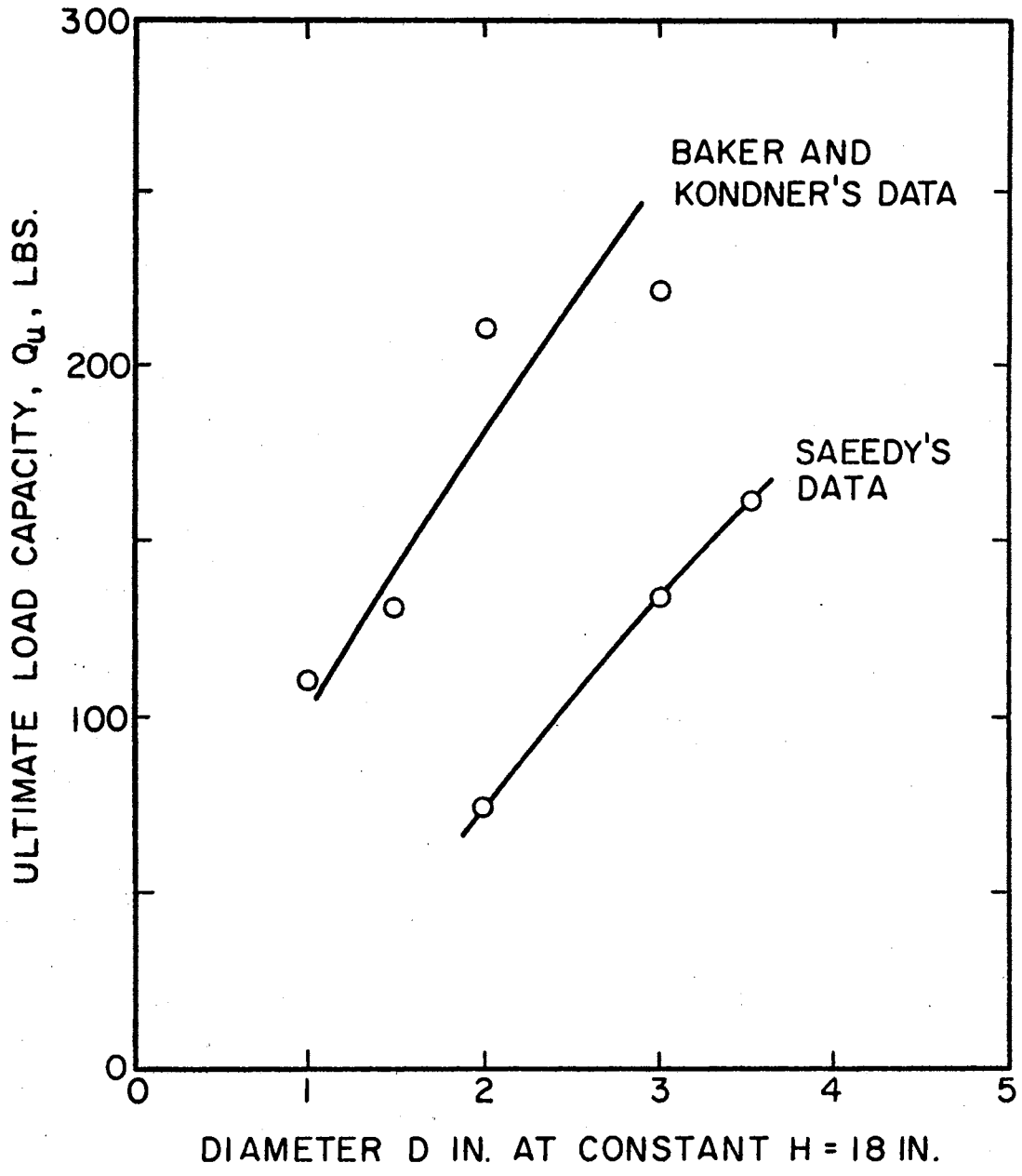

Figure 25. Variation of Q_u Versus D

5.2.3 Plate Thickness

The effects of plate thickness may be pronounced at ratios of diameter to thickness smaller than 1.0, in which case the anchor plate tends to function as a friction pile (Baker and Kondner (2)), due to the shearing resistance created between the peripheral surface area of the plate and the soil. The effect is not very significant when the ratio of diameter to thickness is larger than 1.0. Sams (26) has used a beveled-edge plate to simulate plates without thickness. While this would, at first glance, appear to be an acceptable premise, the effects of this sharpened edge on stress distribution in the vicinity of the plate, and on the collapse mechanism leading to flow of particles into the void created by lifting the plate, have not been considered. The importance of this may be indicated by two tests that were conducted in this study using beveled plates. The resulting load-displacement characteristics, Figure 26, reflect certain peculiarities, shown by a sharp hump at low strain, probably indicating a premature failure caused by high stress concentration around the periphery of the anchor plate.

Other factors affecting the pull resistance of vertical anchors may include the diameter of the anchor shaft, although Sams (26) showed this to be negligible. Also, surface roughness of the anchor may influence the ultimate uplift resistance.

5.3 Effects of Grain Size on Small Models of Anchors

The limitations of model techniques and the frequent necessity for employing similitude in analyzing the results of model tests are well

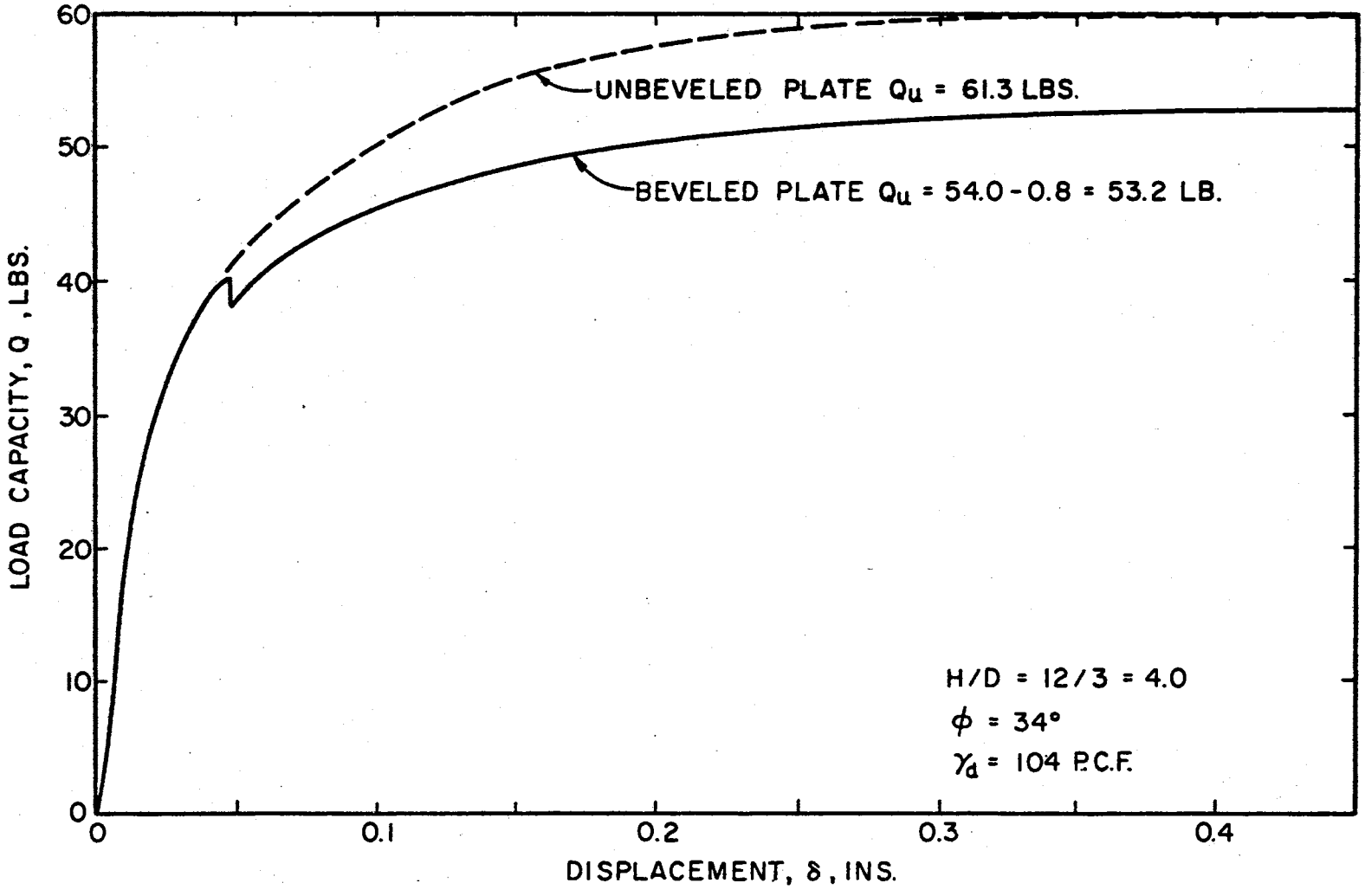

Figure 26. Load-Displacement Characteristic for Beveled Anchor Plate

recognized. Some of those limitations may be eliminated when the analysis is based on the use of dimensionless ratios, such as stress, force, or length ratios. But there is likely to be some effect when there is a substantial difference in the scale of the model and the grain size of the material as compared with prototype. This effect was evidently experienced in this study.

A close examination of Figure 27, which represents a plot of H/D corresponding to points of inflections measured from Figures 23 and 24, versus the diameter D reveals that the relationship is non-linear. Moreover, the curve has a tendency to be asymptotic horizontally at a value of $D \geq 3.0$ inches, and vertically at $D \leq 1.0$ inch. This behavior may perhaps be attributed to the effect of grain size on the stability of anchors, when anchor plates are of small diameter. Figure 27 may also suggest that the modeling effect for this particular soil is eliminated by the use of anchor plates greater than 3.0 inches in diameter. This point deserves further investigation utilizing coarser and finer materials and, also, using plate sizes outside the range used in this study, or in previous ones.

5.4 Comparison of Experimental and Theoretical Results of This Study

The experimental results collected in the testing program, as tabulated in Table I, are utilized in this section to verify the validity of the analytical solution developed in Chapter III. A detailed comparison of experimental and theoretical results is shown in Tables IV, V, and VI, representing values of the ultimate pullout capacity for anchors buried in dry sand. The correlation between the

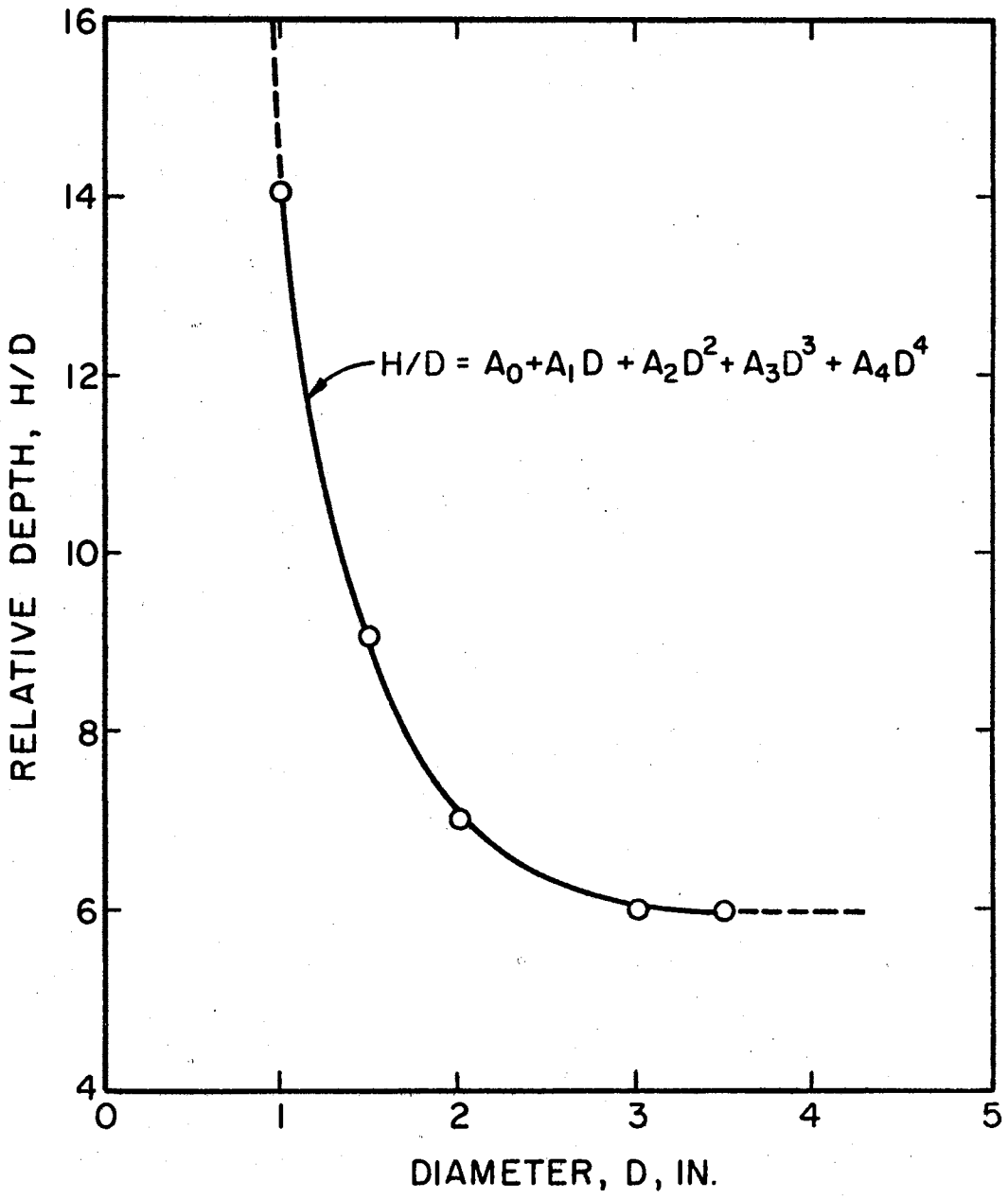

Figure 27. Variations of H/D at Points of Inflection Versus D

TABLE IV

DRY SAND DATA FOR D = 2.0 INCHES

Group Ave. No.	Depth H (in)	H/D	γ Ave. (pcf)	Φ^o	Experimental Q_u (lb) Ave.	Saeedy's Theor. Q_u (lb)	Force Ratio * F_1
2-1-1	8.0	4.0	103.2	34	18.75	18.14	12.18
2-1-2	12.0	6.0	105.0	34	45.9	48.3	21.36
2-2-3	16.0	8.0	103.8	34	72.4	78.3	26.29
2-1-4	20.0	10.0	103.6	34	89.4	92.4	24.83
2-2-5	24.0	12.0	103.2	34	104.65	106.6	23.86
2-1-6	28.0	14.0	104.0	34	110.0	120.7	23.17

$$^*F_1 = Q_u / \{\gamma \cdot H \cdot \left(\frac{\pi}{4}\right) \cdot (D^2 - D_o^2)\}$$

TABLE V

DRY SAND DATA FOR D = 3.0 INCHES

Group Ave. No.	Depth H (in)	H/D	γ Ave. (pcf)	Φ^o	Experimental Q_u (lb) Ave.	Saeedy's Theor. Q_u (lb)	Force Ratio * F_1
3-2-1	6.0	2.0	103.76	34	12.6	13.4	5.28
3-2-2	9.0	3.0	103.99	34	34.7	31.82	8.36
3-2-3	12.0	4.0	104.0	34	62.0	61.3	12.08
3-2-4	15.0	5.0	104.0	34	94.3	104.3	16.45
3-5-5	18.0	6.0	103.78	34	133.2	162.8	21.45
3-5-6	21.0	7.0	104.2	34	167.2	181.8	20.45
3-3-7	24.0	8.0	105.71	34	210.7	203.0	19.70
3-3-8	27.0	9.0	104.4	34	224.3	218.9	19.11
3-3-9	29.25	9.75	104.5	34	225.4	232.9	18.75

$$^*F_1 = Q_u / \{\gamma \cdot H \cdot \left(\frac{\pi}{4}\right) \cdot (D^2 - D_o^2)\}$$

TABLE VI

DRY SAND DATA FOR D = 3.5 INCHES

Group Ave. No.	Depth H (in)	H/D	γ Ave. (pcf)	Φ^o	Experimental Q_u (lb) Ave.	Saeedy's Theor. Q_u (lb)	Force Ratio * F_1
3.5-0-1	4.0	1.14	103.5	34	---	7.2	3.14
3.5-1-2	8.0	2.29	103.5	34	27.0	27.9	6.09
3.5-1-3	12.0	3.43	104.0	34	73.8	68.2	9.86
3.5-2-4	16.0	4.57	104.0	34	129.3	133.4	14.47
3.5-3-5	20.0	5.71	103.8	34	180.6	229.1	19.92
3.5-2-6	24.0	6.86	104.2	34	252.0	261.2	18.86
3.5-1-7	28.0	8.00	104.3	34	275.7	292.1	18.06

$$^*F_1 = Q_u / \{\gamma \cdot H \cdot \left(\frac{\pi}{4}\right) \cdot (D^2 - D_o^2)\}$$

experimental and theoretical results is found to be excellent for all ranges of H/D, and for different plate diameters.

For large values of H/D, the theoretical results were based on a modification of the analytical solution developed in Chapter III, taking into account the reduction of anchor efficiency when H/D exceeds the value corresponding to the point of inflection of the curve representing the ultimate load as a function of H/D (see Section 5.2). The method of modifying the solution is described in Chapter VI.

The results are further compared graphically in Figure 28. In this figure the calculated values are plotted against the experimental values for all tests listed in Tables IV, V, and VI. It may be seen that most of the points lie very close to a line drawn from the origin on a 45° slope, indicating good agreement between theoretical and experimental results.

The experimental results obtained from anchors buried in submerged sand and drained sand are presented in Tables VII and VIII, respectively. Values for the apparent cohesion c', included in Table VIII, represent the additional strength exhibited by the drained sand due to the internal forces of capillarity.

The theoretical solution was utilized to determine a value for the apparent cohesion c' by trial and error. In this procedure, c' was varied until a value was found that, in combination with friction, yielded a pullout capacity Q_u equal to the experimental value. The average value of c', based on tests Nos. 3-1-2 and 3-2-3, was 149.0 psf. Another approximation for c' was made using the surface tension equation, which is found in Means and Parcher (22). In this approximation c' was found to have a value of 112.0 psf. Theoretical values

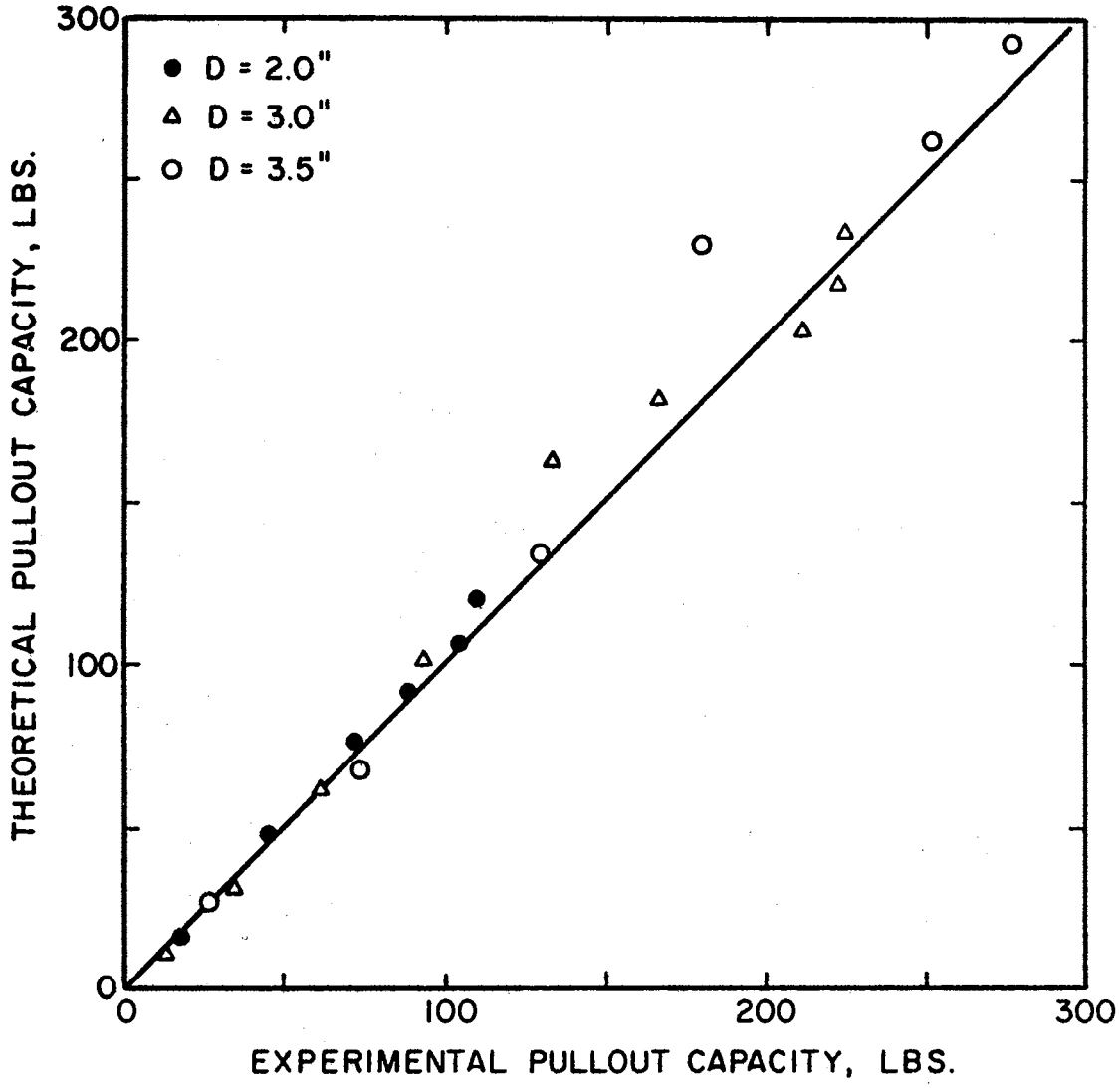

Figure 28. Comparison Between Theoretical and Experimental Results

TABLE VII

COMPARISON OF SUBMERGED SAND RESULTS

Group Ave. No.	Depth H (in)	Diameter D (in)	H/D	γ sub. (pcf)	Φ^o	Experimental Q_u (lb) Ave.	Saeedy's Theor. Q_u (lb)	Force Ratio * F_1
3-2-1	12.0	3.0	4.0	68.3	40.0	44.5	48.6	14.61
3-2-2	15.0	3.0	5.0	68.3	40.0	82.0	84.0	20.19
3-2-3	18.0	3.0	6.0	68.3	40.0	138.0	133.1	26.64
3-1-4	22.5	3.0	7.5	68.3	40.0	229.0	237.0	37.97
3-2-5	24.0	3.0	8.0	68.3	40.0	299.0	280.9	42.18
3-2-6	28.62	3.0	9.54	68.3	40.0	343.0	315.9	39.78

$$^{*}F_1 = Q_u / \{\gamma \cdot H \cdot \left(\frac{\pi}{4}\right) \cdot (D^2 - D_o^2)\}$$

TABLE VIII

COMPARISON OF DRAINED SAND RESULTS

Group Ave. No.	Depth H (in)	Diameter D (in)	H/D	γ sat. (pcf)	Φ^o	Experimental Q_u (lb) Ave.	Saeedy's Theor. Q_u (lb)	Cohesion c' (psf)
3-1-1	9.63	3.0	3.21	114.2	40.0	61.0	97.2	149.0
3-1-2	14.25	3.0	5.11	114.2	40.0	213.0	217.9	149.0
3-2-3	18.25	3.0	6.08	114.2	40.0	374.0	366.6	149.0
3-1-4	21.25	3.0	7.08	114.2	40.0	458.0	389.4	149.0

for Q_u were computed using c' equal to 149.0 psf. for drained sand, and the results are shown in Table VIII. The theoretical and experimental values for Q_u are in good agreement.

Because the experimental data are so limited, no claim is made that the theoretical solution developed in this study is applicable to cohesive soils. However, it would appear that this solution may, in fact, be appropriate for the analysis of problems involving cohesive soils. As a check on this hypothesis, experimental data from three model tests of cohesive soils conducted by the United State Bureau of Reclamation (obtained by private communication) were compared with the theoretical values obtained using the solution developed in this investigation. Those comparisons are given in Table IX, and it may be seen that there is reasonably good agreement. The approximated belled anchor solution was obtained by considering the depth of anchor plate to be measured from the soil surface to the top of the tapered section of the bell shaped plate.

TABLE IX

ANCHORS IN COHESIVE SOILS REPORTED BY HORNER
U. S. BUREAU OF RECLAMATION

Test No.	Depth H (in)	Diameter D (in)	H/D	γ Ave. (pcf)	Φ^o	Experimental Q_u (lb)	Saeedy's Theor. $^*Q_u$ (lb)	Saeedy's Theor. $^{**}Q_u$ (lb)	Shaft Diameter D_o (in)	Remarks Cohesion (psf)
4	11.81	6.5	1.82	107	33.0	1150.0	1141.0	---	3.5	1353.6
6	6.25	6.3	0.99	105	33.0	500.0	458.0	---	3.5	1353.6
8	16.85	6.0	2.81	108	33.0	2200.0	1892.0	---	3.5	1353.6
4	13.0	6.5	2.0	107	33.0	1150.0	---	1317.0	3.5	1353.6
6	7.6	6.3	1.32	105	33.0	500.0	---	595.0	3.5	1353.6
8	18.0	6.0	3.0	108	33.0	2200.0	---	2105.0	3.5	1353.6

*Approximated Belled Anchor Solution

**Flat Plate Anchor Solution

CHAPTER VI

GENERALIZATION OF THEORETICAL SOLUTION

6.1 General

Most of the earth anchor investigations reported in literature have suggested the classification of anchors as deep or shallow, much as for conventional footings, without pointing out a fundamental difference in load resistance characteristics that occurs with the transition from one to the other. The data from the present investigation indicate that it is both possible and logical to distinguish deep anchors from shallow ones on the basis of a significant behavioral characteristic.

It is suggested that the term "shallow" anchor be reserved for those anchors having a ratio H/D equal to or less than that value at which the H/D - Ultimate Load relationship departs from linearity. Up to this point it appears probable that the entire mass of soil above the anchor is contributing directly to the anchor's capability for resisting load. The gain of load resistance per unit of increased depth, as H/D increases beyond this point, steadily diminishes. The load capacity tends toward a constant value that cannot be increased by deeper embedment of the anchor. It appears logical to reserve the term "deep" anchor for those having an H/D within this non-linear range of the H/D - Ultimate Load relationship. Within this region, local shear failure and resultant flow of soil around the anchor begins to be the dominant behavioral characteristic. Beyond a certain depth of

embedment there is no further gain in load resistance of the anchor as depth of embedment increases.

It has been shown in this investigation that diminishing returns are yielded when H/D is increased beyond six, for the anchor diameters studied. Moreover, it would appear from the relationship plotted in Figure 27 that anchor sizes larger than those tested will be governed by the same critical value of H/D (although this needs to be verified by actual tests of larger anchors). From an engineering viewpoint it is, therefore, suggested that the greatest economic advantage will be attained by earth anchors of $H/D \leq 6$. While some increase in load capacity may be gained by deeper embedment of an anchor of specified diameter, the greatest good can be gained by simultaneously increasing anchor size and depth of embedment in such a way as to maintain H/D constant at about six. While valid for anchor dimensions so far studied, this conclusion still needs to be verified by full-scale tests.

These relationships can be most appropriately represented by the use of the dimensionless ratios H/D and F_1. H/D has been previously defined as the ratio of depth of embedment to anchor plate diameter. F_1 is a force ratio (defined in Figure 29) that includes factors that have great influence on the load capacity of anchors. Anchor geometry and soil density are introduced in this ratio.

The behavior described above makes it necessary to modify the theoretical solution to account for the subsequent reduction of anchor efficiency when H/D exceeds the transitional value. The modification may be achieved by assuming that the extent of the failure surface is limited to a depth of H_T above the anchor plate. This suggests that mobilization of shear strength would be limited to a height, H_T.

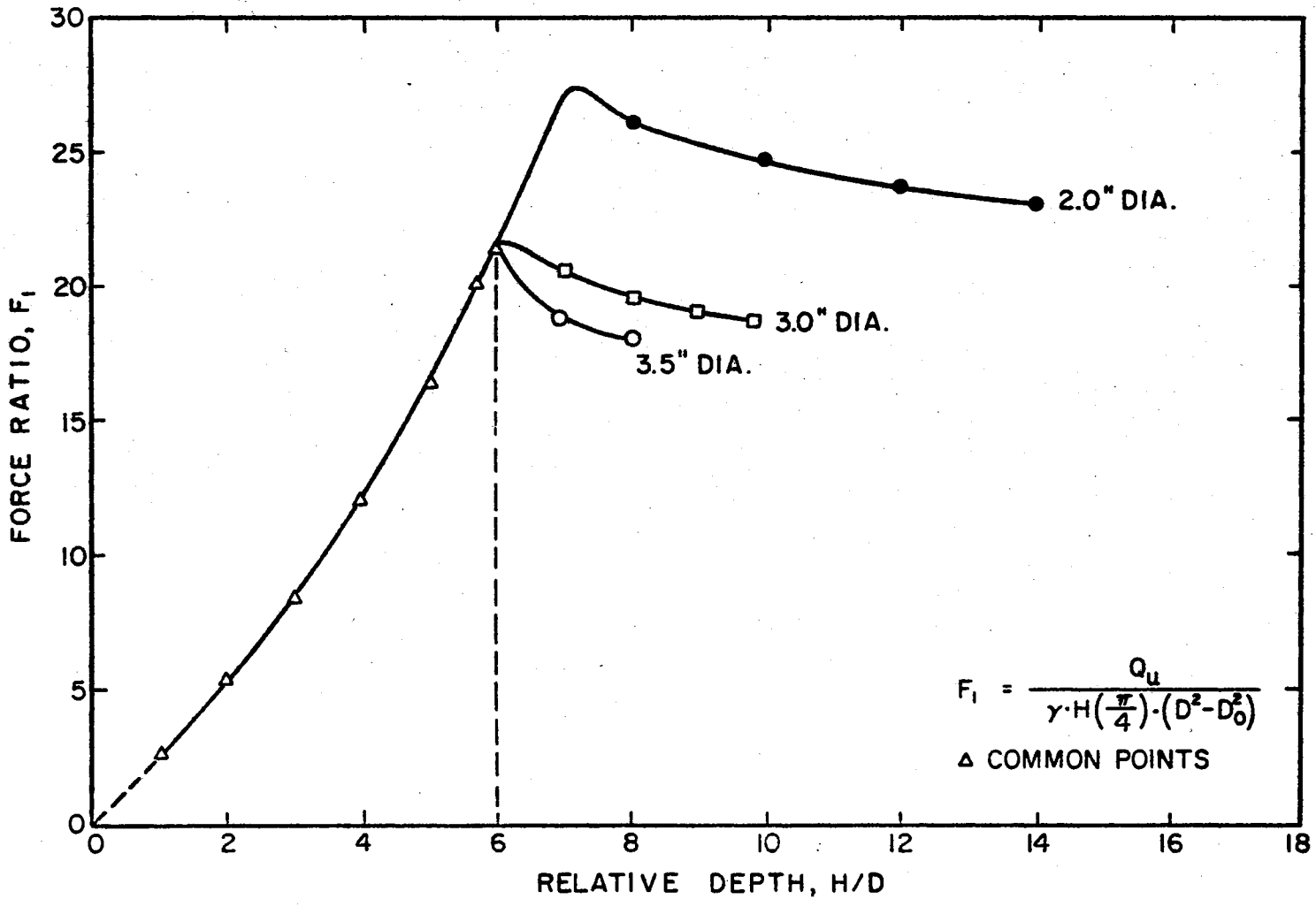

Figure 29. Variations of Force Ratio F_1 with Respect to H/D

Above the height H_T, in the region $(H - H_T)$, the soil is in elastic equilibrium, as shown in Figure 30. The overburden pressure of this part of the mass produces an initial value of the shear strength at the upper boundary of the failure surface; e.g., point (A), Figure 30. The magnitude of this shear strength is found from Coulomb's equation as follows:

$$\tau_u = c + \sigma \cdot \tan \Phi \qquad (6.1)$$

where

τ_u is the ultimate shear stress, acting along the failure surface,

$\sigma = (H - H_T) \cdot \gamma \cdot k_o$, and

k_o = coefficient of earth pressure at rest, since the soil in the region $(H - H_T)$ is being maintained under elastic equilibrium.

Therefore, the value τ_u at the upper boundary is given by:

$$\tau_u = c + \{(H - H_T) \cdot \gamma \cdot \tan \Phi\} \cdot k_o \quad . \qquad (6.2)$$

6.2 Development of the Non-Dimensional Curves for the Uplift Resistance

To provide a general solution for determination of the ultimate load capacity of earth anchors, the method of similitude is utilized to produce a non-dimensional family of curves, in the form of force ratio versus relative depths.

The method of similitude as outlined by Kline (16) is basically simple, providing that the following two conditions are satisfied:

1) The forces that are believed to be important in a given problem are enumerated, including the dependent and all independent forces. Each of these forces is then expressed

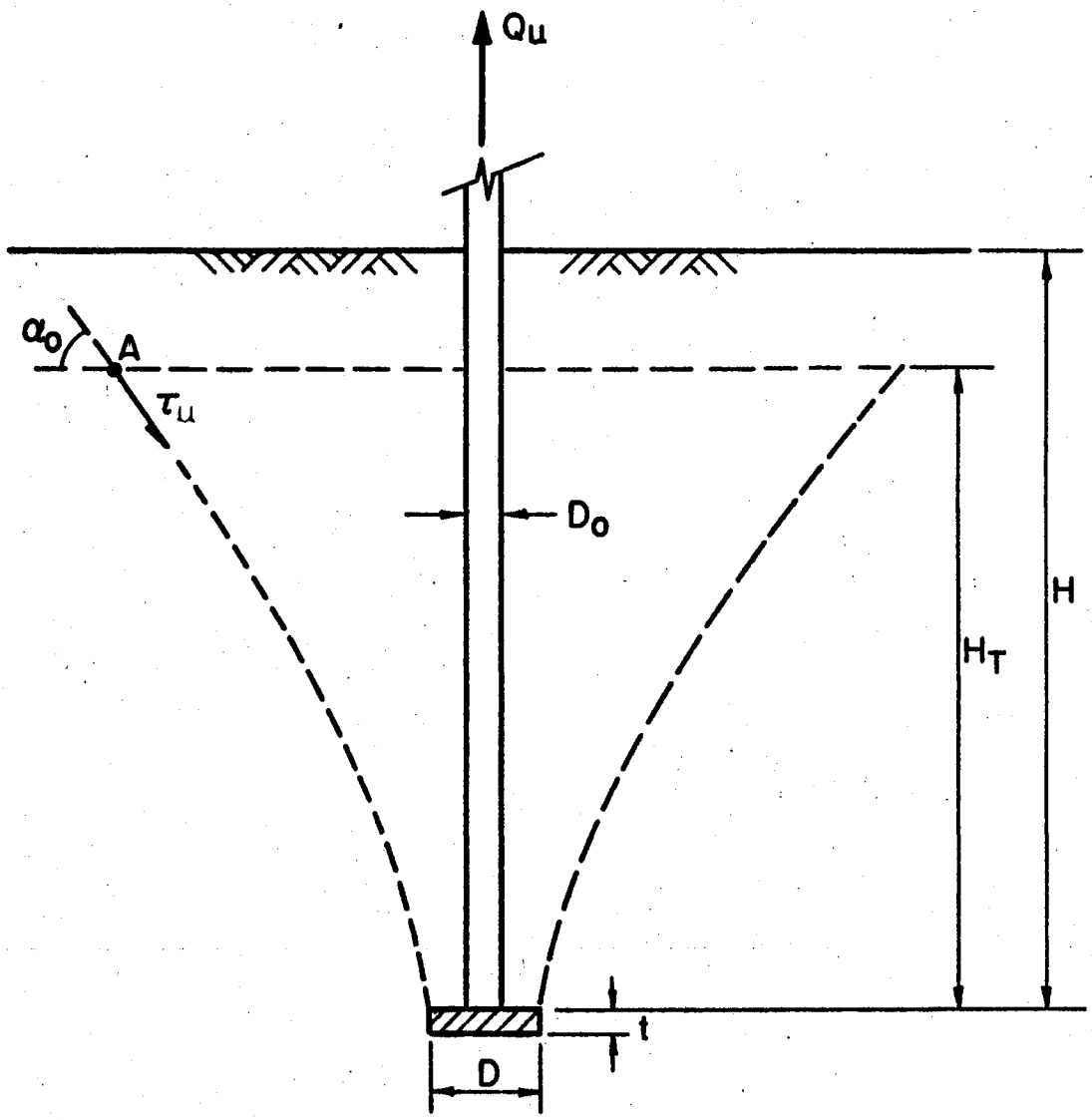

Figure 30. Condition of Shear Stress at the Upper Boundaries for Deep Anchors

in terms of the parameters of the problem by physical or dimensional arguments.

2) The pertinent non-dimensional groups are constructed by forming ratios of these factors, including enough length ratios to insure geometric similarity.

As outlined in Chapter III, the computer program provided in Appendix A contains Fortran statements of the solution which is capable of determining the ultimate load capacity Q_u, and the force ratio F_1 for any particular anchor, given the geometry of anchor and the strength properties of the soil. In formulating the general solution given in Figure 31, the most important forces and geometrical factors governing the stability of anchors have been used. These are the pullout capacity and the gravitational force represented by the weight of a soil cylinder having a diameter D equal to that of the anchor plate, and a height equal to depth of embedment, H. The force ratio F_1 is expressed by:

$$F_1 = \frac{Q_u}{\frac{\pi}{4} \cdot (D^2 - D_o^2)\gamma \cdot H} \quad . \tag{6.3}$$

The dimensionless parameter, F_1, may also be regarded as a stress ratio, namely the normal stress applied by the anchor plate on the soil, $Q_u/[\frac{\pi}{4} \cdot (D^2 - D_o^2)]$, divided by the stress caused by the overburden material $(\gamma \cdot H)$.

In order to produce the curves plotted in Figure 31, the computer was utilized as explained in Chapter III, Section 3.5, to solve several hypothetical problems for the same angle of internal friction, Φ, while varying the geometry of anchor, (H/D). The value of F_1 is then plotted versus its particular relative depth, to define a single curve. Other

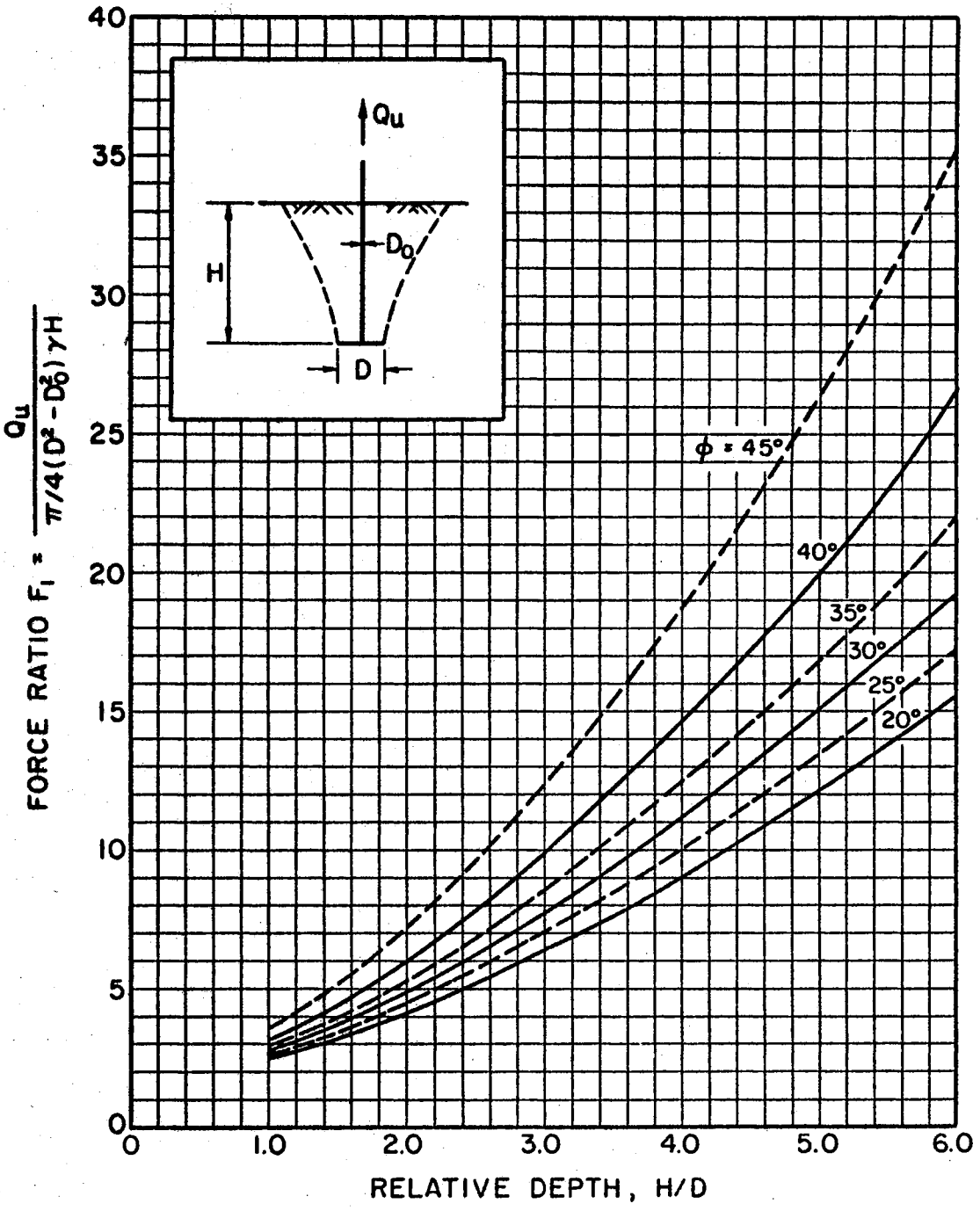

Figure 31. Non-Dimensional Curves for Determination of Q_u

curves were similarly produced by changing the value of Φ from 20° to 45° at intervals of 5°. A summary of all results for these hypothetical problems is given in Appendix B.

Figure 32 is another family of curves, obtained by plotting F_1 versus Φ with H/D varying from one to six. Either one of these figures may be used in connection with the theoretical determination of Q_u as explained in Section 6.4. It is of some interest to note that in Figure 32, at lower values of H/D, the force ratio F_1 does not change appreciably with variation of the friction angle. However, as the value of H/D increases, the force ratio becomes more sensitive to small variations of Φ, and at H/D = 6 a small change in Φ will result in a significant change in F_1. This indicates that for small values of H/D the part of the pullout resistance contributed by internal frictional resistance of the soil is negligible in comparison with that contributed by the weight of the displaced soil.

6.3 Development of the Non-Dimensional Curves for Anchor Spacing

The spacing of earth anchors is governed by factors similar to those that apply to other types of foundation units; e.g., piles. If piles are too closely spaced, the overall carrying capacity of the group of piles is less than the sum of the capacities of the individual piles (17). A similar constraint exists for a group of anchors, due to the overlapping effects of the failure surfaces, unless the anchors are placed sufficiently far apart. The uplift resistance of an individual anchor is proportionately reduced if it is a member of a closely spaced group of anchors.

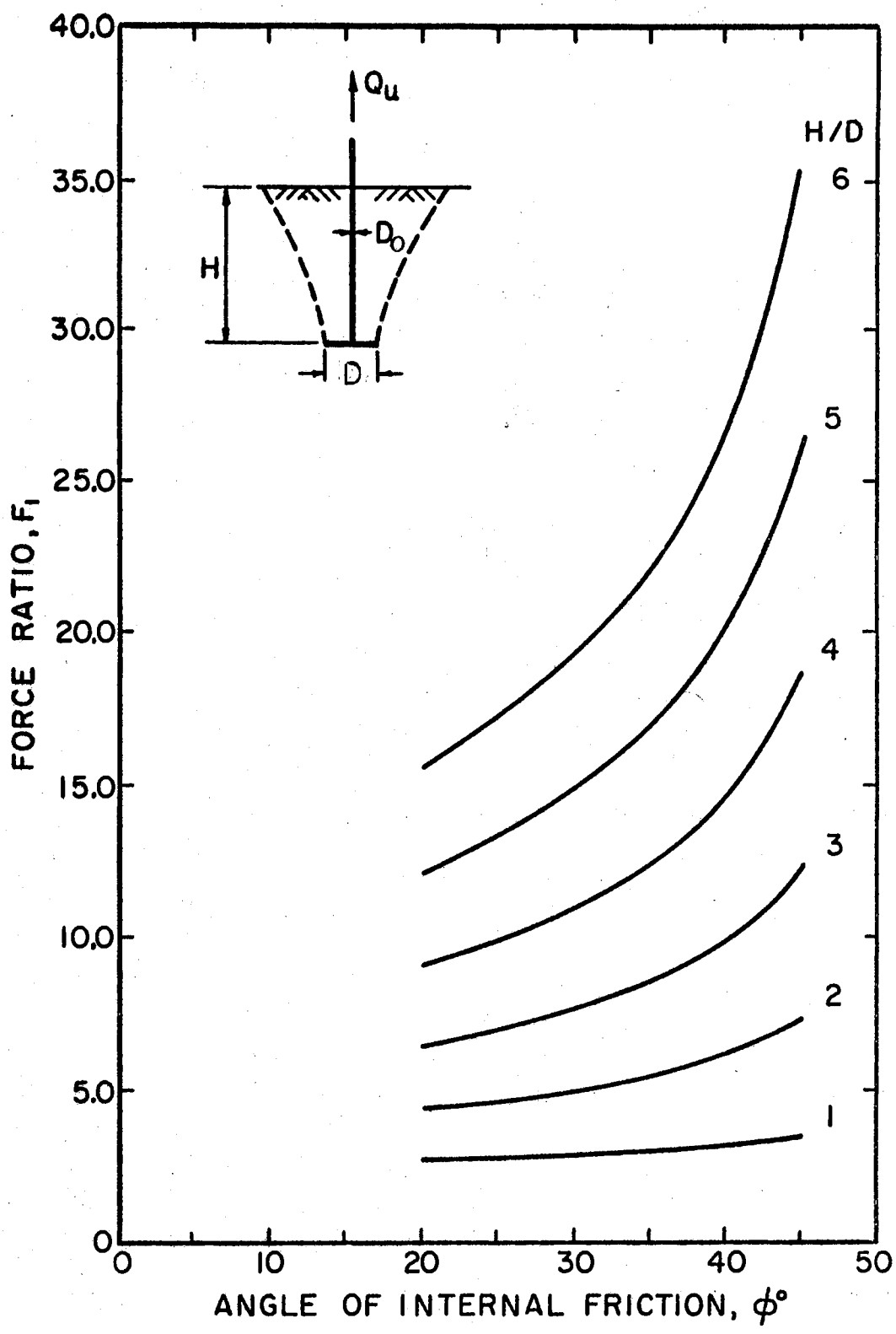

Figure 32. Non-Dimensional Curves for Determination of Q_u

Figure 33 is developed to calculate the minimum distance, 2ρ, at which anchors must be placed in order to develop the full capacity of each anchor. This curve is based on the assumption that the minimum spacing between anchors is equal to the horizontal extent of the assumed failure surface, when the anchor is stressed to its ultimate load capacity.

The values of ρ found from Figure 33 are likely to be conservative since, in practice, anchors are not designed to resist their ultimate load capacities; but, rather, are designed to include a certain factor of safety. Evaluation of the dimensionless ratio $H/(\rho - D/2)$ in Figure 33, was accomplished by calculating the maximum horizontal radius of the theoretical failure surface, measured from the centerline of the anchor shaft for several cases, as listed in Appendix B. From Figure 33, it is evident that ρ is strongly dependent on the angle of the internal friction of soil and the depth of embedment of anchor. The use of this figure in anchor design is outlined in Section 6.4.

6.4 Application of the Theoretical Solution

The various aspects of the solution techniques developed in the preceding sections of this chapter can now be fitted together for practical application. The solution may be illustrated through a solved numerical example, shown later in this section, in which a hypothetical problem is formulated to show the procedure that can be followed when a value of the ultimate load capacity of a vertical anchor is to be found.

As for most problems in soil mechanics and foundations, construction of anchors also requires full exploration of the site as a first step in evaluating the soil properties. According to Wiggins (33), a

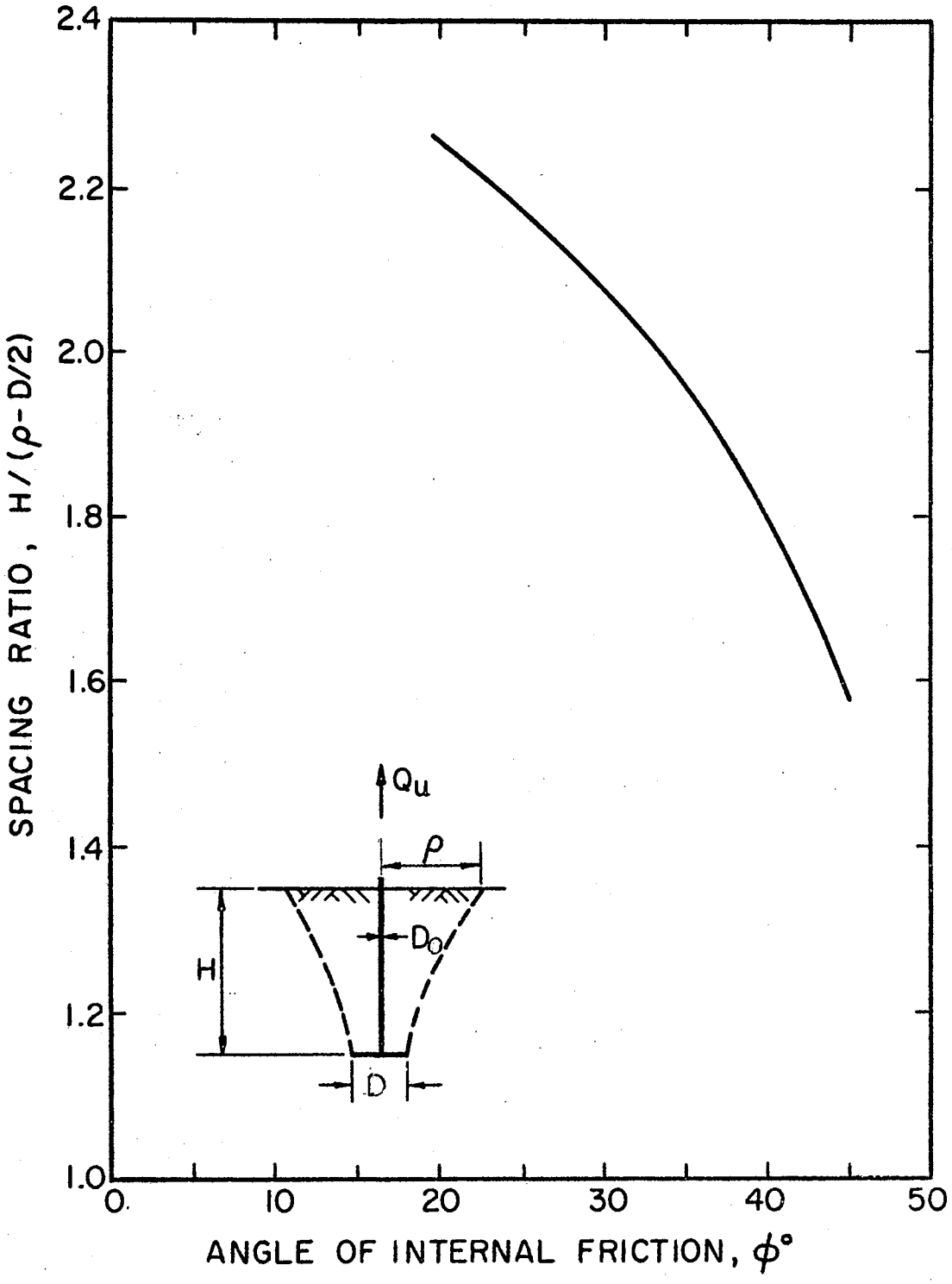

Figure 33. Non-Dimensional Curves for Anchor Spacing Ratio

factor of safety of 2.0 is recommended for the design of anchors. It should be noted that estimation of the factor of safety requires the simultaneous consideration of many factors:

1) Variations of soil profile within the designed effective depth of anchor, including seasonal variations of the soil moisture conditions. The most adverse conditions should be assumed in design, giving some consideration to probability of occurrence.
2) Period of serviceability of the structure, whether permanent or temporary.
3) Climatic conditions, to account for the occurrence of wind, frost, and ice.
4) Possible adverse effects of construction methods employed and quality of construction supervision.

Numerical Example:

An upward force of 25 kips must be resisted by means of an earth anchor. The distance between the supports cannot be less than 15 ft. The anchors are to be constructed in a silty-sand soil. Site exploration and laboratory testing indicate that the soil has the following properties:

Angle of internal friction $\Phi = 30^{\circ}$.

Unit weight of soil $\gamma = 108.0$ pcf.

Ground water table is located at 20 ft. below ground surface.

Solution

Using a factor of safety of 2.0, the required ultimate load capacity is:

$$Q_u = 2.0 \times 25.0 = 50.0 \text{ kips} \quad .$$

The diameter and the thickness of anchor plate may be determined from structural calculations. For the purpose of this example the diameter D_o of the anchor shaft is assumed to be equal to 9.0 inches.

From Figure 31,

$$Q_u = F_1\{H \cdot \gamma(\pi/4)(D^2 - D_o^2)\}$$

First Trial:

Assuming,

$$H = 9.0 \text{ ft.}$$

$$D = 4.0 \text{ ft.}$$

then

$$H/D = 2.25 \ .$$

The value of F_1 which corresponds to

$$\Phi = 30^o$$

$$H/D = 2.25$$

is found from Figure 31. Thus,

$$F_1 = 6.0 \ .$$

Therefore,

$$Q_u = 6 \times 108 \times 9(\pi/4)(4^2 - 0.75^2)$$

$$= 70.6 \text{ kips} \ .$$

The value of Q_u obtained in the first trial is in excess of the required value of 50 kips.

Second Trial:

Assuming,

$$H = 8.0 \text{ ft.}$$

$$D = 4.0 \text{ ft.}$$

then

$$H/D = 2.0 \text{ ft.}$$

Thus

$$F_1 = 5.0 ,$$

therefore,

$$Q_u = 5 \times 108 \times 8(\pi/4)(4^2 - 0.75^2)$$

$$= 52.4 \text{ kips per support, which is close enough to the required value of } Q_u.$$

Spacing:

The value of $H/(\rho - D/2)$ is found from Figure 33, for $\Phi = 30^o$.

$$H/(\rho - D/2) = 2.08,$$

therefore,

$$\rho = \frac{H}{2.08} + \frac{D}{2} = 5.85 \text{ ft.}$$

$2\rho = 11.70$ ft. minimum spacing distance center to center of anchors.

Conclusion:

Ultimate load capacity $Q_u = 52.4$ kips

Minimum spacing $2\rho = 11.70$ ft.

Depth of embedment $H = 8.0$ ft.

Diameter of anchor plate $D = 4.0$ ft.

The above calculations are based on the assumption that the water table will not rise above the level of the anchor plate. If there is any chance of submergence, for instance, during a heavy rainfall, the value of the submerged unit weight of soil should be used instead of

the dry or wet density. In most situations, there is a strong probability that the soil will at times be submerged. Further, the value of Q_u in the above example excludes the weight of the anchor foundation.

CHAPTER VII

COMPARISON OF VARIOUS THEORETICAL RESULTS WITH EXPERIMENTAL DATA

In this chapter, the analytical results obtained by the method developed in this study are compared with those obtained using the procedures proposed by Balla (3), and Vesic (31), and with all available experimental data. The three analytical methods are comparable in simplicity of application. All of them yield a theoretical value for the ultimate load capacity of anchors, which, in each case, excludes the dead weight of the anchor. The superiority of the method developed in this study, over those previously proposed, will be demonstrated in terms of both reliability and range of application.

7.1 Correlation of Experimental Results

The data from the experimental work carried out by Balla (3), Baker and Kondner (2), and Esquivel (9), are listed in Tables X, XI, and XII, respectively. These tables also show the theoretical results obtained using the procedure of Balla, Vesic, and the author. From these tables, it can be seen that there is generally a close agreement between the results produced by Balla's method and by the author's method. However, the results produced by Vesic's method were much lower than the experimental values and the theoretical values found by the other two methods.

TABLE X

EXPERIMENTAL RESULTS REPORTED BY BALLA (3)

Depth H (in)	Diameter D (in)	H/D	γ Ave. (pcf)	Φ^o	Experimental Q_u (lb)	Saeedy's Theor. Q_u (lb)	Balla's Theor. Q_u (lb)	Vesic's Theor. Q_u (lb)
1.97	3.55	0.55	108.0	37.0	3.7	2.4	1.1	1.6
3.94	3.55	1.11	108.0	37.0	11.2	7.8	8.9	6.2
5.91	3.55	1.67	108.0	37.0	23.1	16.9	17.1	10.9
7.88	4.72	1.67	108.0	37.0	49.5	39.9	43.7	25.5
7.88	3.55	2.22	108.0	37.0	42.8	30.5	34.6	21.7
9.85	3.55	2.78	108.0	37.0	69.3	49.6	55.8	37.4
7.87	2.36	3.33	108.0	37.0	33.0	22.1	24.9	14.9
11.80	3.55	3.33	108.0	37.0	89.0	74.5	84.2	50.7

TABLE XI

EXPERIMENTAL RESULTS REPORTED BY BAKER AND KONDNER (2)

Depth H (in)	Diameter D (in)	H/D	γ Ave. (pcf)	Φ^{o}	Experimental Q_u (lb) Ave.	Saeedy's Theor. Q_u (lb)	Balla's Theor. Q_u (lb)	Vesic's Theor. Q_u (lb)
3.0	1.0	3.0	112.09	42.0	2.20	1.63	1.6	1.1
6.0	1.0	6.0	111.96	42.0	11.80	9.00	--	5.5
9.0	1.0	9.0	111.91	42.0	32.90	26.21	--	16.0
12.0	1.0	12.0	112.30	42.0	54.25	57.13	--	13.2
15.0	1.0	15.0	112.44	42.0	81.60	92.00	--	--
18.0	1.0	18.0	112.20	42.0	110.20	104.30	--	--
21.0	1.0	21.0	111.76	42.0	130.10	116.20	--	--
9.0	1.5	6.0	112.33	42.0	35.70	30.2	--	18.6
12.0	1.5	8.0	112.77	42.0	69.45	64.2	--	38.5
15.0	1.5	10.0	111.93	42.0	105.80	93.3	--	68.8
18.0	1.5	12.0	112.33	42.0	141.10	104.8	--	109.8
3.0	2.0	1.5	112.00	42.0	3.50	2.9	2.9	2.0
6.0	2.0	3.0	112.00	42.0	15.40	13.0	13.0	8.5
9.0	2.0	4.5	112.04	42.0	33.70	34.5	34.5	23.8
12.0	2.0	6.0	112.00	42.0	79.40	71.4	--	43.9
15.0	2.0	7.5	112.00	42.0	138.90	113.3	--	82.5
18.0	2.0	9.0	112.00	42.0	200.70	127.3	--	128.7
21.0	2.0	10.5	112.00	42.0	229.35	141.3	--	183.9
3.0	3.0	1.0	112.00	42.0	5.5	4.4	4.4	3.3
6.0	3.0	2.0	112.00	42.0	17.9	17.7	17.6	11.8
9.0	3.0	3.0	112.00	42.0	49.3	43.9	43.9	28.8
12.0	3.0	4.0	111.93	42.0	95.5	87.0	87.4	60.4
15.0	3.0	5.0	111.82	42.0	167.6	151.1	--	103.1
18.0	3.0	6.0	112.04	42.0	269.0	240.9	--	148.9
21.0	3.0	7.0	111.79	42.0	388.1	264.4	--	230.8

TABLE XII

EXPERIMENTAL RESULTS REPORTED BY ESQUIVEL (9)

Depth H (in)	Diameter D (in)	H/D	γ Ave. (pcf)	Φ^o	Experimental Q_u (lb)	Saeedy's Theor. Q_u (lb)	Balla's Theor. Q_u (lb)	Vesic's Theor. Q_u (lb)
4.5	3.0	1.5	96.0	42.9	13.6	8.6	8.3	2.0
9.0	3.0	3.0	95.0	42.9	62.0	38.7	37.6	8.3
13.5	3.0	4.5	95.8	42.9	171.5	104.1	102.0	23.0
18.0	3.0	6.0	95.5	42.9	360.0	215.9	--	42.4
24.0	3.0	8.0	95.8	42.9	734.5	258.3	--	91.0
29.4	3.0	9.8	94.2	42.9	997.0	290.4	--	150.0
4.5	3.0	1.5	81.0	35.3	4.0	6.0	7.0	1.7
9.0	3.0	3.0	81.4	35.3	13.9	25.6	31.7	7.0
13.5	3.0	4.5	81.6	35.3	22.5	65.8	86.0	19.4
18.0	3.0	6.0	81.1	35.3	29.7	132.3	--	35.0
29.4	3.0	9.8	81.9	35.3	60.6	190.2	--	126.6

The method outlined by Balla, was only applicable to anchors having $H/D \leq 4.0$. The application of Vesic's method was based on the values of N_q, which are plotted in Esquivel's report. The experimental data presented by Esquivel (9) were not in agreement with any of the theoretical results; and, indeed, appear unreasonable in terms of the author's own experience with experimental investigations. For example, the experimental value for Q_u reported by Esquivel for one of the tests of a 3.0 in. diameter plate, and $H/D = 9.8$, represents a force equal to about 80 per cent of the total weight of the material used in the experiment. It may also be pointed out that the difference between his test results for dense and loose sand are far greater than can be reasonably accounted for.

7.2 Correlation of Field Results

A comparison similar to that in the previous section is made for the three theoretical methods and field results obtained by Sutherland (27) for vertical anchors buried in cohesionless soils. A comparison is also made with field testing results of Brown - Boweri and Fielitz as reported by Balla (3). The two comparisons are given in Tables XIII and XIV, respectively.

It is believed that the data in Tables X through XIV indicate a clear superiority of the method developed in this study over those previously proposed. The author's procedure in general yields more reliable predictions of Q_u, although some anomalies exist, and has a broad range of application. Discrepancies, in some instances, would appear to be attributable to experimental errors rather than to theoretical deficiencies.

TABLE XIII

FIELD TESTS REPORTED BY SUTHERLAND (27)

Depth H (in)	Diameter D (in)	H/D	γ Ave. (pcf)	Φ^o	Experimental Q_u (Kip)	Saeedy's Theor. Q_u (Kip)	Balla's Theor. Q_u (Kip)	Vesic's Theor. Q_u (Kip)
96.0	94.0	1.02	66.0	45	90.0	91.23	84.15	60.8
180.0	94.0	1.9	66.0	45	368.0	329.76	298.5	214.7
180.0	94.0	1.9	66.0	45	352.0	329.76	298.5	214.7
204.0	94.0	2.2	66.0	45	512.0	435.25	389.1	270.4
204.0	94.0	2.2	66.0	45	500.0	435.25	389.1	270.4
252.0	94.0	2.7	66.0	45	464.0	706.36	629.6	414.2
276.0	94.0	2.94	66.0	45	576.0	875.15	770.9	563.4
276.0	94.0	2.94	66.0	45	900.0	875.15	770.9	563.4

TABLE XIV

FIELD RESULTS OF (BROWN-BOWERI AND FIELITZ) FROM BALLA (3)

Authority	Depth H (in)	Diameter D (in)	H/D	γ Ave. (pcf)	Φ^o	Experimental Q_u (Kip)	Saeedy's Theor. Q_u (Kip)	Balla's Theor. Q_u (Kip)	Vesic's Theor. Q_u (Kip)
Brown-Boweri	57.1	74.8	0.79	124.0	36.0	45.76	43.14	46.0	39.9
	59.1	74.8	0.79	124.0	36.0	45.54	45.68	51.6	43.1
Fielitz	98.4	55.2	1.78	101.5	30.0	51.48	60.41	68.1	45.6
	98.4	43.3	1.92	105.3	30.0	42.9	49.34	68.4	30.8
	106.3	51.2	2.45	84.5	30.0	53.9	54.40	57.4	44.7

CHAPTER VIII

CONCLUSIONS AND RECOMMENDATIONS

8.1 Conclusions

The primary purpose of this investigation was to provide additional knowledge concerning the stability of earth anchors buried in cohesionless material. Based on extensive theoretical and experimental study, the following conclusions are drawn:

1) Classification of earth anchors as shallow or deep should be governed by their capability to resist uplift forces, as reflected by a departure from transient linearity of the relationship between ultimate load and relative depth, rather than on observations related to the occurrence of bulging of the soil surface. The latter depends too greatly on the state of compaction of the soil. Furthermore, load capacity is the main concern of the design engineer in evaluating the stability of anchors.

2) The ultimate load capacity of anchors increases with the plate diameter and depth of embedment. The rate of load increase attains a maximum value that remains constant over a linear part of the Q_u versus H/D curve, for an appreciable range of intermediate H/D values. Following this, the rate of load increase again decreases, tending toward zero for large values of H/D. It is necessary to take these observed

behavioral characteristics into account if maximum economy is to be effected in the design of anchors.

3) Modeling effects arising from differences in the relative dimensions of anchor and soil grains may be minimized by selecting appropriate dimensions for the anchor system. It appears from this investigation that modeling effects are substantially eliminated when anchor plates in sand are three inches or more in diameter.

4) The moisture condition of the soil has a pronounced effect on the magnitude of Q_u. The submerged condition produces the least resistance to pullout, while the drained condition gives the greatest. The resistance of dry sand is intermediate between the two. The difference in resistance for the dry and saturated-drained states cannot be accounted for by the difference in unit weight, alone. Consideration must also be given to the effects of capillarity in the pore water.

5) The shape of anchor plate has a considerable influence on the stability of anchors. The ultimate load capacity of a bevel-edged plate is about 20 per cent less than that of a flat plate with a uniform thickness.

6) The excellent correlation of various experimental and field values of the ultimate load capacity with those theoretical values found from the solution developed in this study, shows the proposed method to be superior to methods previously proposed, in terms of reliability, range of applicability and simplicity.

8.2 Recommendations for Future Investigations

Additional investigations are recommended to extend the range of applicability of the solution developed in this study, and to provide additional verification of the validity of the solution for use in full scale anchor installations. Specifically, the following areas of investigation appear to be needed:

1) Experimental studies of anchor plates having diameters larger than 3.5 inches. Additional verification is needed of the independency of Q_u on H/D for large values of H/D. It now appears that Q_u approaches a constant value that cannot be increased by deeper embedment, after H/D has attained some large, but as yet unspecified magnitude. Additional evidence is also needed to confirm the indication that the value of H/D marking the upper limit of the linear part of the Q_u versus H/D curve remains constant for D greater than 3.5 inches.

2) A study of the behavior of anchors in cohesive soils to substantiate the indication that the theoretical solution developed in this study is applicable to cohesive as well as cohesionless soils.

3) An extension of both the theoretical and experimental studies to include anchor plates that are inclined to the horizontal and subjected to pulls perpendicular to their bedding planes; and horizontal anchor plates that are subjected to pulls other than in a vertical direction.

SELECTED BIBLIOGRAPHY

(1) Ali, M. S. "Pullout Resistance of Anchor Plates and Anchor Piles in Soft Bentonite Clay." (unpub. M. S. thesis, Duke University, 1968).

(2) Baker, W. H., and R. L. Kondner. "Pullout Load Capacity of Circular Earth Anchors Buried in Sand," H.R.B., No. 108 (1965), pp. 1-10.

(3) Balla, A. "The Resistance to Breaking-Out of Mushroom Foundations for Pylons," Proc. Fifth International Conference on Soil Mechanics and Foundations Engineering, Volume 1 (1961), pp. 569-576.

(4) Bhatnagor, R. S. "Pullout Resistance of Anchors in Silty Clay." (unpub. M. S. thesis, Duke University, 1967).

(5) Brinch Hansen, J. Earth Pressure Calculations. The Danish Technical Press, 1953, pp. 54-55.

(6) Brinch Hansen, J. "The Internal Forces in a Circle of Rupture," The Danish Institute Bulletin, No. 2 (1957).

(7) "Construction Methods and Equipment: Tie Back Wall Braces Building Excavation," Construction Methods and Equipment (Nov. 1962), pp. 116-119.

(8) "Engineering News Record: Tie Backs Remove Clutter in Excavation," Engineering News Record, Vol. 165 (1962), pp. 34-36.

(9) Esquivel, R. F. "Pullout Resistance of Deeply Buried Anchors in Sand." (unpub. M. S. thesis, Duke University, 1967).

(10) Giffels, W. C. "Concrete Cylinder Anchors Proved for 345 KV Tower Live," Electrical World, Vol. 154 (1960), pp. 46-49.

(11) Henrici, P. Elements of Numerical Analysis. New York: John Wiley and Sons, 1963.

(12) Jaky, J. "Stability of Earth Slopes," Proc. First International Conference on Soil Mechanics and Foundations Engineering, Harvard University, Cambridge, Massachusetts, Vol. 2 (1936), pp. 200-207.

(13) Jaspar, J. L., and V. W. Shtenko. "Foundation Anchor Piles in Clay Shales," Canadian Geotechnical Journal, Vol. 6, No. 159 (1969).

(14) Jumikis, A. R. Theoretical Soil Mechanics. New York: Van Nostrand Co., 1968, pp. 258-263.

(15) Jumikis, A. R. "Stability Analysis of Soil-Foundation Systems," Rutgers State University, Eng. Research Publications, No. 44 (1965).

(16) Kline, S. J. Similitude and Approximation Theory. New York: McGraw Hill Co., Inc., 1965, pp. 36-51.

(17) Leonards, G. A. Foundation Engineering. New York: McGraw Hill Co., Inc., 1962, pp. 670-676.

(18) Mariupol'skii, L. G. "The Bearing Capacity of Anchor Foundations," (English Translation), Russian Soil Mechanics and Foundation Eng. (1965), pp. 26-32.

(19) Markowsky, M., and J. I. Adams. "Transmission Towers Anchored in Maskey," Electrical World, Vol. 155 (1961), pp. 36-37.

(20) Matsuo, M. "Study on the Uplift Resistance of Footing," Soil Mechanics and Foundations, Tokyo, Vol. 7, No. 4 (1967), pp. 1-37.

(21) McCracken, D. D., and W. S. Dorn. Numerical Methods and Fortran Programming. New York: John Wiley and Sons, 1968.

(22) Means, R. E., and J. V. Parcher. Physical Properties of Soils. Ohio: Merrill Publishing Co., 1963, pp. 307-314.

(23) Meyerhof, G. G., and J. I. Adams. "The Ultimate Uplift Capacity of Foundations," Canadian Geotechnical Journal, Vol. 5, No. 4 (1968), pp. 225-244.

(24) Nadai, A. Theory of Flow and Fracture of Solids. New York: McGraw Hill, Vol. II, 1963, pp. 454-463.

(25) Parcher, J. V., and R. E. Means. Soil Mechanics and Foundations. Ohio: Merrill Publishing Co., 1967, pp. 381-391.

(26) Sams, R. "Laboratory Modeling of Anchor Stability," (unpub. M.S. thesis, Colorado State University, 1970).

(27) Sutherland, H. B. "Model Studies for Shaft Raising Through Cohesionless Soils," Proc. Sixth International Conference on Soil Mechanics and Foundations Engineering, Vol. 2 (1965), pp. 410-413.

(28) Terzaghi, K. Theoretical Soil Mechanics. New York: John Wiley and Sons, 1965.

(29) Timoshenko, S., and J. N. Goodier. Theory of Elasticity. New York: McGraw Hill, 1951, pp. 55-56.

(30) Turner, E. A. "Uplift Resistance of Transmission Tower Footings," Journal of Power Division, ASCE, Vol. 88, No. PO2 (July 1962), pp. 17-33.

(31) Vesic, A. S. "Cratering by Explosives as an Earth Pressure Problem," Proc. Sixth International Conference on Soil Mechanics and Foundations Engineering, Vol. 2 (1965), pp. 427-431.

(32) Wiggins, R. L. "Analysis and Design of Tower Foundations," Journal of Power Division, ASCE, Vol. 95, No. PO1 (March 1969), pp. 77-100.

(33) Yong, R. W., and B. P. Warkentin. Introduction to Soil Behavior. New York: Macmillan, 1966, pp. 259.

APPENDIX A

LISTING OF COMPUTER PROGRAM

```
      $JOB    *****,***-**-****          H.S. SAEEDY
      C*****************************************************************
      C      THIS PROGRAM IS TO ANALIZE THE ULTIMATE LOAD CAPACITY     *
      C      OF VERTICAL EARTH ANCHORS BASED ON THE ULTIMATE STRENGTH  *
      C      OF SOIL, AND ASSUMED LOG. SPIRAL RUPTURE SURFACE.         *
      C*****************************************************************
 1          DIMENSION A(10) ,PK(10),HED(20),TV(105),RR(105),AL(105),RHO(105),
           1AREA(105),TTU(105),TTUB(105),W(105) ,RW(105),HD(105)
 2          DATA FINISH/'FINI'/
 3        1 READ 106,HED
 4          IF(FINISH-HED(1)) 5,107,5
 5        5 PRINT 2,HED
      C**** PHI    = ANGLE OF INTERNAL FRICTION  - DEGREES
      C**** C      = COHESION OF SOIL - P.S.F.
      C**** GAMMA  = UNIT WT. OF SOIL -P.C.F.
      C**** HT     = TOTAL DEPTH OF ANCHOR - IN.
      C**** BE     = ANCHOR PLATE DIAM. -IN.
      C**** DE     = ANCHOR SHAFT DIAM. -IN.
      C**** TH     = ANCHOR PLATE THICKNESS - IN.
      C**** N      = NO. OF INTERVALS OF ANGLE ALPHA.
      C**** GAM2   = UNIT WT. OF PLATE.
      C**** GAM1   = UNIT WT. OF SHAFT.
      C**** H      = EXTENDED HEIGHT OF FAILURE SURFACE.
 6          READ 100, PHI, C, GAMMA, HT, BE, DE, TH, N
 7          READ 101, GAM1, GAM2, FF
 8          PRINT 200
 9          PRINT 201, GAMMA , PHI, C
10          PRINT 202
11          PRINT 203 , HT, DE, BE, TH
12          PIE =3.14159
13          HT = HT / 12.
14          DE = DE /12.
15          ALPHAD = (45. - PHI/2.)
16          PHI=PHI*(3.14159/180.)
17          ALPHAR=ALPHAD*(3.14159/180.)
18          BET = (PIE/2. - ALPHAR )
19          DBET =BET /N
      C**** TRANSITIONAL RELATIVE DEPTH
20          A0 = 27.85971
21          A1 =-22.43521
22          A2 = 8.441958
23          A3 =-1.372482
24          A4 = 0.0806472
25          Q = A0 + A1 * BE + A2 *(BE**2) + A3 * (BE **3) + A4 * (BE **4)
26          BE=BE/12.
27          ORATIO = HT / BE
28          IF ( HT / BE .GT. Q ) H = Q * BE
29          IF ( HT / BE .LE. Q ) H = HT
30          IF ( HT .GT. H ) GO TO 11
31          TAU=C*(1.+SIN(PHI))
32       11 TAU =  C +( HT - H)* GAMMA * TAN(PHI)) *  0.5
33          X = H *TAN(ALPHAR)
34          RR(1) = H/COS(ALPHAR)
35          OW = PIE/2.- ALPHAR
36          RW (1) = RR(1) *SIN(ALPHAR)/ (COS(PIE/2. - ALPHAR -PHI ))
37          RPHI = RW(1)
38          Y =RW(1) *SIN(PIE/2.-ALPHAR -PHI)
39          HPHI =H -Y
40          AN=N
41          DO 18 I=1,N
```

```
42          W(I  )=(I  )* OW/ AN
43          RW(I+1) = RPHI* EXP(W(  I)* TAN(PHI))
44          RR(I+1)=SQRT((RW (I+1))**2+(HPHI)**2-2.*RW (I+1)*HPHI*COS(PIE/2.
           1-PHI + (OW-W(I))))
45        18 CONTINUE
46          TAUS=TAU
47          CALL FUNC1(TAUS,RR(1), ALPHAR, GAMMA, FTAU, PHI)
      C       INITIAL  VALUES
48          AL(1) =ALPHAR
49          TTUB(1)=TAU
50          TTU(1)= TAU
51          DH =H /N
52          OW = ARSIN(DH/ (RR(1) * EXP(OW  *TAN(PHI))))
53          DO 10 I=1,N
54          ALPHA1=ALPHAR
55          W( I ) =( I) *OW
56          DO 20 K=1,4
57          RK=(K+1)/2.
58          CALL FUNC1(TAUS,RR(I+1),ALPHAR, GAMMA, FTAU, PHI)
59          PK(K) =FTAU *DBET
60          IF(K-4) 6,12,12
61         6 TAUS=TAU+(PK(K)/2.)*RK
62          ALPHAR =ALPHA1 +(DBET /2.)*RK
63        20 CONTINUE
64        12 TAU=TAU+(PK(1)+2.*PK(2)+2.*PK(3)+PK(4))/6.
65          CALL FUNC2(TAUB ,ALPHAR ,PHI,GAMMA,C,TAUBV,RB,H,BE)
66          ALPHAD=ALPHAR*(180./3.14159)
67          AL(I+1)= ALPHAR
68          TTU(I+1)=TAU
69          TTUB(I+1)= TAUB
70        10 CONTINUE
71          L=N+1
72          DO 30 I=1,L
73          RHO(I)=RR(L) -(RR(I)*SIN(AL(I))) +BE/2.
74          TV(I  )=TTU(I  )*2.*PIE*RHO(I  )*H/N
75          AL(I)=AL(I)* 180./PIE
76          HD(I)= (I-1)* H/AN
77        30 CONTINUE
78          SPACE = HT / ( RHO(1) - (BE/ 2.))
79          PRINT 88, TAUBV ,RB
80          PRINT 29
81          PRINT 99
82          PRINT 19, (AL(I),RR(I),TTU(I),RHO(I),HD(I),TV(I),TTUB(I),RW(I),
           1 I=1,L)
      C SIMPSON RULE TO FIND THE SUMMATION OF THE VERTICAL FORCES ALONG THE FAILURE
83          ODD= 0.
84          EVEN =0.
85          M=L-3
86          DO 16 I= 2,M,2
87          EVEN =EVEN + TV(I)
88          ODD =ODD + TV(I+1)
89        16 STV =(TV(1) +4.*(EVEN+TV(L-1))+ 2.* (ODD+TV(L)))/3.
90          RPHI = RPHI* 12.
91          OW = OW *(180./PIE)
92          PRINT 7, OW, RPHI
93          PRINT 108, STV
94          EVEN1=0.
95          ODD1=0.
96          DO 50 I=1,L
97          AREA(I)  =PIE *RHO(I)**2
```

```
 98      50 CONTINUE
 99         DO 40 I=2,M,2
100         EVEN1= EVEN1+ AREA(I)
101         ODD1= ODD1+AREA(I+1)
102         AN=N
      C**** NET VOLUME OF BREAKING-OUT SOIL
103         VOL =(AREA(1) +4.*(EVEN1+AREA(L-1))+2.*(ODD1+AREA(L))) * H/(AN*3.)
104         VOL1 =(H * PIE * DE**2) / 4.
      C**** NET WEIGHT OF BREAKING-OUT SOIL
105         F1= GAMMA *( VOL-VOL1)
106         VOL2 =(PIE *TH* BE**2        )/(4.* 12.)
      C**** WEIGHT OF ANCHOR   FOUNDATION
107         F2 = GAM1* VOL1 +GAM2* VOL2
108         FMAX = STV + F1 +F2
109      40 CONTINUE
110         PRINT 39, VOL,F1
111         PRINT 49,FMAX
112         GF = (PIE /4. ) * (HT*(BE**2 - DE**2)* GAMMA )
      C******* FPHI = FRICTIONAL FORCE
      C******* FF= FORCE RATIO FROM FRICTION
      C******* F = COHESIVE FORCE
      C******* FC= FORCE RATIO FROM COHESION
113         IF ( C  .LT. 1.0 ) GO TO 150
114         FPHI = FF* GF
115         F = FMAX - FPHI
116         FC = F/ (C*HT* BE)
117         FPHIC = FF + FC
118          FRATIO = FPHIC
119         FC1 = F *C /( GF* GAMMA*BE/2. )
120         PRINT 89, F,FC
121         GO TO 151
122     150 FRATIO = FMAX / GF
123         F2 =FMAX /(( BE**3 - DE**3) * GAMMA )
124     151 CONTINUE
125         PRINT 59, GF
126         PRINT 69, FRATIO
127         PRINT 79, DRATIO, Q, SPACE
128       2 FORMAT (1H1,//,20A4)
129       3 FORMAT (7F10.0)
130       4 FORMAT(/,1H,'H=',F10.3,2X,'GAMMA=',F10.3,2X,'C=',F10.3,2X,'PHI=',
           1F10.3,2X,'BE=',F10.3,2X,'N =',I4/)
131       7 FORMAT(//5X,'OMEGA =',F10.3,2X,'DEGREES', 4X, 'INITIAL SPIRAL RAD.
           1 =',F8.2,2X,'IN.')
132       9 FORMAT (11F5.2)
133      19 FORMAT(    8(2X,F10.3))
134      29 FORMAT( /,6X,'ALPHAD',8X,'RAD.',4X,'TAU-SAEEDY',6X,'RHO',8X,
           1'DEPTH',8X,'TV',6X,'TAU-BRINCH',2X,'RAD.OF SPIRAL' )
135      39 FORMAT(/ ,5X,'VOL. OF SOIL =',F10.3,'CU. FT.',5X,'WT. OF SOIL=',
           1F10.3,'  LBS.' /)
136      49 FORMAT(5X,'MAX. PULL-OUT FORCE=',F10.3,'  LBS.' )
137      59 FORMAT(/,5X,'GRAVITATIONAL FORCE OF  SOIL=',F10.3,2X,'  LBS.' )
138      69 FORMAT (/,5X,'FORCE RATIO F1 =', F10.3)
139      79 FORMAT(/,5X,'RELAT.DEPTH =',F7.3 , 5X,'TRANSITIONAL RELATIVE DEPTH
           1 =',F 7.3,5X ,'ANCHOR SPACE RATIO =',F7.3)
140      88 FORMAT ( /, 5X ,'VERT. SHEAR FORCE (TAU-BRINCH)=',F10.3,1X,'LB',
           1 4X ,'CIRCULAR RAD. RB =',F10.3,1X,'FT'/)
141      89 FORMAT (/,5X,'COHESIVE FORCE =',F10.3,2X,'POUNDS',5X ,'COHESIVE FO
           1RCE RATIO =',F10.3)
142      90 FORMAT (/,5X,'FRICTIONAL FORCE RATIO =',F10.3,10X,
           1'COHESION FORCE RATIO =',F10.3)
```

```
143      99 FORMAT (6X,'******',8X ,'***', 5X ,'**********' , 6X,'***',
        1 8X,'*****', 8X, '**', 6X,'**********' ,2X,'**********')
144     100 FORMAT (7F10.0,I4)
145     101 FORMAT (3F10.0)
146     105 FORMAT (5F15.5)
147     106 FORMAT (20A4)
148     108 FORMAT (/, 5X,' VERTICAL FORCE DUE TO SHEAR STRESS =',F10.3,' LBS.
        1' )
149     110 FORMAT (2X,4E15.3)
150     111 FORMAT (2X,2E15.5)
151     200 FORMAT (  /, 1H , 43X,'*** PROPERTIES OF SOIL ***')
152     201 FORMAT (  18X,'UNIT WT. =',F7.2,1X,'PCF.', 4X,'ANGLE PHI =',F6.2,
        11X ,'DEG.', 4X ,'COHESION =',F7.2,' PSF.')
153     202 FORMAT (/ ,44X ,'*** GEOMETRY OF ANCHOR ***')
154     203 FORMAT ( 5X,'DEPTH =',F7.2,1X,'IN.',4X,'SHAFT DIA. =',F6.2,' IN.'
        1,4X,'PLATE DIA. =' ,F7.2,' IN.',4X, 'PLATE THICK. =',F6.2, ' IN.')
155         GO TO 1
156     107 STOP
157         END
158         SUBROUTINE FUNC1(TAU,RR,ALPHAR,GAMMA,FTAU,PHI)
159         BET=ALPHAR+PHI
      C**** THIS IS KOTTER'S DIFF. EQ. SOLVED BY RUNGE-KUTTA METHOD
160         FTAU=-2.*TAU*TAN(PHI)+RR   *GAMMA* SIN(PHI) *SIN(BET)
161         RETURN
162         END
163         SUBROUTINE FUNC2(TAUB,ALPHAR ,PHI,GAMMA,C,TAUBV,RB,H,BE)
      C     THIS IS THE CIRCULAR CURVE SOLUTION( AFTER BRINCH & BALLA )
164         PIE =3.14159
165         RB=H/(COS(PIE/4.-PHI/2.))
166         Y= 1./(EXP(2.*TAN(PHI)*ALPHAR))
167         Z= EXP((3.14159/4.-PHI/2.)*2.* TAN(PHI))
168         D=(3.14159/4.+PHI/2.)
169         B=(1.+SIN(PHI))
170         B1=C/(RB*GAMMA)
171         B3=(2.*TAN(PHI)*TAN(D)-1.)
172         B5 = ALPHAR+PHI
173         B4=2.*TAN(PHI)*SIN(B5 )
174         R=(SIN(PHI))/(1.+4.*TAN(PHI)*TAN(PHI))
175         B2=R*COS(D)
176         AB=RB*GAMMA*Z*((B1*B)-(B2*B3))
177         TAUB=AB*(  Y )+(RB*GAMMA*R*(B4-COS( B5)))
178         D1 = (3.14159/4.) -(PHI/2.)
179         D2=1./(1.+4.*TAN(PHI)**2)
180         H1= (C/(RB*GAMMA))*(1.+SIN(PHI))
181         H2= SIN( PHI)*D2*COS(D)
182         H3=2.*TAN(PHI)*TAN(D)-1.
183         H4=(1.+BE/(2.*RB))*(D2)
184         H5=2.*TAN(PHI)*EXP(-D*2.*TAN(PHI))
185         H6=COS(D1)*(2.*TAN(PHI)*TAN(D1)+1.)
186         H7= (1./    (1.+TAN(PHI)**2))   *(EXP(-D1*2.*TAN(PHI))-1.)
187         H8=1./(4.*(1.+TAN(PHI)**2))
188         H9= (EXP(-D1*2.*TAN(PHI))+SIN(PHI))*TAN(PHI)-COS(PHI)
189         H10= (D2/4.)*(1. +BE/(2.*RB))
190         H11=3.*SIN(PHI)**2*(3.14159/2.+PHI+COS(PHI))
191         H12=SIN(PHI)*(COS(PHI)-2.*SIN(PHI)*TAN(PHI))*(1.+SIN(PHI))
192         H13=D2/6.
193         H14=3.*SIN(PHI)**2*(5.-SIN(PHI))*COS(D1)
194         H15=SIN(PHI)*(COS(PHI)-2.*SIN(PHI)*TAN(PHI))
195         H16=(1.-SIN(PHI))*SIN(D1)-2.
196         TAUBV=(RB**3)*GAMMA*2.*3.14159*((H1- H2*H3)*(H4*(-H5+H6)+H7+(H8*H9
           ))+H10*(H11-H12)-H13*(H14+(H15*H16)))
197         RETURN
198         END

      $FNTRY
```

** SAEEDY-LOG. SPIRAL SOLUTION FOR EARTH ANCHORS **

*** PROPERTIES OF SOIL ***

UNIT WT. = 100.00 PCF. ANGLE PHI = 35.00 DEG. COHESION = 0.00 PSF.

*** GEOMETRY OF ANCHOR ***

DEPTH = 15.00 IN. SHAFT DIA. = 0.25 IN. PLATE DIA. = 3.00 IN. PLATE THICK. = 0.38 IN.

VERT. SHEAR FORCE (TAU-BRINCH)= 64.256 LB CIRCULAR RAD. RB = 1.409 FT

ALPHAD	RAD.	TAU-SAEEDY	RHO	DEPTH	TV	TAU-BRINCH	RAD.OF SPIRAL
******	***	**********	***	*****	**	**********	**********
27.500	1.409	0.000	0.764	0.000	0.000	0.000	0.734
33.750	1.407	7.381	0.633	0.125	3.670	7.449	0.792
40.000	1.401	14.009	0.514	0.250	5.656	14.164	0.855
46.250	1.392	19.873	0.409	0.375	6.391	20.158	0.923
52.500	1.379	24.964	0.321	0.500	6.294	25.436	0.996
58.750	1.363	29.281	0.250	0.625	5.743	30.005	1.075
65.000	1.345	32.826	0.196	0.750	5.050	33.867	1.160
71.250	1.327	35.618	0.159	0.875	4.441	37.026	1.252
77.500	1.309	37.686	0.137	1.000	4.042	39.486	1.252
83.750	1.296	39.075	0.127	1.125	3.883	41.257	1.459
90.000	1.290	39.842	0.125	1.250	3.912	42.346	1.575

OMEGA = 62.500 DEGREES INITIAL SPIRAL RAD. = 8.80 IN.

VERTICAL FORCE DUE TO SHEAR STRESS = 48.805 LBS.

VOL. OF SOIL = 0.543CU. FT. WT. OF SOIL= 54.303 LBS.

MAX. PULL-OUT FORCE= 103.108 LBS.

GRAVITATIONAL FORCE OF SOIL= 6.093 LBS.

FORCE RATIO F1 = 16.922

RELAT.DEPTH = 5.000 TRANSITIONAL RELATIVE DEPTH = 6.007 ANCHOR SPACE RATIO = 1.956

APPENDIX B

RESULTS OF HYPOTHETICAL EXAMPLES

RESULTS OF HYPOTHETICAL EXAMPLES USED IN PREPARING FIGURES 31, 32, AND 33

Φ Deg.	γ pcf.	Diameter D in.	Relative Depth H/D	Ultimate Load Capacity Q_u lb.	Force Ratio F_1	Anchor Space Ratio $H/(\rho - D/2)$
20	100.0	3.0	1.0	2.9	2.40	2.26
20	100.0	3.0	2.0	10.2	4.18	2.26
20	100.0	3.0	3.0	23.4	6.40	2.26
20	100.0	3.0	4.0	44.0	9.03	2.26
20	100.0	3.0	5.0	73.6	12.09	2.26
20	100.0	3.0	6.0	113.8	15.57	2.26
25	100.0	3.0	1.0	3.1	2.55	2.18
25	100.0	3.0	2.0	11.1	4.54	2.18
25	100.0	3.0	3.0	25.6	7.01	2.18
25	100.0	3.0	4.0	48.5	9.96	2.18
25	100.0	3.0	5.0	81.5	13.38	2.18
25	100.0	3.0	6.0	126.3	17.28	2.18
30	100.0	3.0	1.0	3.3	2.70	2.08
30	100.0	3.0	2.0	12.0	4.92	2.08
30	100.0	3.0	3.0	28.1	7.69	2.08
30	100.0	3.0	4.0	53.7	11.01	2.08
30	100.0	3.0	5.0	90.7	14.89	2.08
30	100.0	3.0	6.0	141.2	19.31	2.08
35	100.0	3.0	1.0	3.5	2.87	1.96
35	100.0	3.0	2.0	13.1	5.38	1.96
35	100.0	3.0	3.0	31.3	8.56	1.96
35	100.0	3.0	4.0	60.5	12.41	1.96
35	100.0	3.0	5.0	103.1	16.90	1.96
35	100.0	3.0	6.0	161.6	22.11	1.96
40	100.0	3.0	1.0	3.7	3.12	1.79
40	100.0	3.0	2.0	14.8	6.07	1.79
40	100.0	3.0	3.0	36.2	9.90	1.79
40	100.0	3.0	4.0	71.2	14.61	1.79
40	100.0	3.0	5.0	123.0	20.19	1.79
40	100.0	3.0	6.0	194.8	26.64	1.79
45	100.0	3.0	1.0	4.3	3.51	1.58
45	100.0	3.0	2.0	17.9	7.33	1.58
45	100.0	3.0	3.0	45.3	12.40	1.58
45	100.0	3.0	4.0	91.5	18.77	1.58
45	100.0	3.0	5.0	160.9	26.42	1.58
45	100.0	3.0	6.0	258.5	35.35	1.58

Φ Deg.	γ pcf.	Diameter D in.	Relative Depth H/D	Ultimate Load Capacity Q_u lb.	Force Ratio F_1	Anchor Space Ratio $H/(\rho - D/2)$
30	60.0	3.0	4.0	32.2	11.01	2.08
30	70.0	3.0	4.0	37.6	11.01	2.08
30	80.0	3.0	4.0	42.9	11.01	2.08
30	90.0	3.0	4.0	48.3	11.01	2.08
30	100.0	3.0	4.0	53.7	11.01	2.08
30	110.0	3.0	4.0	59.1	11.01	2.08
30	120.0	3.0	4.0	64.4	11.01	2.08

VITA

Hamed Salem Saeedy

Candidate for the Degree of

Doctor of Philosophy

Thesis: ANALYTICAL AND EXPERIMENTAL STABILITY OF EARTH ANCHORS

Major Field: Civil Engineering

Biographical:

Personal Data: Born in Basrah City, Republic of Iraq, December 25, 1937, the son of Salem and Safia Saeedy.

Education: Attended elementary school in Basrah, Iraq; graduated from Basrah High School, Basrah, Iraq, in June, 1957; received a certificate in Teaching and Education from Basrah Educational Course, June, 1958; received a Diploma of Technology in Civil Engineering from Kingston College of Technology, Kingston on Thames, Surrey, England, in July, 1962; granted a Diploma of Technology in Construction Engineering from Twickenham College of Technology, Twickenham, Middlesex, England, in May, 1963; received a Master of Science Degree in Civil Engineering from Colorado State University, Fort Collins, Colorado, in August, 1968; completed requirements for the Doctor of Philosophy degree in Civil Engineering at Oklahoma State University in May, 1971.

Professional Experience: Apprentice in the Engineering Divisions, KOC, Basrah, Iraq, from October, 1953, to September, 1955; Personnel Office Education Directorate, Basrah, Iraq, from September, 1955, to September, 1958; Structural Engineer, Atkins and Partners, Epsom, England, 1963-1964; Lecturer, College of Engineering, Basrah, Iraq, from January, 1965, to June, 1967; Soils Engineer, Ardaman and Associates from May to September, 1969; Graduate Assistant, School of Civil Engineering, Oklahoma State University from September, 1969, to date.

Professional Societies: Associate Member, The Institution of Civil Engineers, London, England; Member, The Iraqi Society of Engineers, Baghdad, Iraq; Associate Member, American Society of Civil Engineers.